U-007-303.50

5489

GLACIAL OVERBURDEN/UPPER GREAT MIAMI AQUIFER SYSTEM MODEL DEVELOPMENT REPORT REVISION NO. 1 APRIL 1994

04/20/94

DOE-FN/EPA
139
REPORT
OU5

- 5489

Glacial Overburden/ Upper Great Miami Aquifer System Model Development Report

Fernald Environmental Management Project
April 1994
Revision No. 1

Submitted by:
U.S. Department of Energy
Fernald Office
P.O. Box 398705
Cincinnati, Ohio 45239-8705

5489

Glacial Overburden/ Upper Great Miami Aquifer System Model Development Report

Fernald Environmental Management Project
April 1994
Revision No. 1

Submitted by:
U.S. Department of Energy
Fernald Office
P.O. Box 398705
Cincinnati, Ohio 45239-8705

Prepared by:
PARSONS
Fairfield, Ohio

Prepared for:
Fernald Environmental Restoration Management Corporation

PARSONS

FERMCO
Restoration Management Corporation

000002

Glacial Overburden/Upper Great Miami Aquifer System Model Development Report

CONTENTS

SECTION

1.0 Introduction 1-1
- 1.1 Objectives 1-2

2.0 Technical Approach 2-1
- 2.1 Two-Model Approach 2-1
- 2.2 Selection of the Auxiliary Unsaturated Code 2-3
- 2.3 Selection of the Primary Saturated Code 2-4
- 2.4 Preliminary Development of the Primary and Auxiliary Models 2-4
- 2.5 Cross-Verification of the Modeling Codes 2-5
- 2.6 Primary Model Final Steady-State Flow Calibration 2-5
- 2.7 Evaluation of Lateral Plume Migration with the 3-D GO/UGMAS Model 2-6
- 2.8 Linkage of the GO/UGMAS and GMA Models 2-7

3.0 Hydrogeological Conditions and Conceptual Model 3-1
- 3.1 Hydrogeological Conditions 3-1
- 3.2 Generalized Stratigraphy of the Conceptual Model 3-10
- 3.3 Primary Assumptions in the Conceptual Model 3-12

4.0 Preliminary Model Development 4-1
- 4.1 Preliminary Development of the Primary 3-D Flow Model 4-1
- 4.2 Preliminary Auxiliary Flow Model Development 4-7

5.0 Cross-Verification of Auxiliary and Primary Models 5-1
- 5.1 Model Grids for Cross-Verification 5-1
- 5.2 Soil Hydraulic Properties for Cross-Verification 5-2
- 5.3 Boundary Conditions for Cross-Verification 5-4
- 5.4 Cross-Verification Results 5-4

6.0 Primary Model Final Steady-State Flow Calibration 6-1
- 6.1 Approach 6-1
- 6.2 Criteria 6-2
- 6.3 Results 6-2

5489

CONTENTS (Continued)

7.0 Uranium-238 Transport Simulation 7-1

7.1 Uranium-238 Transport Parameters 7-1

7.2 Uranium-238 Initial Conditions 7-2

7.3 Uranium-238 Transport Run Results 7-2

8.0 Conclusions and Recommendations 8-1

8.1 Recommendations for the CRU-5 RI/FS Glacial Overburden Modeling 8-1

9.0 References 9-1

APPENDICES

A MSTS Soil Characteristic Curve Parameters

B Cross-Sectional Steady-State Flow Figures and Tables

C 3-D Flow Model Figures and Tables

D 1,000-Year Uranium-238 Transport Run Figures and Tables

E 1,000-Year Uranium Run Material Balance Summary

LIST OF ILLUSTRATIONS

5489

FIGURES

2-1 GO/UGMAS Model Development Process Diagram

3-1 General Pressure Head Profile
3-2 Major Features of the Conceptual Model
3-3 Distribution of Coarser-Grained Sediment Bodies
3-4 Average Perched Groundwater Elevations
3-5 Conceptual Model

4-1 GO/UGMAS Model Grid (Subset of GMA Model Grid)
4-2 Cross-Sections A-A' and at Row 80 for 2-D Steady-State Flow Runs
4-3 MSTS Grid - Soil Type Cross-Section at Row 80
4-4 Discharge Across the Bottom Boundary - Row 80 Cross-Section

5-1 MSTS Grid - Soil Type Cross-Section A-A'
5-2 Discharge Across the Bottom Boundary - Cross-Section A-A'

TABLES

3-1 Hydraulic Conductivity Geometric Mean by Sediment Group
3-2 Hydraulic Conductivity of Coarse-Grained Sediment

4-1 Initial Steady-State Flow Parameters by Soil Type

6-1 Final Steady-State Flow Parameters by Soil Type Used in Run 3DFLOW32

7-1 Transport Properties Specified in Flow Run 3DFLOW32/U238 Transport Run 3DTRAN01
7-2 Flow-Transport Run 32 - Total Dissolved U-238 Mass by Layer vs. Time and Dissolved U-238 Mass Rate of Change by Layer vs. Time

5489

LIST OF ACRONYMS AND ABBREVIATIONS

CERCLA	Comprehensive Environmental Response, Compensation, and Liability Act
CPC	Constituent of Potential Concern
CRU	CERCLA/RCRA Unit
ERMA	Environmental Resource Management Analysis
FEMP	Fernald Environmental Management Project
GIS	Geologic Information System
GMA	Great Miami Aquifer
GO/UGMAS	Glacial Overburden/Upper Great Miami Aquifer System
HELP	Hydrologic Evaluation of Landfill Performance
MSTS	Multiphase Subsurface Transport Simulator
ODAST	One-Dimensional Analytical Solute Transport
1-D	One-Dimensional
PRG	Preliminary Remediation Goal
RCRA	Resource Conservation and Recovery Act
RI/FS	Remedial Investigation/Feasibility Study
SWIFT	Sandia Waste Isolation Flow and Transport
3-D	Three-Dimensional
2-D	Two-Dimensional
UGMA	Upper Great Miami Aquifer

000006

SECTION 1

INTRODUCTION

A modeling effort was conducted to assess and improve the modeling of groundwater flow and contaminant transport through the Glacial Overburden and Upper Great Miami Aquifer System (GO/UGMAS). A one dimensional analytical code for solute transport in homogenous, semi-infinite media (One-Dimensional Analytical Solute Transport [ODAST]) was being used to model fate and transport in the GO/UGMAS. There was a concern that ODAST was not effectively simulating actual conditions due to the presence of multiple sources of contamination and the possibility of contaminants migrating laterally through coarser grained sediment pathways.

Flow and transport in the GO/UGMAS were modeled with the three dimensional Sandia Waste Isolation Flow and Transport (SWIFT) finite difference code using the following assumptions: (1) the glacial overburden is saturated, (2) the upper unsaturated sands and gravels of the Great Miami Aquifer (GMA) can be treated as saturated, (3) the upper layer of the model is very permeable (weathered, oxidized sediments). It was concluded that lateral uranium plume migration from major contaminated perched groundwater areas is not significant in relation to vertical uranium plume migration. Modeling results indicate that uranium in perched groundwater under the Plant 2/3 and Plant 6 areas can not reach surface water exposure points west of the Production Area in 1,000 years through lateral migration.

The Multiphase Subsurface Transport Simulator (MSTS) Code, which is capable of modeling flow and transport under variably saturated conditions, was used to assess whether flow and transport predictions made assuming full saturation provide larger estimates of flux (err on the conservative side). It was concluded that when lateral transport is a concern, assumption of fully saturated conditions produces higher estimates of lateral flux than assumption of partial saturation.

Based on the comparison of the saturated model to the unsaturated model it was concluded that a saturated three-dimensional (3-D) model can be used to reasonably assess plume migration through the GO/UGMAS. However, because lateral plume migration is insignificant in relation to vertical plume migration a one dimensional transport code is adequate. It was also concluded that a one-dimensional vertical transport code (e.g., ODAST) can be used as the main modeling tool for Constituent of Potential Concern (CPC) screening, simulating baseline conditions, and Preliminary Remediation Goal (PRG) development in the glacial overburden. Simple analytical models (e.g., ECTran) will be used to supplement ODAST to screen and evaluate the impact due to lateral (as well as vertical) migration of contaminants in the perched water zone of the GO/UGMAS.

1.1 Objectives

The overall objectives associated with the development of a 3-D GO/UGMAS model were:

1) Assess the significance of lateral contaminant transport for the purpose of determining the optimal approach to GO/UGMAS modeling for the Remedial Investigation/Feasibility Study (RI/FS). In areas where heavy loading occurs and a high potential for lateral migration exists, model simulations will be conducted to investigate the relative significance of lateral and vertical transport. These model simulations in conjunction with interpretation of field data will be used to provide a sound basis for the use of one-dimensional (1-D) vertical models at these locations to support the RI/FS decision process.

2) Support RI/FS studies and remedial design efforts for assessing the significance, where judged appropriate, of lateral transport from multiple sources under natural or induced flow conditions.

3) Provide a level of conservatism that is appropriate for the RI/FS risk assessment process.

This report summarizes the development of the 3-D GO/UGMAS model. The primary objective of the current model development is to determine the most efficient modeling approach for: (1) CPC screening in the groundwater pathway; (2) estimating the future impacts of perched groundwater contamination on the GMA for the CERCLA/RCRA Unit 5 (CRU-5) RI baseline risk assessment; and (3) perched groundwater PRG development for CRU-5 FS. All the available stratigraphy and geological information collected in the past and preliminary results (i.e., soil-type-specific slug test results and perched groundwater table contours) from recently completed field hydraulic studies in the glacial overburden were used to determine the 3-D model grid and flow model parameters. Contaminant information in the perched groundwater zone was also used to select the predominant constituent of concern and its current conditions for transport simulation. The transport simulation using the Phase I 3-D GO/UGMAS model quantified and compared the long-term lateral and vertical migrations of uranium-238 from two major source areas of perched groundwater contamination at the FEMP.

Since the GO/UGMAS model is only calibrated to steady-state conditions for simulating the long-term no action scenario, further improvements of the GO/UGMAS model are required for simulating remedial actions. If pump and treat of perched groundwater is selected as the main remedial alternative for the contaminated glacial overburden the GO/UGMAS model will need to be calibrated to pumping conditions.

SECTION 2

TECHNICAL APPROACH

Figure 2-1 outlines the process which was followed for development of the GO/UGMAS Model. At the time that the modeling process began it was recognized that additional hydraulic data was needed (hydraulic conductivity, yield estimates, etc.) from the glacial overburden to better understand and properly conceptualize flow and transport processes. The collection of this additional data (Till Hydraulic Studies) was integrated with the GO/UGMAS model development process.

The GO/UGMAS was modeled as a saturated system using the three dimensional SWIFT code (primary code). The impact that the assumption of full saturation has on flow was assessed using the MSTS code (auxiliary code) in a cross-sectional mode. This code was selected through a screening process which is described in the Glacial Overburden/Upper Great Miami Aquifer Modeling Improvement Technical Approach/Work Plan (Parsons 1993b). Preliminary results from the Till Hydraulic Studies were used in the assessment process to establish preliminary conceptual model boundary conditions and to construct a model mesh for code verification. The result of the assessment process is identified in Figure 2-1 as, "Preliminary Model Development and Code Cross-Verification (Primary and Auxiliary)".

Once it was understood that saturated and unsaturated approaches would produce similar flow fields, the primary model (SWIFT) underwent final steady-state flow calibration. By the time this calibration step was reached, final results from the Till Hydraulic Studies were available. These results were used to finalize the conceptual model, boundary conditions, and input parameters. Uranium transport simulations were then conducted using the calibrated primary model.

2.1 Two-Model Approach

After consideration of the hydrologic features of the GO/UGMAS and the scale of the problem, it was decided to use a two-model approach. This approach consisted of using a saturated code for the primary 3-D model (SWIFT) and a more complex (and presumably more physically realistic) unsaturated code (MSTS) for two-dimensional (2-D) cross-sectional simulations. The unsaturated code was then used to assess the impact of assumptions made with the saturated code. The assumptions only affect the flow portion of the modeling. This approach was adopted to demonstrate that the saturated and unsaturated approaches produce similar flow fields, and therefore that the solute transport solutions will be similar for both. For this reason, flow results for saturated and unsaturated conditions were compared. This "cross-verification" was performed by running the unsaturated code for a particular cross-sectional flow problem, and then solving the same flow problem by running the saturated 3-D code in a 2-D cross-sectional mode. Close agreement of results (see Subsection 5.4 and Figures 5-2, 9B, and 10B) indicate that the assumptions and use of the saturated code are justified.

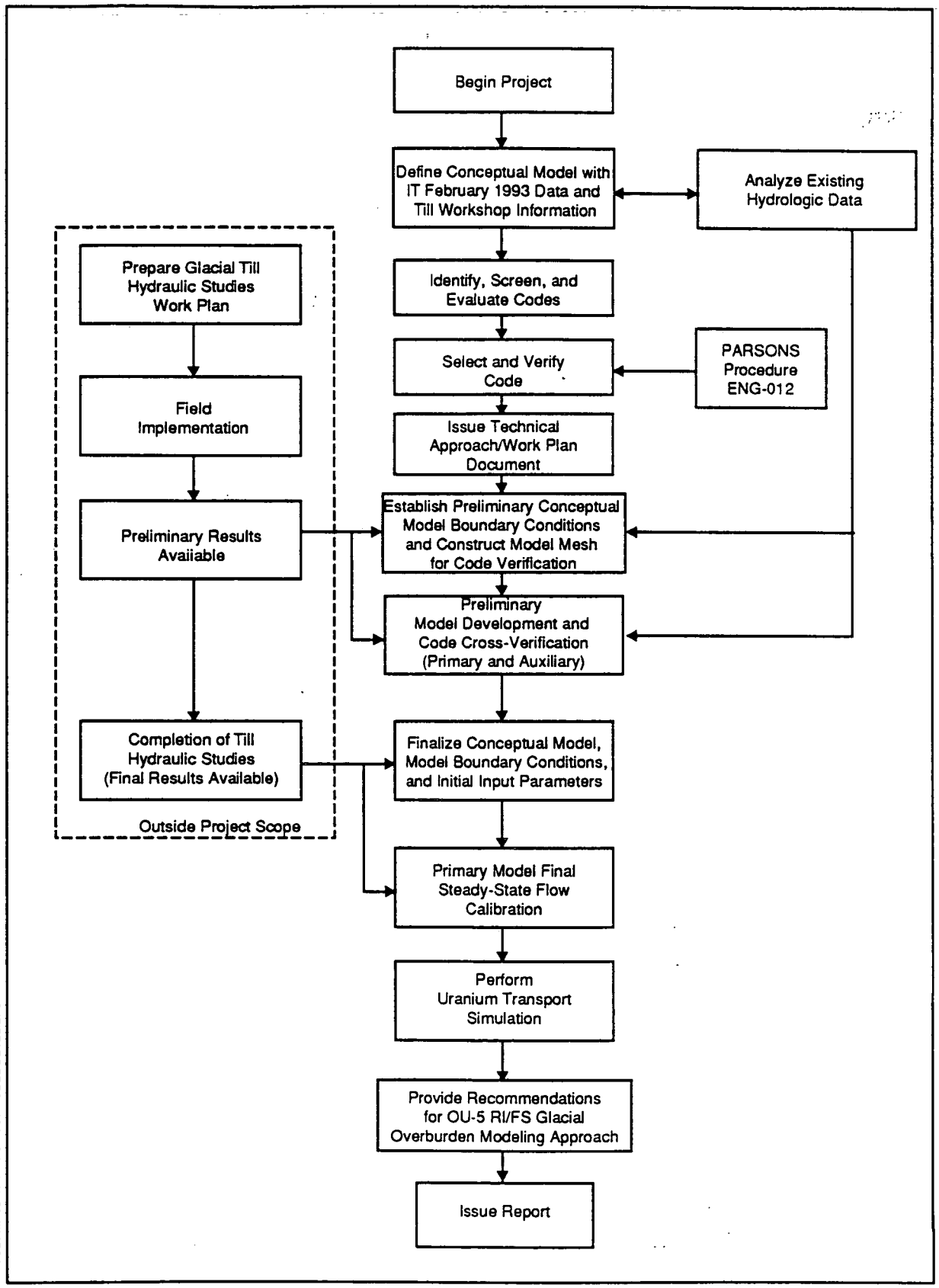

Figure 2-1 - GO/UGMAS Model Development Process Diagram

There are several factors that led to the described two-model approach. During April 15-16, 1993, the Fernald Environmental Management Project (FEMP) Industrial Workshop "Characterization of the Vadose Zone" (DOE 1994) was held. One of the conclusions reached at this workshop was that the glacial overburden at the FEMP is saturated with a perched water table within a few feet of the ground surface (see Figure 10C for contour map of perched groundwater surface, and Figures 1B and 5B for cross-sections). The Upper Great Miami Aquifer (UGMA) underlying the glacial overburden is unsaturated, however. A conclusion of the workshop was that if appropriate assumptions (described in Section 3) were made to conservatively account for transport through the unsaturated GMA, a saturated code could be used to simulate the variably saturated GO/UGMAS. In addition to the workshop conclusions, it was also recognized that unsaturated codes require functional specifications of hydraulic conductivity versus moisture content. The parameters typically used in such soil characteristic curves may be highly variable, difficult to measure, and are generally unavailable for the FEMP site.

Finally, because the area of interest is rather large (roughly 2,500 acres) and the GO/UGMAS model output serves as input for the saturated GMA Model, it was desired to use the horizontal grid of the GMA Model (120 by 112) for the GO/UGMAS Model. Because of the large variation of hydraulic conductivity with soil moisture content and the high degree of nonlinearity this produces in an unsaturated code, vertical grid discretization would need to be sufficiently fine to obtain accurate answers. This would lead to an excessively large grid which, when coupled with the numerous iterations required for the nonlinear solution, would lead to run times on the order of hundreds of hours for an unsaturated flow solution.

It was decided that the use of an unsaturated code on the scale of interest needed for the FEMP is impractical. An unsaturated code, constructed to a smaller 2-D scale, would be used to assess the accuracy of the saturated approach.

2.2 Selection of the Auxiliary Unsaturated Code

A screening of candidate unsaturated codes was performed during the development of the work plan for the GO/UGMAS Modeling Improvement Task (PARSONS 1993a). A list was developed of unsaturated codes that meet criteria established for the selection of the auxiliary code. At the outset, selection criteria for the auxiliary code were more restrictive than was ultimately necessary. Primary selection criteria included: (1) the code must be capable of simulating both saturated and unsaturated conditions; (2) the code must be verified and peer reviewed; (3) the code must be able to simulate 3-D flow; (4) the code must be able to simulate flow through fractures; and, (5) the code must be able to simulate both steady-state and transient conditions. Secondary selection criteria included: (1) the ability to simulate chemical transport including the effects of dispersion, adsorption, and source and solute decay; (2) the ability to simulate mass transport in multiple phases (e.g., liquid and gas); (3) the method of domain discretization should include the finite-difference method to be compatible with the existing SWIFT GMA model; and (4) the code should be widely used by groundwater modelers.

Several codes were identified that are capable of simulating 3-D unsaturated groundwater flow and chemical transport (PARSONS 1993a). A partial listing of these codes includes: 3DFEMWASTE/3DFEMWATER (Yeh 1987 and 1992), FLAMINCO (Huyakorn 1985), and 3-D SUFM/ 3-D SUTM (Segol 1975 and 1976) to name a few. However, only the MSTS code developed by Battelle Pacific Northwest Laboratory (Nichols and White 1993, and White and Nichols 1993) met all the primary selection criteria. MSTS met all the secondary selection criteria except for having an established reputation for being a widely used code by groundwater modelers. This was believed to be a consequence of its recent development.

2.3 Selection of the Primary Saturated Code

The SWIFT code was selected as the primary code for the full 3-D GO/UGMAS Model. SWIFT was designed specifically for uranium transport modeling, has a long history of use at the FEMP, and has been extensively verified and peer reviewed. Compatibility between the GO/UGMAS and GMA Models was also an important factor in the selection. Because the existing GMA Model uses SWIFT, use of the same code for GO/UGMAS facilitates linkage between the two models. With SWIFT, it is also possible to integrate the two models into a single model of the glacial overburden and aquifer if determined necessary.

2.4 Preliminary Development of the Primary and Auxiliary Models

Preliminary development of the primary and auxiliary models focused primarily on the model grid and layer designs. Information for defining stratigraphy of the modeling area was available from cross-sectional maps produced in previous work, but some needed hydraulic data (hydraulic conductivities, soil moistures, yield estimates) were not yet available. At the time that the modeling process began it was recognized that additional hydraulic data was needed from the glacial overburden to better understand and properly conceptualize flow and transport processes. The collection of this additional data (Till Hydraulic Studies) was integrated with the development of the GO/UGMAS model. Available results from the Till Hydraulic Studies were integrated with existing data to establish preliminary conceptual model boundary conditions and to construct a model mesh for code verification. Final calibration of the primary model (described in Section 6) was initiated after the completion of the Till Hydraulic Studies.

Some of model parameters needed for the preliminary development of the primary and auxiliary models had to be estimated (hydraulic conductivities, soil moistures, etc.). Estimates were made based on preliminary calibrations or literature values. Using estimates for some model parameters allowed the assessment portion of modeling project to move forward while the remaining data needed for the final calibration of the primary model was being collected.

For SWIFT, initial model development consisted of producing grid generation routines that transformed the latest Environmental Resource Management Analysis (ERMA) surface, isopach, and geologic maps into a 3-D grid with zoned material properties reflecting the distribution of soil types. The properties attached to each soil type were estimated using the best available data at the time. Likewise, initial estimates were made of recharge and internal sources/sinks, and initial assignments of other boundary conditions were made.

For MSTS model development, a 2-D cross-section of the preliminary 3-D GO/UGMAS grid was selected. The cross-section chosen was a cut along Row 80 (Y = 9937.5 feet) of the 3-D SWIFT finite-difference grid. Initial soil properties, boundary conditions, and sources/sinks were taken from the initial 3-D model development. Results for the auxiliary model initial development show the capability of MSTS to provide the necessary cross-verification for the SWIFT 3-D GO/UGMAS Model.

2.5 Cross-Verification of the Modeling Codes

Because of its capability to simulate unsaturated conditions (UGMA is unsaturated), MSTS modeling results represent more realistic flow conditions in the GO/UGMAS than SWIFT which was developed for saturated flow only. The assumption of full saturation is required in order to model the GO/UGMAS using SWIFT. The purpose of cross-verification between the preliminary SWIFT and MSTS models is to evaluate the impact of the assumption of full saturation in the final SWIFT model. This comparison was conducted by simulating flow conditions in a representative cross-section of GO/UGMAS with both codes.

The 2-D cross-verification was performed along a cross-section (A-A') cut diagonally across the 3-D GO/UGMAS grid in an east-west direction. (This is shown in Figure 4-2.) Cross-section A-A' was chosen because it cuts across both the sand body underlying the production area and the uranium-238 plumes used as initial conditions for the 3-D 1,000-year transport run described below. For the MSTS flow runs, values of some hydraulic conductivities were changed to produce the best possible fit of calculated and measured water tables along the cross-section. Parameters for soil characteristic curves were determined from literature data on soils similar to those found in the FEMP GO/UGMAS. Once the MSTS flow run for A-A' was finalized, the SWIFT GO/UGMAS model was run for the same cross-section and the same set of input parameters. This process and results are further discussed in Sections 4 and 5.

2.6 Primary Model Final Steady-State Flow Calibration

The final steady-state flow calibration of the 3-D GO/UGMAS model was initiated when results of the Till Hydraulic studies in the glacial overburden were available. During the final calibration, the preliminary 3-D model grid was refined and model parameter values were adjusted based on the results

of field studies. The objective of this calibration was to incorporate all the available hydrogeological information on the glacial overburden into a 3-D model which can simulate the flow condition in the GO/UGMAS.

The saturated code SWIFT was used to develop the 3-D GO/UGMAS model. A special calibration procedure was required to match the saturated model output with the measured saturated/unsaturated conditions. In order to calculate both a perched water table position near the top of the overburden and the discharge of water out the bottom of the model and into the GMA, a positive pressure condition must be specified at the bottom GO/UGMAS boundary. This boundary, however, coincides with the unconfined, steady-state water table of the GMA, where the pressure must be equal to zero (see Figure 3-1). Therefore, the specified positive bottom pressure in the GO/UGMAS model cannot be physically realistic and a typical calibration (specify fixed boundary conditions, vary conductivities and/or infiltration rates to match a measured water table) cannot be performed. When the measured water table is used to establish a hydrostatic condition at the bottom surface and then top surface recharge is added, the calculated water table is too high. An iterative procedure (which adjusts the top surface used to define water column height) was devised so that the calculated water table converges to the measured surface. This calibration procedure was also used in the preliminary model development and cross-verification calibrations of the SWIFT model.

2.7 Evaluation of Lateral Plume Migration with the 3-D GO/UGMAS Model

To assess lateral plume migration and determine the optimal modeling approach for CPC screening, long-term baseline simulation, and PRG development in the RI/FS, a 3-D flow run and 1,000-year uranium-238 transport run were performed using the 3-D GO/UGMAS Model. The flow results are from the final calibrated primary model. The transport run started from initial measured uranium-238 plumes in the soils and perched groundwater beneath Plants 2/3, 6, and 9. These plumes have the highest measured perched groundwater concentrations of uranium-238 in the GO/UGMAS. The initial plumes in the Plant 2/3 area are located near the center of the FEMP production area in an area where a larger concentration of coarser grained sediment (sand and gravel) occurs (see Section 3). These coarser-grained sediments provide the highest potential for lateral migration. The sediments underlying the Plants 6 and 9 are degraded (weakened by acids) and are not an effective barrier. Therefore, these initial plumes represent sources of the highest potential future impacts from contaminated perched groundwater to the GMA and surface water bodies. All the transport parameters in the model are selected so that the model can produce conservative estimates of the extent of uranium-238 migration.

In typical cases of low molecular diffusion, the ratio of lateral to vertical transport is dependent mainly upon mechanical properties of the porous medium (dispersivity and pore velocity) rather than constituent-dependent parameters. This means that the ratio of lateral to vertical transport seen in the uranium run

is indicative of the ratio that would be seen for other constituents from the same source area. Therefore, no other constituent was simulated during the model development.

2.8 Linkage of the GO/UGMAS and GMA Models

The use of SWIFT for both the GMA and GO/UGMAS Models facilitates linkage between the two. The linkage consists of using constituent mass loading histories (mass per unit time) exiting the bottom of the GO/UGMAS Model as input to the top of the GMA Model. Mass loading histories to be used as input to the GMA Model can be obtained directly from SWIFT output files created at the option of the user. A post-processing code translates the mass loading histories in this SWIFT file into loading input cards to be integrated into the GMA model input file.

Optionally, the GO/UGMAS and GMA Models could be integrated into a single model. This would require only a moderate amount of modification to the two models since they both use the same grid. However, this linkage was not established since the major concern was contaminant migration within the GO/UGMAS.

SECTION 3

HYDROGEOLOGICAL CONDITIONS AND CONCEPTUAL MODEL

The GO/UGMAS refers to the vadose zone beneath the FEMP which extends from the ground surface to the water table of the GMA. A major portion of the glacial overburden is saturated. Saturation begins approximately 3 to 5 feet below the ground surface. Groundwater in the glacial overburden is perched above the water table of the GMA. Approximately 20 feet of unsaturated sand and gravel exists between the base of the overburden sediments and the water table of the GMA. Therefore, the vadose zone (in descending order) consists of up to 60 feet of glacial overburden material overlying approximately 20 feet of unsaturated sand and gravel. A general profile of pressure head relative to depth is presented in Figure 3-1. Both the water table in the perched groundwater system and the underlying GMA are unconfined.

3.1 Hydrogeological Conditions

Figure 3-2 illustrates the major hydrogeological features of the GO/UGMAS. Perched groundwater is encountered in the glacial overburden at a depth of 3 to 5 feet below the ground surface. The movement of groundwater within the overburden sediments occurs in both primary and secondary pathways. For the purpose of this modeling study primary pathways refer to pathways created by coarser grained sediments contained within the finer grained clays, and secondary pathways include such features as fractures, root tubes, and bioturbation. Data collected at the FEMP and data reported in the literature for similar hydrogeologic environments indicate that secondary pathways tend to dominate groundwater movement at shallow depths and primary pathways dominate the movement of groundwater at greater depths. The transition between the two is evidenced in the field by a reddish-brown to blue-gray color change noted in the overburden sediments. No lithologic or depositional differences are evident in sediments above the color change compared to sediments below the color change. The color change is believed to be the result of iron oxidation caused by infiltrating groundwater.

5489

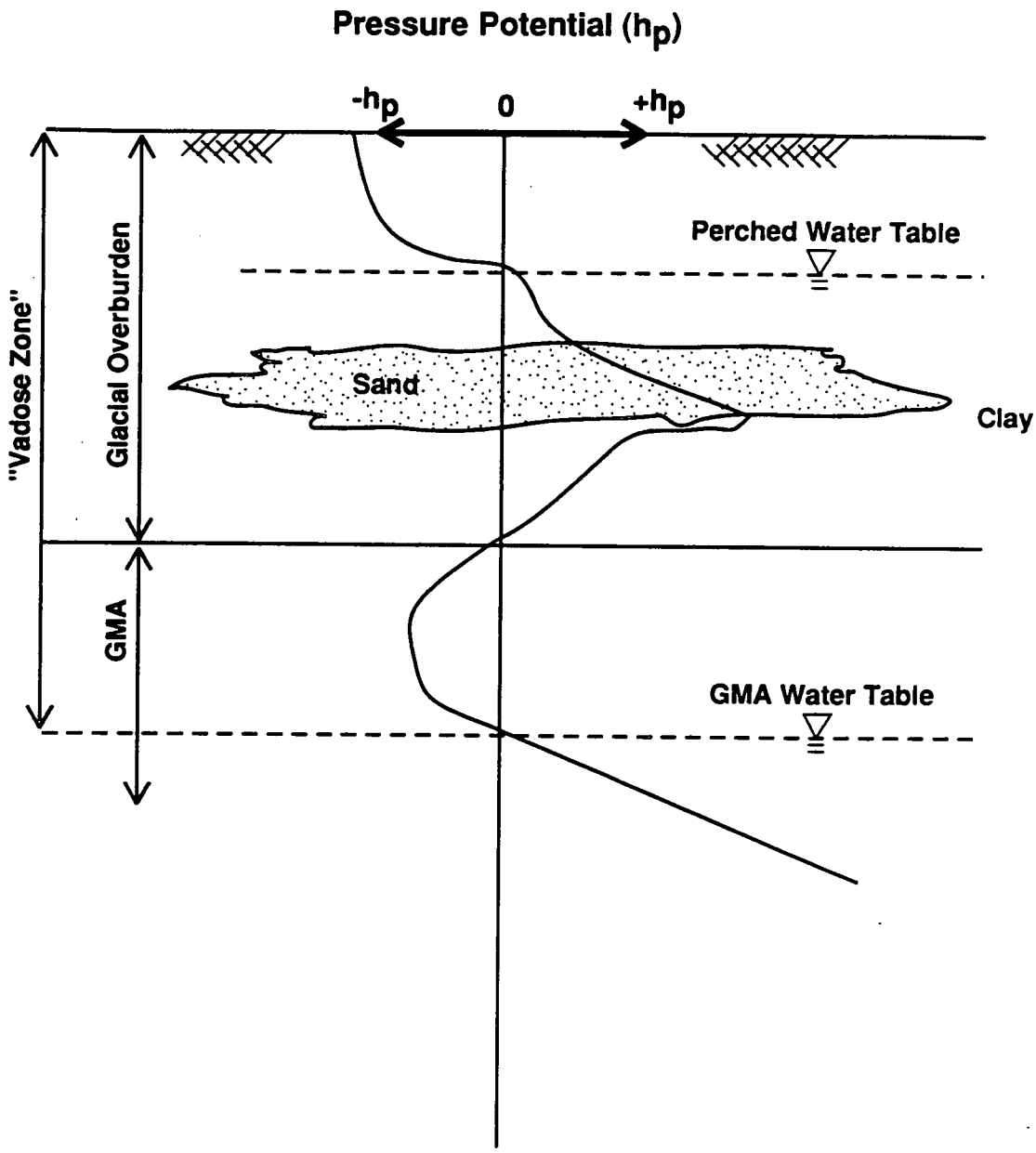

Figure 3-1 - General Pressure Head Profile

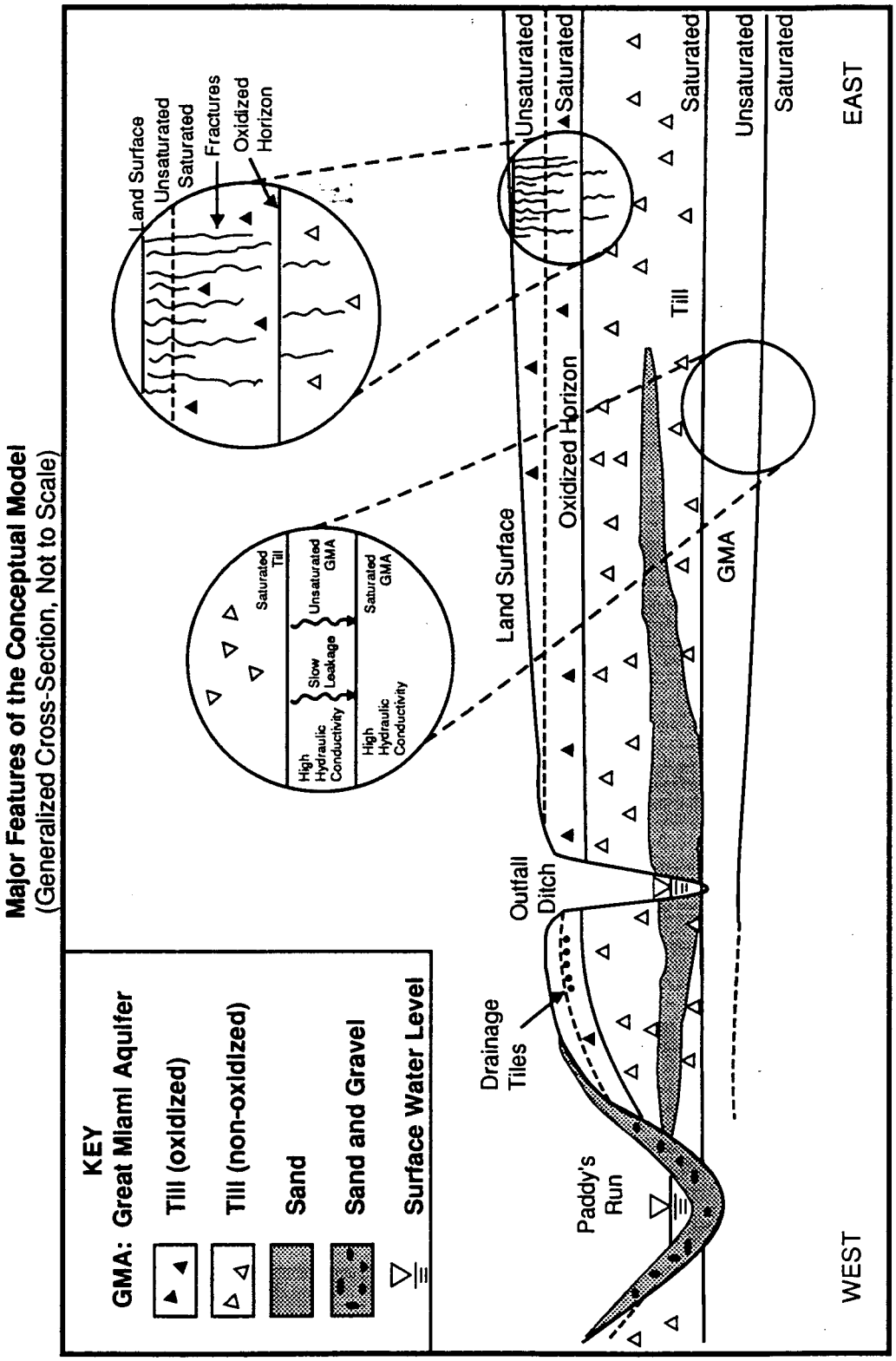

Figure 3-2 - Major Features of the Conceptual Model

3.1.1 Major Coarser-Grained Sediment Zone

Figure 3-3 is a map which illustrates where most of the coarser sediment (sand and gravel) within the glacial overburden is located. The highlighted areas do not represent contiguous units of sediments. The highlighted areas simply indicate where most of the coarser grained material is located (i.e., laterally discrete deposits treated as net deposits). The dark heavy line outlines the extent of a basin feature. The map indicates that most of the coarser grained material is present within the basin feature or trends to the basin from the north. Within the basin feature itself, coarser grained sediment is located along the northeast rim. This implies that the source of sediment entering the basin was also to the northeast. Sediments under the western portion of the FEMP have been interpreted as being lacustrine. Sediments under the eastern portion of the FEMP are interpreted as being predominantly glacial till. The glacial till beneath the eastern portion of the FEMP consists mostly of clay, but contains pockets of silt, sand, and gravel. No evident depositional pattern or features are recognizable to the east.

A larger percentage of coarser grained material (silt, sand, and gravel) is found in the lacustrine sediments beneath the western portion of the FEMP than within the till beneath the eastern portion of the FEMP. These coarser grained sediments could interconnect and create lateral or stair step pathways for the movement of groundwater through the glacial overburden. The potential for such a pathway is greater beneath the western portion of the FEMP.

3.1.2 Near Surface Weathered Zone

Near surface fracturing within the glacial overburden sediments beneath the FEMP has been observed. Fracturing at depth has not been observed. Smearing along the sides of the boreholes, though, often masks the physical evidence of fractures, and the vertical orientation of drillholes decreases the probability of encountering a fracture. The density of fractures observed in the near surface at the FEMP is believed to decrease with depth. This belief is consistent with reports that the upper layers of clay-rich till deposits are typically weathered and fractured and that the secondary porosity features increase the low-hydraulic conductivity of the deposits (McKay et al. 1993). When fractures are present, they can dominate groundwater flow and greatly increase the potential for rapid lateral or vertical migration of fluids. Although direct evidence of fracturing is elusive at the FEMP, indirect evidence is present.

Oxidation color changes, noted in the field, are perhaps the best indirect evidence for fracturing. The oxidation of iron causes overburden sediments to change from a bluish-gray color to a reddish-brown color. The blue-gray color is due to trace amounts of iron in the soil that are in the ferrous (Fe^{+2}) oxidation state. As weathering takes place, the ferrous iron is converted to ferric iron (Fe^{+3}), a hydrous oxide of iron that colors the soil brown. The oxidation of the iron is probably assisted by bacteria in the soil, although it could be due to a simple chemical reaction. Regardless of the process, the presence of brown coloration is evidence that oxygenated groundwater is circulating to that depth.

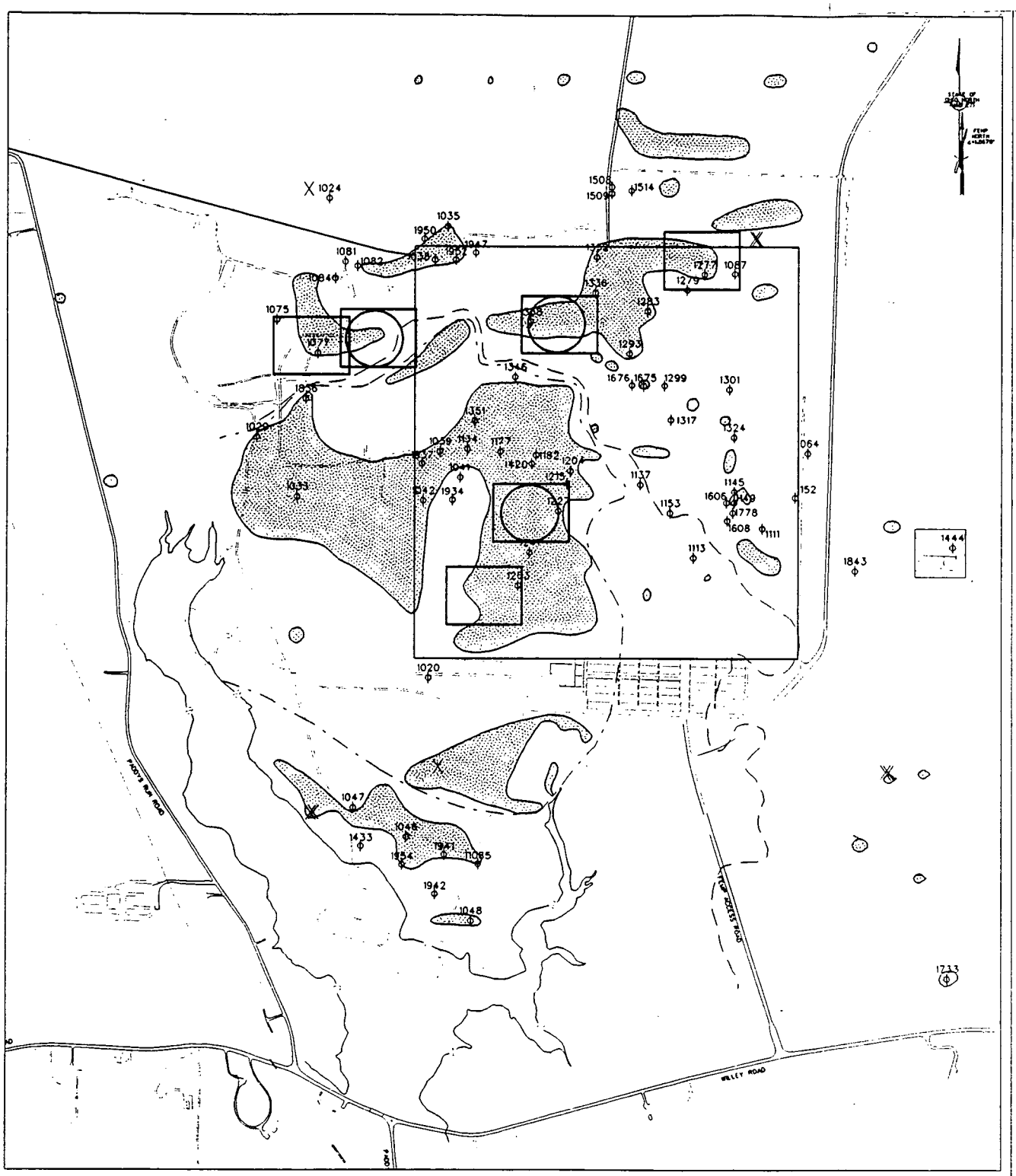

Figure 3-3 - Distribution of Coarser-Grained Sediment Bodies

Groundwater is probably circulating deeper, but because it is depleted in oxygen, it does not cause additional iron oxidation. The bottom of the reddish-brown oxidation front is typically defined by a 1- to 2-foot-thick transition zone in which gray clay material exhibits mottled brown stringers in the clay-rich material. Brown staining also diffuses outward from the stringers a short distance. The fact that the brown coloration is strongest along stringers is an indication that secondary permeability enhances groundwater circulation in the upper clay-rich portions of the glacial overburden and facilitates infiltration of surface water into the glacial overburden.

The depth of active infiltration is probably controlled by secondary porosity features (desiccation fractures, bioturbation, etc.) As the density of the secondary porosity features decreases with depth, infiltration slows down. As the infiltration slows down, the oxidation of iron also slows down. Given enough time the brown oxidation front, in theory, would progress deeper and deeper into the underlying saturated gray sediments. In a relative sense though, infiltration into the gray sediments is low compared to the infiltration in the brown sediments because the gray sediments lack as many secondary porosity features as the brown sediments do.

Profiles of volumetric moisture content indicate that the moisture content of the glacial overburden sediments generally decreases with depth. Work completed in the northeast corner of the production area indicates the following profile:

DEPTH	AVERAGE
0 to 10 feet	14.0%
10 to 20 feet	11.8%
20 to 30 feet	11.5%

Data collected along the northern and eastern FEMP boundary indicates the following profile:

DEPTH	AVERAGE
0 TO 10 feet	17.3%
10 to 20 feet	15.5%
20 to 30 feet	14.4%

3.1.3 Physical Properties of Gray Clay

Within the glacial overburden it is the low permeability of the gray clay that controls the potential for movement and creates the perched groundwater system. The porosity of the gray clay has been determined from density measurements performed on core samples collected with Shelby Tubes. Porosity calculations range from 16.03 percent to 20.28 percent with an average porosity of 17.2 percent. Porosity ranges for glacial till have been reported to be between 10 percent and 20 percent (Fetter 1988, pg. 68).

The moisture content of the gray clay located beneath the FEMP has been determined using core samples collected with Shelby Tubes (DOE 1994). Moisture content measurements range from 10.3 percent to 25.4 percent with an average moisture content of 14.3 percent.

3.1.4 Hydraulic Conductivity

Slug tests have been performed in the glacial overburden at the FEMP. Data from 70 of these tests have been grouped according to the sediment types and increasing hydraulic conductivity. Table 3-1 presents the geometric means for the sediment groupings.

Table 3-1 - Hydraulic Conductivity Geometric Mean by Sediment Group

	Hydraulic conductivity	
Group	**feet/day**	**cm/s**
Brown clay	1.0×10^{-1}	3.59×10^{-5}
Gray clay	5.30×10^{-3}	1.87×10^{-6}
Brown silt	2.8×10^{-1}	9.88×10^{-5}
Gray silt	2.5×10^{-1}	8.83×10^{-5}
Brown sand	5.0	1.75×10^{-3}
Gray sand	2.3	8.04×10^{-4}
Brown gravel	8.7×10^{1}	3.07×10^{-2}
Gray gravel	1.1×10^{1}	4.03×10^{-3}

During the calculation and interpretation of slug test data, the location of the well screen relative to the sediment type and water level in the well was compared to determine whether the well behaved according to confined or unconfined conditions. If the water level in a well completed in sand rose above an upper confining unit of clay it was considered confined. It was noted that the water level in wells which were completed in clay did not rise above the clay so they were considered unconfined. Wells completed in silt, sand, or gravel, with a few exceptions, behaved as if they were confined. This data suggests that the clays are controlling the potential for fluid movement within the glacial overburden at the FEMP. Furthermore, even though coarser sediments are present in the overburden, they are surrounded by the finer-grained sediments and therefore behave as if they are confined.

Three pump tests were conducted in the glacial overburden for the purpose of determining hydraulic conductivities and the degree of hydraulic interconnection found within the overburden sediments. The

tests were conducted in areas of the FEMP that contain saturated, coarse-grained sediments. The hydraulic conductivity calculations are therefore biased to sand and gravel with enough permeability to yield water for a pump test. Table 3-2 presents hydraulic conductivities for various coarse-grained sediments calculated from pump tests.

Table 3-2 - Hydraulic Conductivity of Coarse-Grained Sediment

Area	Hydraulic (feet/day)	Conductivity (cm/s)	Storativity
Plant 1 pad	15.1	5.3×10^{-3}	0.006
Plant 2/3	23.8	8.4×10^{-3}	0.005
Waste pit	4.3	1.5×10^{-3}	0.004

Drawdown trends from the pump test correlated with coarse grain sediment trends.

3.1.5 Yield

Seven areas of the glacial overburden (Figure 3-3) were pumped to determine the rate at which and length of time during which they would supply water to a well. Areas were selected for testing based upon the amount of coarser grained sediment present and upon the apparent presence of a readily obtainable amount of groundwater. The purpose of pumping was to determine how much water the sediments would yield before a well went dry. It is assumed that a large, interconnected flow system should be able to yield water to a well faster and longer than a small, discontinuous system.

The results of the yield tests indicate that the calculated, sustainable discharge from the glacial overburden ranges from less than 1 to 2.5 gallons per minute.

3.1.6 Flow Directions and Potentials

The heterogenous nature of the glacial overburden complicates the interpretation of flow direction (Figure 3-4). As explained above, silts, sands, and gravels found within the overburden exhibit confined conditions whereas clay exhibits unconfined conditions. Yield test results indicate that the clays control the migration of water. Field observations indicate that groundwater is generally encountered within the overburden at a depth of 3 to 5 feet below the ground surface. Water table data contoured in Figure 3-4 depicts a heterogeneous, anisotropic system as homogenous and isotropic.

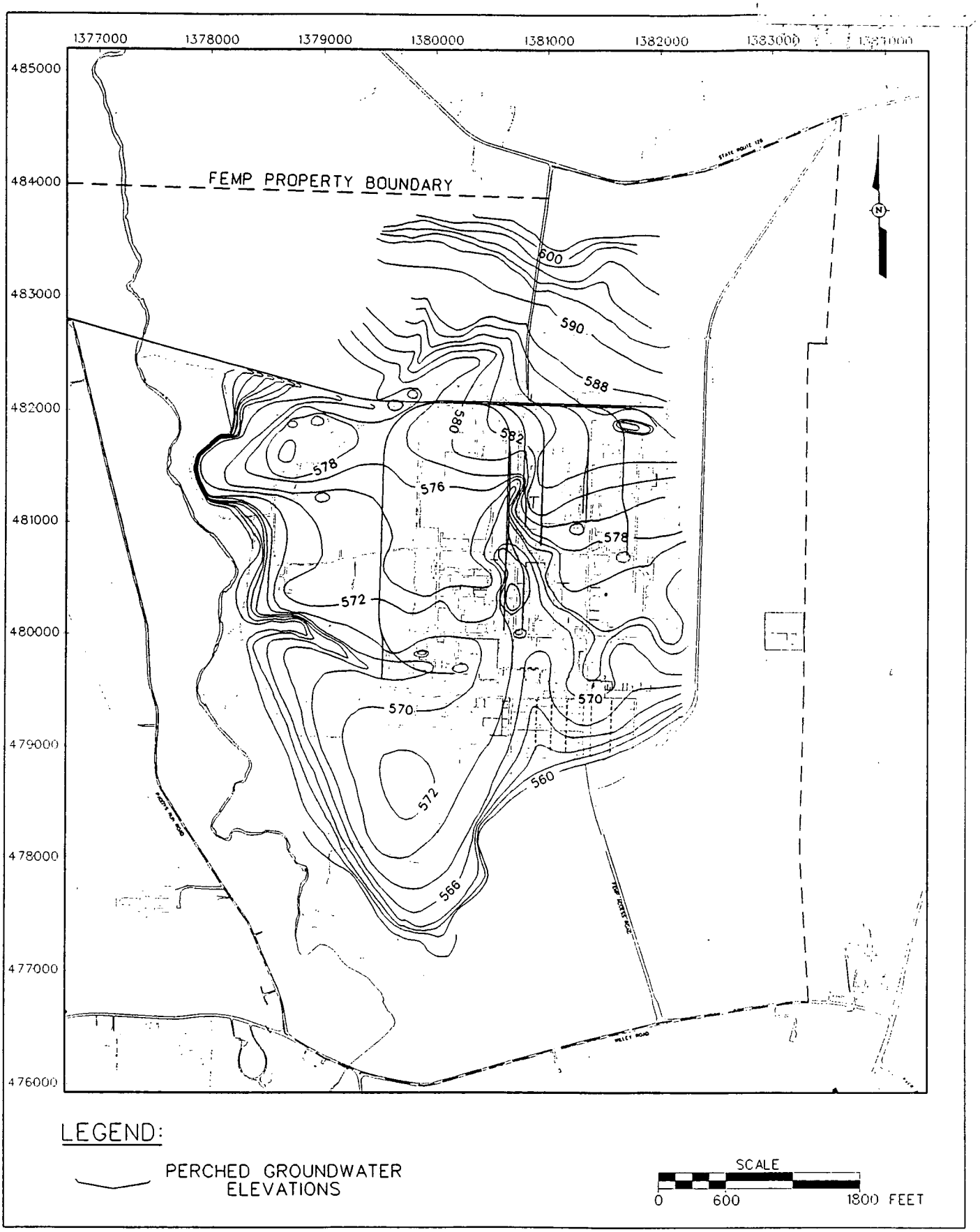

Figure 3-4 - Average Perched Groundwater Elevations

3.2 Generalized Stratigraphy of the Conceptual Model

There are multiple potential pathways from any near-surface waste source downward to the GMA. These pathways include:

1) Vertical infiltration through the clay layers to the unsaturated GMA

2) Vertical infiltration through the clay layers to a sand lens, migration laterally along the sand lens to other deeper lenses which could connect to the GMA

3) Vertical infiltration through the clay layers to a sand lens, laterally along the sand lens which connects to Paddys Run (or the outfall ditch), and from the stream to the GMA

Figure 3-5 shows the conceptual model. The conceptual model is based upon field data and conclusions reached at the FEMP Industrial Workshop (DOE 1993a). This conceptual model simplifies the major features shown in Figure 3-2 and was designed so that transport and risk estimates would not be underestimated. The conceptual model consists of five layers. Layer 1 is the oxidized and fractured near surface glacial overburden (brown clay). This layer was included to provide a free surface for the saturated zone.

Layer 2 consists of non-oxidized saturated glacial overburden. Layer 3 is either modeled as saturated sand or clay. Lateral transport would primarily take place within this layer. Lateral flow along this layer could discharge into surface drainage features (Outfall Ditch or Paddys Run). Layer 4 consists of gray clay. At specific locations, this layer may consist of more permeable soils (sand) representing a more permeable pathway to the upper GMA. Layer 5 is the bottom layer of the model. It consists of unsaturated GMA sands. The bottom boundary of Layer 5 is the water table of the GMA.

It should be noted that in a few spots the actual model grid deviates from the conceptual model. In several locations the measured oxidized horizon dips below the bottoms of layers 2 and 3, resulting in the presence of more than one layer of fractured clay.

The flux through the bottom of Layer 5 couples to the GMA SWIFT model in that it forms the upper boundary condition to the saturated GMA. This technique builds conservatism into travel times but, more importantly, it eliminates the calculational and conceptual problems of saturated and unsaturated flow boundaries. Measurements from the Glacial Till/Vadose Zone Hydraulic Investigations field work were used to refine the conceptual model. The hydraulic characteristics of the various lithologic units found within each layer of the model are varied to simulate the degree of interconnection between the surface and the underlying GMA.

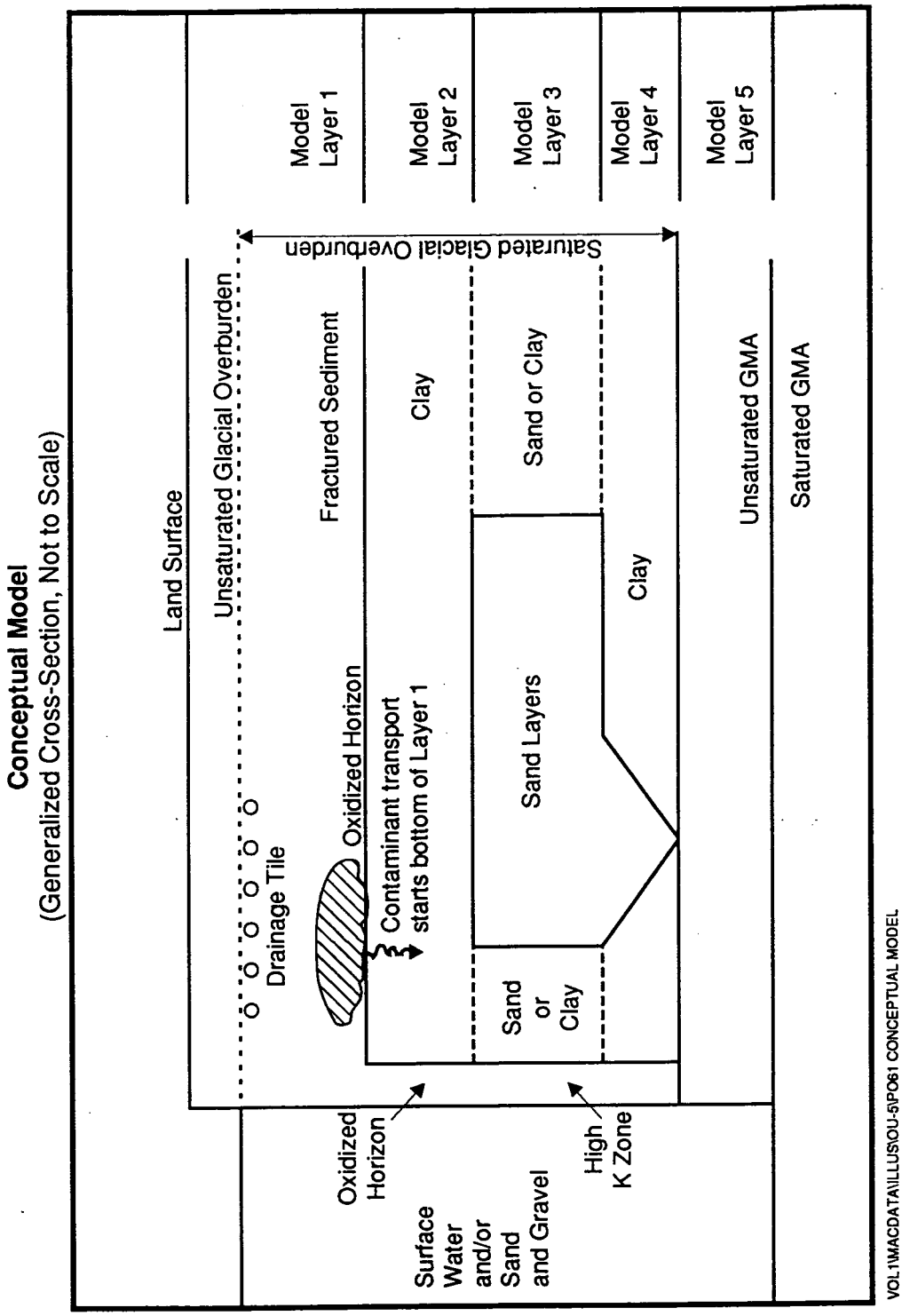

Figure 3-5 - Conceptual Model

Primary Assumptions in the Conceptual Model

The conceptual model creates a conservative simplification of the real system so that it can be effectively modeled. At every point in the modeling process where uncertainty existed, the modeling process proceeded along the most conservative path. The primary assumptions used in creating the conceptual model include:

1) The perched water system contained within the glacial overburden is unconfined.

2) The UGMA sands are assumed to be fully saturated with only vertical transport. Since saturated transport is faster than unsaturated transport under similar conditions, this assumption is a conservative representation of flow and contaminant transport throughout the unsaturated zone. In essence, this layer represents a time delay between the overburden and the saturated GMA which can effectively be simulated with saturated conditions.

3) The upper oxidized zone (Layer 1) was used to allow a free water surface in the model. Layer 1 may be highly fractured and will not provide an effective barrier to transport. Therefore, values of Layer 1 vertical hydraulic conductivity used in the model were increased accordingly. Vertical hydraulic conductivity is greater than horizontal hydraulic conductivity when fractures are present. Again, this is a conservative representation of the system since the model assumed no attenuation in this layer.

4) An equivalent porous medium approach (hydraulic conductivity of sediment accounts for the effect of fractures) was used to account for potential fractures through the glacial overburden. This approach was adopted since the Industrial Workshop suggested it was impractical to calibrate a fracture flow model. Hydraulic conductivities obtained through slug tests represent bulk properties and provide for the effect of fractures. The modeling objectives were on a large enough scale that simulation of contaminant migration through an equivalent porous medium could effectively meet the modeling objectives.

5) Steady state flow conditions were considered adequate to represent flow conditions in the GO/UGMAS. Similar to item 3 above, the modeling objectives were on a large enough time scale that simulation of contaminants moving under steady state flow conditions could effectively meet the modeling objectives.

SECTION 4

PRELIMINARY MODEL DEVELOPMENT

4.1 Preliminary Development of the Primary 3-D Flow Model

4.1.1 Model Grid Construction

The horizontal SWIFT GMA model grid was also used for GO/UGMAS model. This consists of a 120 by 112 block grid composed of 125-foot, square grid blocks. The area of glacial overburden modeled in the GO/UGMAS model was smaller than the area modeled in the SWIFT GMA model, which made it possible to use only a subset of the SWIFT GMA Model grid for the GO/UGMAS calibration and uranium transport runs. This allowed these runs to focus on the areas of the site where contaminant transport potential is highest and where characterization data is most complete. It also had the beneficial effects of shortening run times and saving computer file space. The subset used has its lower left corner at block (17,18) of the GMA grid and the upper right corner is at GMA grid block (91,112). These grid blocks have 1927 State Planar Coordinates of E = 1,380,641, W = 472,123.21 and E = 1,382,776.5, W = 486,923.71, respectively. The resulting grid is 75 by 95 blocks in the horizontal plane and is depicted in Figure 4-1.

For vertical discretization, the ERMA Geologic Information System (GIS) system was used to provide elevations and isopachs on a block-by-block basis. Well and boring data were contoured and overlaid on the horizontal model grid. Values of elevation or thickness were then calculated for each grid block and assigned to the grid block centroid. Geologic maps were also overlaid with the ERMA GIS system to provide soil type flags (integers associated uniquely with particular soil types) on a block-by-block basis. Text files containing the block-by-block information were generated and used as input for a global grid generation program. The grid generation program integrated each surface and isopach file into a single, 3-D grid file. A SWIFT preprocessor then converted the 3-D grid file into input cards, which were assembled into a single SWIFT input file.

In several locations, elevation changes from one grid block to an immediately adjacent block were equal to or greater than the grid block thicknesses. This would result in the absence of an interface between adjacent blocks in the same layer. Another problem was the inversion of surfaces in certain regions; for example, the surface defining the bottom of model Layer 1 was found to be below the surface defining the bottom of Layer 2 in several locations. These two problems, resulting from the highly variable geometry of the GO/UGMAS, were the biggest obstacles to generating a representative 3-D grid. To produce a smoothly varying grid that closely approximated the GO/UGMAS geometry, the following algorithm was used within the global grid generation program:

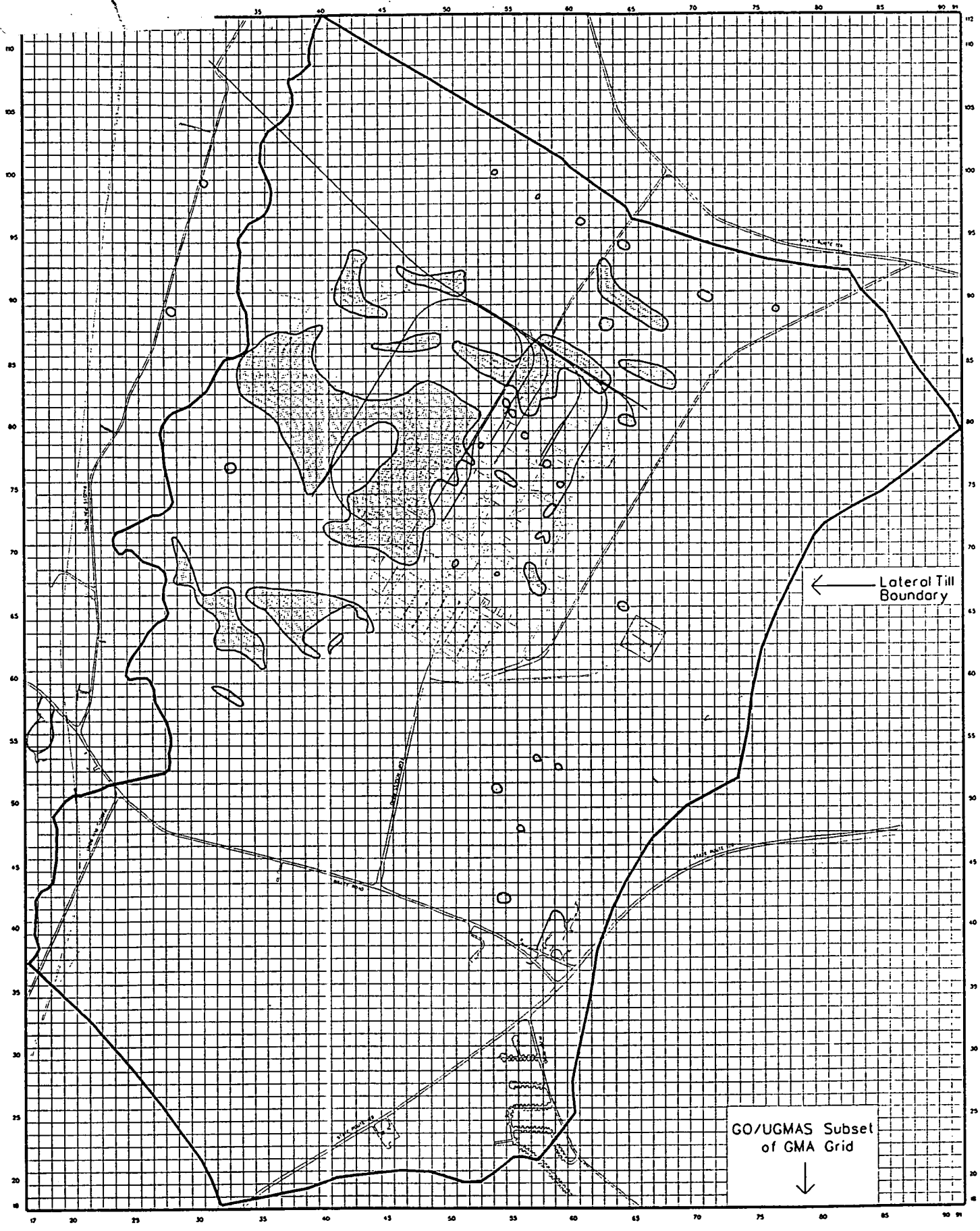

Figure 4-1 - GO/UGMAS Model Grid (Subset of GMA Model Grid)

1) Originally, five vertical layers were defined as being bounded by six surfaces. These surfaces will be referred to as surfaces 1 through 6, with surface 1 being the ground surface and surface 6 coincident with the GMA water table. Figure 4-3 shows an example of the arrangement of the six surfaces, which are represented by the solid black lines separating the different model layers. The second solid line from the bottom was not one of the original six surfaces, but was added later (see step 6). With this scheme, surfaces 1 and 6 were best supported in the ERMA system by field data, and did not need to be altered in any way.

2) A deltaic sand body embedded in glacial till was identified over a limited area in the vicinity of the FEMP production area west to Paddys Run. Because the third model layer was to contain this sand body, elevation relationships in the area were examined closely. Average sediment trends within the sand body region were extrapolated to the rest of the grid, where little vertical variation of soil type within the till exists. For grid blocks within the sand body, the following steps were performed:

   (1) Surfaces 2 through 5 were sorted by elevation, so that surface 2 was closest to ground surface and surface 5 was the lowest. This resolved the problem of local elevation inversions.

   (2) Surface 5 elevation was subtracted from surface 2 elevation to provide the total thickness of layers 2, 3, and 4. The ratios of the distances of surfaces 4, 3, and 2 above surface 5 to the thickness of the entire three-layer sequence was computed for each grid block and averaged over the sand body region. These average ratios were applied later to the entire grid.

   (3) Top and bottom elevations of the sand body were saved for later allocation of sand lithologies.

   (4) The surface 2 elevation originally depicted the weathering horizon. All soil types above the surface are denoted as brown, presumably due to oxidation. Below the surface, soils have not been oxidized and are specified as gray. The original surface 2 was saved for later allocation of brown and gray lithologies.

3) Another pass was made through the entire grid, this time assuming the newly sorted surface 2 and 5 elevations would remain unchanged. Surfaces 3 and 4 were then placed using the average ratios determined in step 2(2) above.

4) With all surfaces now fixed, grid block thicknesses and centroid elevations were obtained by differencing and averaging bounding elevations over the entire horizontal grid. In the region containing the sand body, layer 3 was assigned the lithology flag for sand. Then the sand top and bottom elevations saved from step 2(3) above were compared to the centroid elevations of layers 2 and 4. If the sand body took up more than 50 percent of either layer 2 or 4 based on this elevation comparison, that layer was also assigned the sand flag. In a similar manner, the

original weathering horizon saved in step 2(4) was used to classify soil types as either brown or gray.

5) A minimum layer thickness of 2 feet was enforced to avoid excessively thin layers. If any grid blocks were increased in thickness to 2 feet, the sequence of layers at that particular block was regenerated from the bottom up so that the bottom of the GO/UGMAS Model remained coincident with the GMA steady-state water table. This resulted in the model ground surface being slightly above actual ground surface at a few locations.

6) Finally, a sixth layer was added at the bottom of the model to increase the accuracy of aquifer contaminant loading histories. This was accomplished by splitting a thin, 2-foot layer off the bottom of Layer 5.

Figures 1C through 6C (Appendix C) are areal maps depicting grid block soil type by layer. Table 1C in Appendix C is a key for the layer maps, associating the symbols used with a soil description. The diagonal blank lines in the layer maps show locations of cross-sections cut through the 3-D grid. The shorter of the two cross-section lines, running from upper left-hand to lower right-hand on the maps, is section A-A' which was used for 2-D comparisons of SWIFT GO/UGMAS with variably saturated MSTS runs (i.e., cross-verification).

4.1.2 Flow Parameter Selection

Flow parameters initially input to SWIFT consist of soil properties assigned to the interior of the model, boundary conditions, and internal sources/sinks. Because steady-state flow runs are used to approximate the net effect of transient behavior, the only soil properties required are the components of hydraulic conductivity in the three coordinate directions and porosity. The boundary conditions are a combination of specified pressures, specified recharge, and no-flux conditions. Internal sources/sinks used consist only of specified discharges coinciding with major drainages near the FEMP site production areas. Although the site-specific information available prior to the completion of field hydraulic studies was used, all the values of flow parameters selected in this stage were for the purpose of evaluating and performing cross-verification of the modeling codes only.

4.1.2.1 Soil Properties

To simplify the generation of SWIFT input cards, each soil type identified in the geologic maps was assumed to have the same set of properties throughout its areal and vertical extent. As can be seen from the previous layer-specific soil type maps, twelve different soil types were used. The initially assigned horizontal and vertical hydraulic conductivities (K_h and K_v) and porosities of the different soil types are summarized in Table 4-1. Note that the soil conductivities were assumed to be isotropic in the horizontal plane and a single value of horizontal conductivity was used for each soil type. Initial values of

conductivities were taken from slug test results calculated from the Till Hydraulics Investigation which was being conducted in parallel with the development of the GO/UGMAS model. For each of the soil types, horizontal conductivity was taken as the geometric mean of the analyzed slug test conductivities. Vertical conductivities were calculated using anisotropy factors obtained from a limited set of Neuman Analyses of pump test data. Porosities were estimated from literature values and values used in previous 1-D vadose zone modeling (Schroeder et al. 1988). Porosity does not affect the volume rate of perched groundwater flow in a steady-state simulation and has minor impact on the steady-state calibration.

Table 4-1 - Initial Steady-State Flow Parameters by Soil Type

Soil Type	K_h (ft/day)*	K_v (ft/day)*	Porosity	Description
1	1.E-5	1.E-5	.1	Inactive Block
2	.100	1.	.45	Brown Till
3	.00550	.00110	.34	Layer 2 Gray Till
4	2.30	.0230	.39	Gray Deltaic Sand
5	.00550	.00110	.34	Layer 3 Gray Till
6	.00550	.00110	.34	Layer 4 Gray Till
7	1.E-5**	45.	.39	Upper GMA Sand
8	10.	10.	.35	Paddys Run/SSOD Alluvium
9	10.	10.	.35	Paddys Run/SSOD Streambed
10	.250	.00250	.35	Gray Lacustrine Silt
11	5.00	.0500	.39	Brown Deltaic Sand
12	.280	.00280	.35	Brown Lacustrine Silt

* Multiply by 3.5278×10^{-4} to convert to cm/s

** Low conductivity used to restrict horizontal flow in the unsaturated GMA

4.1.2.2 Boundary Conditions

A specified net recharge was the boundary condition used for the top surface of the model. Figure 7C in Appendix C is an areal map of the initial recharge distribution and Table 2C in Appendix C is the key defining the symbols used in the map. Initial values of recharge were chosen to produce a total

volumetric influx approximately equal to the total volumetric rate of water entering the top of the GMA Model.

The recharge values were also checked for approximate correctness using a representative Hydraulic Evaluation of Landfill Performance (HELP) run. The HELP run approximated the average vertical GO/UGMAS sequence as a three-layer sequence. The first layer was a 10-foot thick lateral drainage layer of brown clay with saturated conductivity of .36 feet per day (ft/day), a slope of .83 percent, and a drainage length of 5,000 feet. The second layer was a 15-foot thick barrier soil layer of gray clay with conductivity of .0011 ft/day, and the third layer was a 30-foot thick vertical percolation layer of GMA sand with conductivity of 45 ft/day. The vegetative cover was specified as fair grass. The steady-state infiltration rate obtained with this configuration and climatological data for Cincinnati was 7.23 inches per year (in/yr). Therefore, the initial value for recharge (except in the vicinity of Paddys Run) specified in the GO/UGMAS Model was 7.25 in/yr.

The Paddys Run/alluvium recharge was estimated to be 1.5 times the background recharge, or 10.875 in/yr. A two-layer HELP run was performed to verify the accuracy of this estimate. The first layer consisted of 6 feet of alluvium with conductivity of 10 ft/day, the second layer was 30 feet of GMA sand with conductivity of 45 ft/day, and the vegetative cover was specified as fair grass. Steady-state infiltration for this case was 11.1 in/yr, approximately equal to the initially specified value of 10.875 in/yr.

Boundary conditions at the vertical faces bounding the periphery of the active modeled area are of two types. At Paddys Run, a no-flux condition is imposed while the remainder of the boundary has a specified pressure condition. To specify the pressures, a hydrostatic condition is assumed. Under this assumption, the pressure is equal to water density (in pounds/cubic foot) times the measured height of the water column above the grid block centroid in question.

The boundary condition at the base of the GO/UGMAS model is somewhat problematic. Clearly, a specified pressure must be used to calculate the flux leaving the GO/UGMAS Model and entering the GMA Model. Because the bottom of the GO/UGMAS model coincides with the GMA water table, the physically realistic condition is that of atmospheric pressure (pressure equals zero). However, because a fully saturated code is being used to approximate a variably saturated system, such a condition is not permissible if one of the objectives is to calculate a second, perched water table position. Since SWIFT places the calculated water table at the phreatic surface, a specification of atmospheric pressure at the base of the SWIFT GO/UGMAS Model results in the entire model domain being unsaturated. The most straightforward solution to this problem is to initially assign a hydrostatic pressure at the base in the same manner as the sides of the model, thus allowing overburden sediments to be modeled as being saturated.

Because the Paddys Run streambed and the adjacent alluvium have relatively high permeabilities, no perched water table exists over these areas. Bottom pressures are set to zero in these grid blocks.

4.1.2.3 Internal Sources/Sinks

Three major drainage areas in the vicinity of the FEMP production area are represented as discharges. Figure 8C in Appendix C is an areal map of the drainage blocks, which are all located within the first layer of the model. Because these features are drains, the discharge rate was not allowed to exceed incoming recharge. Three levels of constant discharge rate were allowed based on the degree of depression seen in the local perched water table. The discharges have the effect of lowering the net recharge entering GO/UGMAS at the grid block in question. Rates in pounds per day were calculated by subtracting the desired net recharge from the specified surface recharge and multiplying the result by water density and horizontal grid block area. The highest discharge rate removes all but 1 in/yr of the incoming recharge, while the medium and lowest rates remove all but 2 and 3 inches, respectively.

4.2 Preliminary Auxiliary Flow Model Development

4.2.1 Model Grid Construction

During the early stages of the site-characterization effort, a 2-D cross-section model of the GO/UGMAS was developed for use with the MSTS code in order to evaluate its ability to perform 2-D cross-section runs for comparison with 2-D SWIFT GO/UGMAS results. The cross-section model was constructed along Row 80 of the SWIFT 3-D finite-difference grid (Figure 4-2).

The cross-section model represents a southwest to northeast section of the GO/UGMAS that is 8,000 feet long and ranges from approximately 45 to 98 feet in thickness. The model area is bounded on the west by Paddys Run and on the east by an escarpment that delineates the extent of the glacial overburden at the site. The lower model boundary represents the water table surface of the underlying GMA and the upper surface represents land surface. The MSTS model grid included 49 two-foot thick layers with a uniform bottom elevation in the vertical direction and 64 columns each measuring 125 feet wide in the horizontal direction. Figure 4-3 illustrates the soil types represented in the MSTS cross-section model. The geology represented was taken from the 3-D SWIFT model existing at the time.

Although the geology of the 3-D SWIFT model consisted of only six layers, it was necessary to use a finer mesh with 49 layers for MSTS. This is because SWIFT can have stair-stepped grid blocks while MSTS cannot. The solution to this restriction was to use the finer discretization for MSTS while specifying the appropriate blocks as inactive to closely approximate the actual cross-sectional geometry. As noted previously, a finer discretization is also desirable from a numerical point of view considering the highly nonlinear nature of the unsaturated flow model.

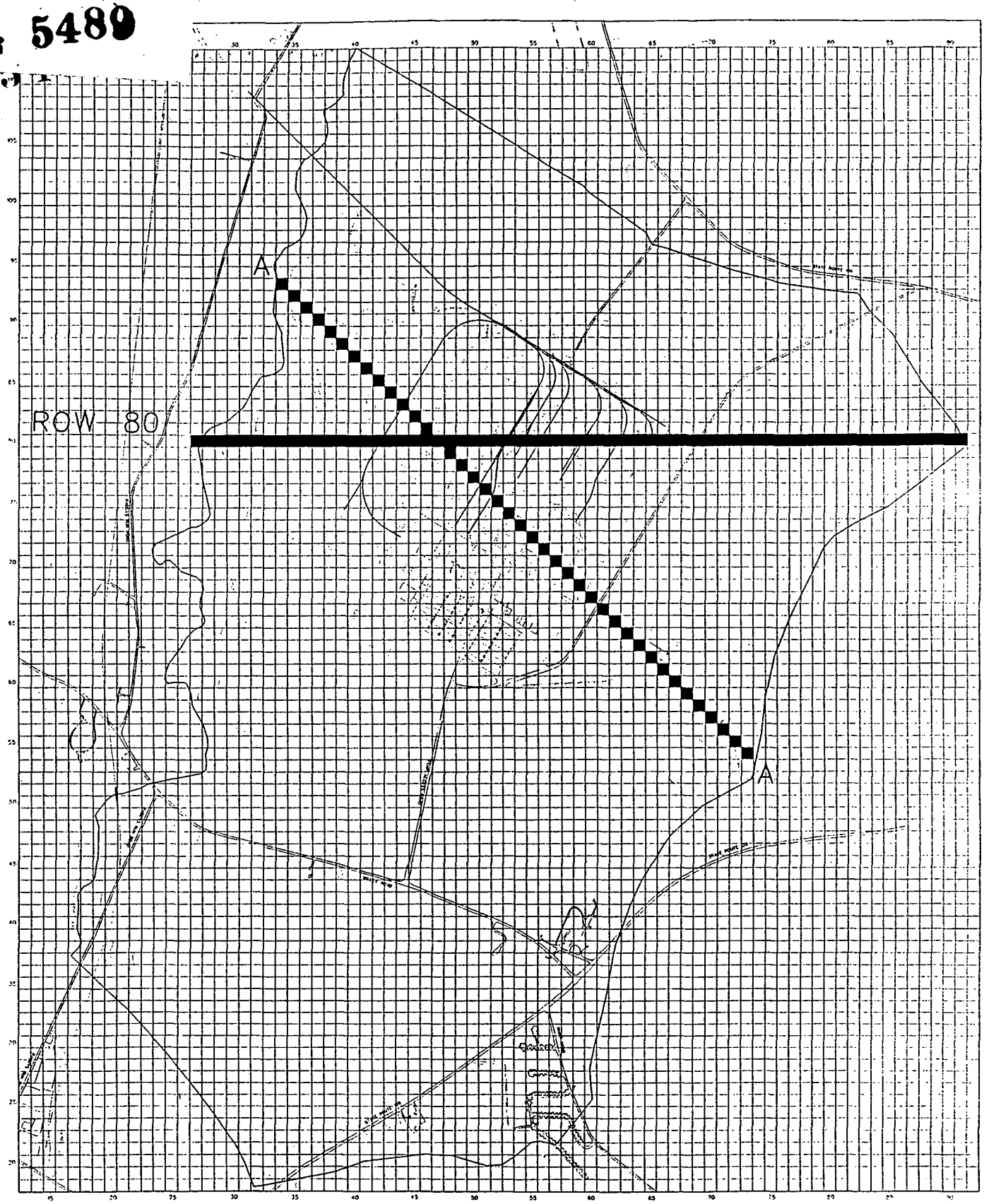

LEGEND

Highlighted Grid Blocks

CROSS-SECTIONS A-A' AND AT ROW 80
FOR 2-D STEADY-STATE FLOW RUNS

Figure 4-2 - Cross-Sections A-A' and at Row 80
for 2-D Steady-State Flow Runs

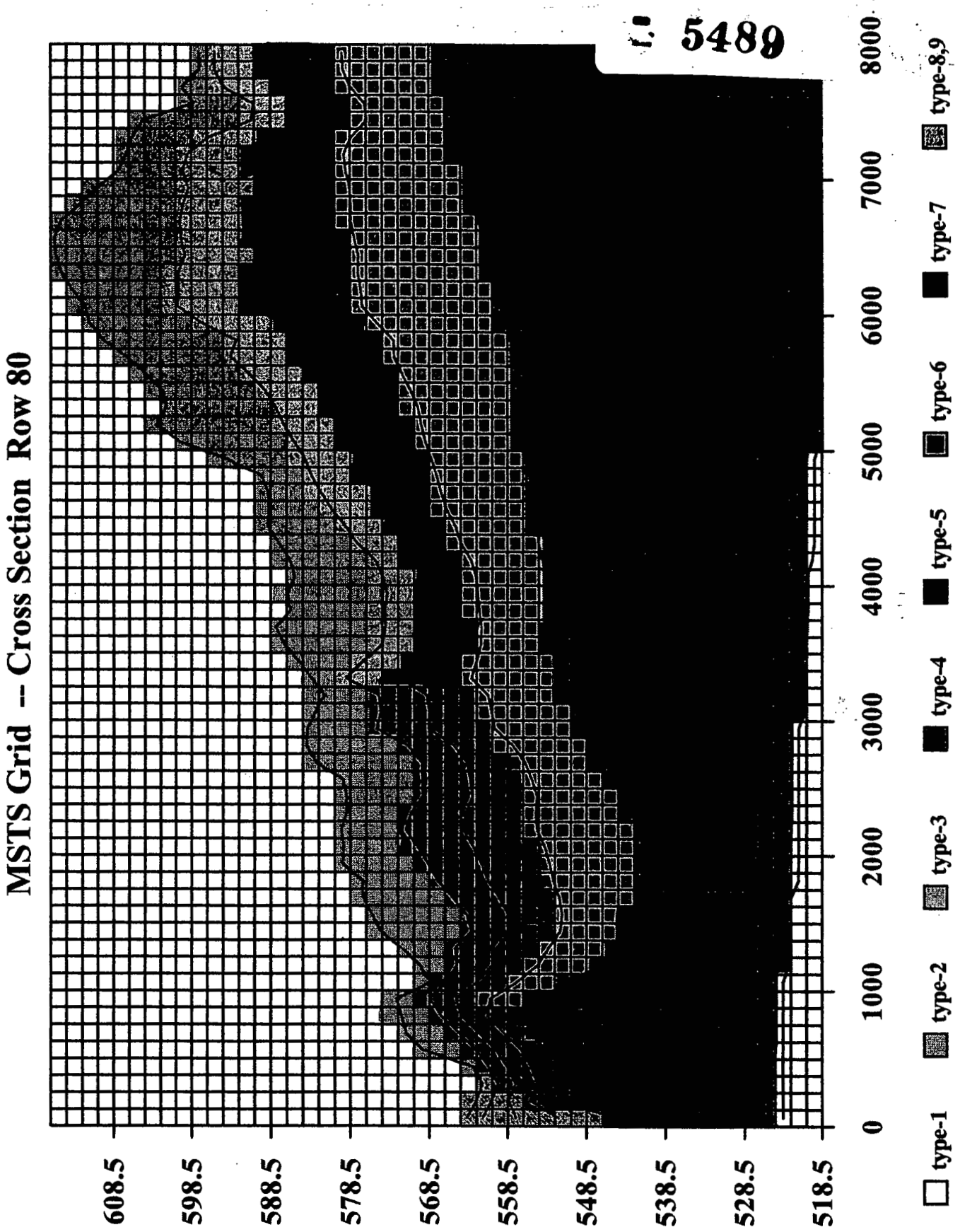

Figure 4-3 - MSTS Grid - Soil Type Cross-Section at Row 80

4.2.2 Estimated Soil Hydraulic Properties for Model Testi...

The initial development of the auxiliary model was performed before preliminary results from the glacial till hydraulic characterization were available. Therefore, initial soil hydraulic properties were estimated from values used in earlier 1-D vadose zone modeling (i.e., ODAST modeling used in CRUs 1, 2, and 4). Gray till was hypothesized to become less permeable with depth, and brown till horizontal conductivities were based on Layer 2 gray till values, with increased vertical conductivity to account for vertical fracturing. Only nine soil types were defined at this stage of development. Table 1B in Appendix B summarizes the initial hydraulic properties used. Initial hydraulic parameters were adjusted until the MSTS model produced a simulated water table within the uppermost layer. This qualitatively "calibrated" water-table surface is shown on Figure 1B of Appendix B.

Table 2B in Appendix B summarizes the final adjusted hydraulic parameters obtained with MSTS. A reasonable perched water table position was obtained by decreasing the initial vertical hydraulic conductivity of the gray till in Layer 4 from 0.0079 ft/day to 0.00088 ft/day and by decreasing the horizontal and vertical hydraulic conductivity of the gray sand from 450 ft/day to 2.5 ft/day and from 45 ft/day to 0.25 ft/day, respectively. The horizontal hydraulic conductivity of the upper GMA was also adjusted since it was set artificially low in the SWIFT model to simulate strictly vertical flow.

4.2.3 Boundary Conditions

The initial development of the MSTS model incorporated a no-flow boundary on the east and west edges of the model domain and a specified recharge boundary along the upper land surface. Once again, because the initial development of the auxiliary model occurred early in the overall GO/UGMAS development, refined estimates of recharge were not available. Because of this, the recharge values for the GMA Model were used. Recharge was set equal to 6 in/yr across the upper model boundary except in the first column where 32 in/yr of recharge was specified at Paddys Run. Pressure at the lower boundary was specified as equal to atmospheric pressure because it is coincident with the water table surface in the underlying GMA. The way in which the lower boundary was treated was a major distinction between the SWIFT 3-D model and the MSTS cross-section model. In the SWIFT 3-D model, it was necessary to designate the lower boundary as a specified pressure boundary with pressures greater than atmospheric because SWIFT is incapable of simulating unsaturated groundwater flow.

4.2.4 Preliminary Flow Results

Results of the MSTS simulation are presented in the form of plots of saturation, hydraulic head, groundwater flow vectors, and discharge for the Row 80 Cross Section Model. Figure 2B in Appendix B shows that the glacial overburden below the uppermost layer is fully saturated and that the GMA is unsaturated down to the lower boundary of the model. Another unsaturated portion of the GO/UGMAS

occurs along Paddys Run where highly permeable alluvial deposits drain adjacent soils. Hydraulic heads in the GO/UGMAS range from approximately 518.5 feet to 600 feet (Figure 3B in Appendix B). Heads are highest near the east end of the cross section where there is a topographic high, and decrease both to the east and the west and downward.

Significant horizontal flow occurs below the water table in the glacial overburden, whereas, flow in the unsaturated GMA and below Paddys Run is primarily vertical. Flow vectors which illustrate the direction of groundwater movement through the GO/UGMAS are shown on Figure 4B in Appendix B. The vertical flux across the lower boundary was converted to discharge in inches per year by dividing the volumetric flow rate (dimensions of L^3/t) through each column by the horizontal area of the column (Figure 4-4).

Discharge represents the amount of recharge that reaches the water table in the underlying GMA and has important implications regarding the fate and transport of contaminants. The total amount of discharge from the model is equal to the total amount of recharge because steady-state conditions were simulated. However, local variations in the discharge are apparent from Figure 4-4. The highest discharge occurs at the western edge of the model below Paddys Run, resulting from higher recharge in that area. Elsewhere, discharge is approximately equal to the specified recharge value of 6 in/yr.

The results of the preliminary development of the auxiliary model clearly show that MSTS is capable of producing the type of results needed to assess the impact of the assumptions made in the 3-D primary GO/UGMAS model. A reasonable perched water table position was obtained, as were an underlying unsaturated sequence representing the Upper GMA and an unsaturated sequence representing Paddys Run.

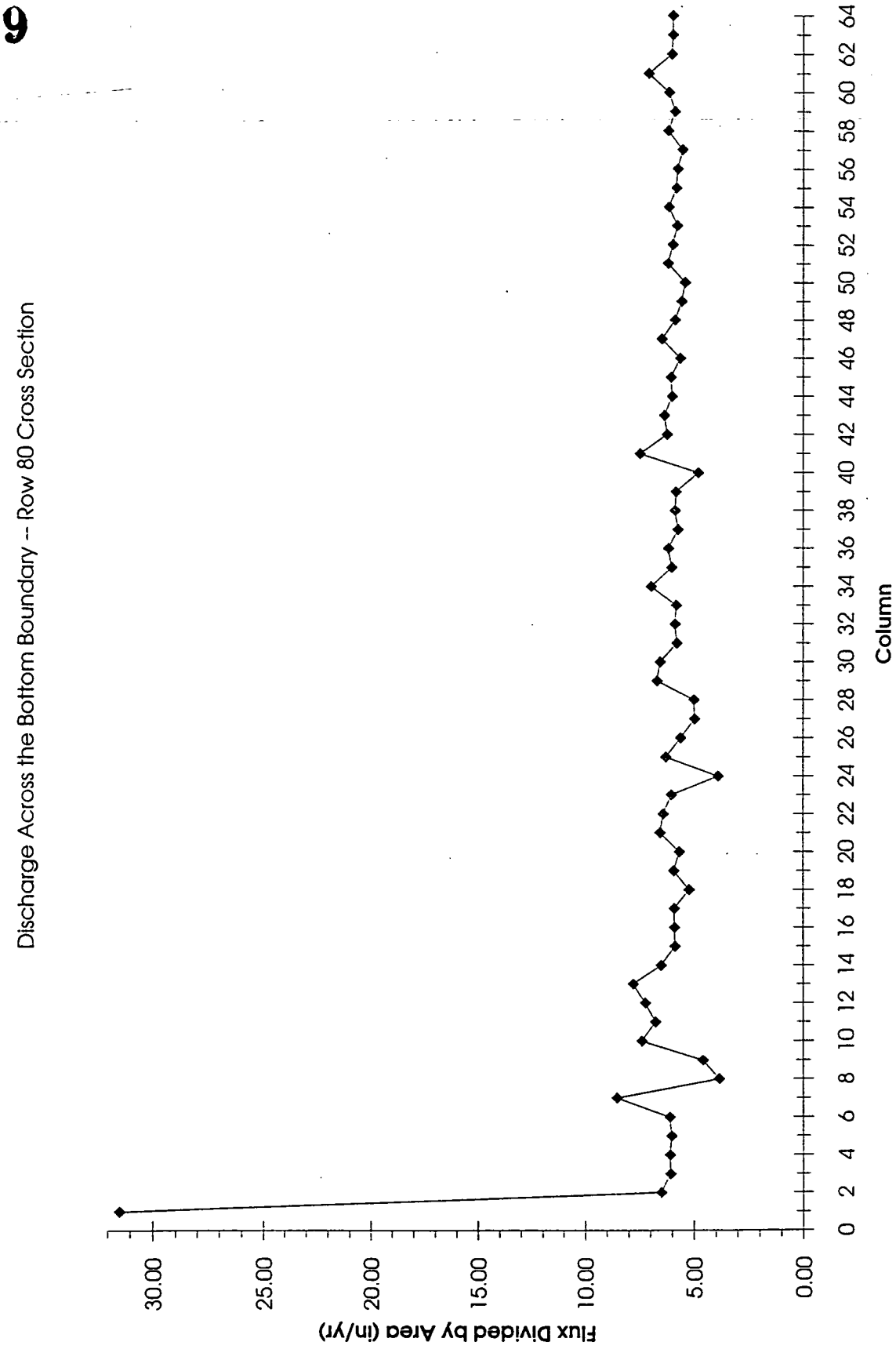

Figure 4-4 - Discharge Across the Bottom Boundary - Row 80 Cross-Section

SECTION 5

CROSS-VERIFICATION OF AUXILIARY AND PRIMARY MODELS

The purpose of the auxiliary model was to evaluate the implications of the primary model assumption that the unsaturated GMA can be treated as fully saturated with strictly vertical transport. This assumption is implemented in the primary model by specifying negligible horizontal conductivities for the GMA and by specifying positive pressures at the bottom boundary. An evaluation of this assumption was made by constructing 2-D cross-section models of the GO/UGMAS with both the auxiliary and the primary code, and comparing their results.

The strategy used was to first design and completely finish a cross-sectional steady-state flow problem with MSTS only. This included a calibration in which hydraulic conductivities and/or recharge were adjusted to produce the best match between simulated and measured perched water tables. Once the auxiliary model run was finalized, the same problem was run with the SWIFT primary model. This approach was used to assure a consistent comparison with the same set of problem parameters except for horizontal conductivity in the unsaturated GMA sand and the specified pressure at the bottom boundary. By making all parameters the same except those dealing with the assumption of a saturated upper GMA, any differences in results between the two models can be attributed to the assumption.

For the MSTS flow runs, parameters for soil characteristic curves were determined from literature data on soils similar to those found in the FEMP GO/UGMAS. Instead of using the measured perched water table as the target head distribution for the SWIFT primary model, the final calculated water table produced by MSTS was used. Once again, this was to make sure that any differences in results were attributed solely to the primary model assumption of a saturated upper GMA. All the soil and hydraulic parameter values of different soil types determined in the preliminary developments of the primary and auxiliary models described in the previous section were used as the initial values during the model calibrations of the cross-verification task.

5.1 Model Grids for Cross-Verification

Two-dimensional cross-section models were constructed with SWIFT and MSTS along line A-A' shown on Figure 4-2. The cross-section is oriented approximately northwest to southeast and extends diagonally 45 degrees across the SWIFT 3-D grid. The modeled section of the GO/UGMAS is 7,071 feet long and ranges from approximately 40 to 90 feet in thickness. Cross-section A-A' was chosen because it cuts across both the major sand body underlying the production area and the major uranium-238 plumes in the glacial overburden (i.e., plumes under the Plant 2/3 and Plant 6 areas). The SWIFT finite-difference grid is comprised of six layers in the vertical direction and 40 columns each measuring 176.77 feet wide in the horizontal direction. The MSTS finite-difference grid is comprised of 41 two-foot thick layers and

40 columns identical to the SWIFT grid. Figure 5-1 illustrates the MSTS finite-difference grid and the layers designated in the SWIFT model. Two special hydrologic features were incorporated into the models including a drain located in the uppermost layer at columns 18 and 19, and a "window" in the glacial till at column 23. The window represents an area in the glacial till, underlying Plant 6, where the vertical hydraulic conductivity has been increased as a result of clay mineral degradation from acid spills.

The modeled area is bounded on the west by Paddys Run and on the east by the escarpment which delineates the eastern extent of the glacial overburden at the site. The lower boundary of the cross-section model represents the GMA water table and the upper boundary represents land surface.

5.2 Soil Hydraulic Properties for Cross-Verification

Hydraulic conductivities calculated from slug tests conducted for the Till Hydraulics Investigation were used in the MSTS cross-section model. A rough calibration of the MSTS model was performed by adjusting soil hydraulic conductivity values until the simulated water table closely approximated the target water table in the glacial overburden. A comparison of the initially used site-characterization data to the parameter values determined by the calibration of the MSTS model is presented in Table 3B in Appendix B. The following parameters were adjusted during the calibration process: the horizontal and vertical hydraulic conductivity of the Gray Till in layers 2 and 3 was increased by a factor of 10 from 0.0055 ft/day to 0.055 ft/day and from 0.0011 ft/day to 0.011 ft/day, respectively; and the vertical hydraulic conductivity of the gray and brown silts were increased by one order of magnitude from 0.0025 ft/day to 0.025 ft/day and from 0.0028 ft/day to 0.028 ft/day, respectively.

It should be noted that the parameters calibrated with the auxiliary model for cross-section A-A' were not the final set used for the subsequent 3-D steady-state flow and uranium transport runs performed with the primary GO/UGMAS Model. The set determined here simply reflects the changes necessary for MSTS to most closely match the target water table for a single cross-section. Because of the unique difficulties of using a saturated code such as SWIFT for a partially saturated flow problem (described in Section 6), a 3-D calibration procedure was devised and implemented for the primary GO/UGMAS Model. It was this procedure which yielded the calibrated parameters for the 3-D flow and transport runs.

Following the calibration of the 2-D MSTS model, modified parameter values were substituted into the SWIFT 2-D cross-section model which was then run to compare results to the MSTS model. The only difference in saturated conductivities between the MSTS and SWIFT runs was in the unsaturated GMA horizontal conductivities. SWIFT used negligible horizontal conductivity (1×10^{-5} ft/day) while MSTS used a value of 45 ft/day.

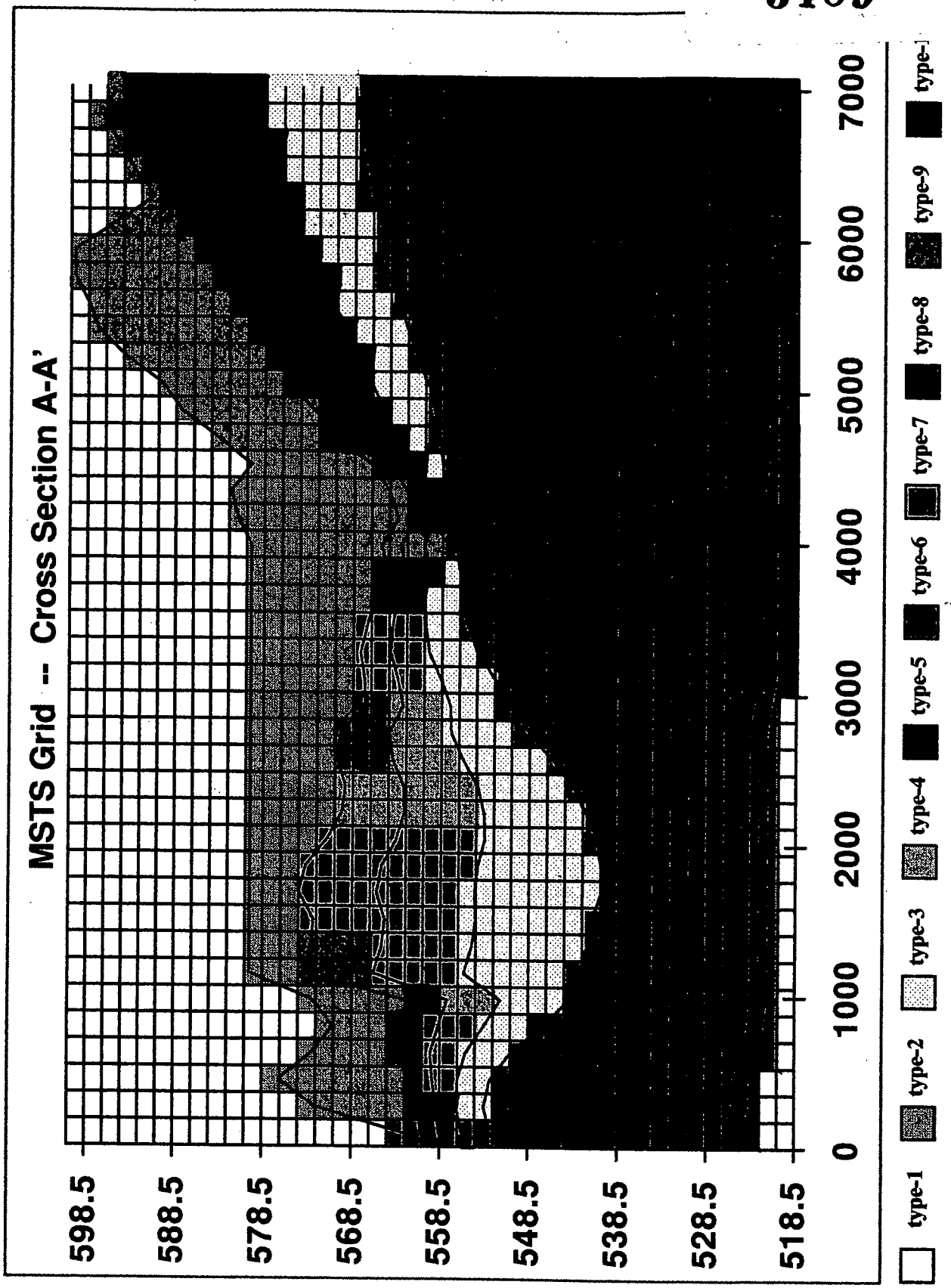

Figure 5-1 - MSTS Grid - Soil Type Cross-Section A-A'

5.3 Boundary Conditions for Cross-Verification

The west and east boundaries of the model were treated as no-flow boundaries. Uniform recharge of 7.5 in/yr was specified along the upper model boundary except in the western-most column where a recharge of 10.875 in/yr was specified to simulate leakage from Paddys Run. At the bottom boundary, atmospheric pressure was specified to represent the GMA water-table surface in the MSTS model. In the SWIFT cross-section model, the bottom boundary was also treated as a specified-pressure boundary, but the pressures were set greater than atmospheric pressure. An initial calibration of the SWIFT model was achieved by adjusting these bottom pressures until the simulated water table approximated the measured water table in the glacial overburden. Other model parameters were then subsequently adjusted to match the values used in the calibrated MSTS model.

5.4 Cross-Verification Results

The simulated water-tables calculated by MSTS and SWIFT are shown on Figure 5B in Appendix B. An apparent large discrepancy between the simulated water-tables and the target/measured water table occurs in the vicinity of the window feature in column 23; however, measured water-table elevations are not available at this location. The target water-table surface represents a contoured interpolation of the available water-table-elevation data and does not account for localized irregularities under the Plant 6 area. At the east end of the modeled area where target water-level data is not available, the simulated water table is above land surface. This is a result of the no flow boundary on the eastern edge of the model which prevents lateral flow from exiting the model, thereby causing water to build up in this area. Despite these discrepancies, the calibration is adequate for the purpose of this comparison. Further improvements to the calibration would require zoning hydraulic conductivity within layers of the same soil type, however, available data does not support such a detailed characterization of the soils.

In the MSTS model, soils are unsaturated in the following areas: below Paddys Run (column 1), across the top of the model; and along the bottom of the model in the GMA (Figure 6B in Appendix B). The glacial overburden is simulated as a saturated water-bearing zone perched above the unsaturated GMA. The window feature in column 23 results in the soils in this column being unsaturated, therefore, the perched water table does not exist in this location. The same phenomenon occurs below Paddys Run, resulting from the more permeable alluvium in this location.

Hydraulic heads in the MSTS model range from approximately 520 to 595 feet (Figure 7B in Appendix B). Heads are highest at the upper east end of the model and decrease downward and to the west. The hydraulic head distribution calculated by SWIFT appears to be quite different from that calculated by MSTS (Figure 8B in Appendix B). Heads calculated by SWIFT range approximately from 540 to 580 feet, and at first glance head contours appear nearly vertical, indicating horizontal flow. However, the 50X vertical exaggeration makes the contours appear more vertical than they actually are. For example, the 560 foot head contour line in the center of the plot is one of the steepest on the plot, but when the

scale exaggeration is taken into account its slope is only 0.4 (which represents the ratio between the local pressure gradient in horizontal and vertical directions). For an isotropic medium, this would mean that the vertical flow component is actually greater than the horizontal. In the Upper GMA, where lateral conductivity is negligible, this head distribution leads to flow that is overwhelmingly vertical. In contrast, the MSTS has Upper GMA lateral conductivity equal to the vertical component. The only way purely vertical flow can occur is if the pressure contours are horizontal, as at the bottom of Figure 7B in Appendix B.

The primary reason for the differences in head distributions is that the auxiliary model simulates partially saturated conditions while the primary model simulates full saturation only. In the unsaturated MSTS model, a sudden dropoff in saturation (as seen at the base of the glacial till and top of the GMA in Figure 6B) leads to a large drop in hydraulic conductivity. Because flux is conserved by the steady-state model, Darcy's Law implies that an accompanying sharp head gradient must occur. This is seen in the base of till/Upper GMA region of Figure 7B. On the other hand, the fully saturated SWIFT model assumes that higher, saturated values of hydraulic conductivity hold everywhere. The result is a head contour plot with less variability and lower gradients. These differences in the two models lead to the conclusion that the fully saturated SWIFT model will predict a conservatively higher degree of lateral flux in the perched water zone than the MSTS model.

Groundwater flow vectors illustrate the pattern of groundwater flow through the GO/UGMAS (Figure 9B in Appendix B). Groundwater flow vectors calculated by the SWIFT model are similar to those calculated by MSTS (Figure 10B in Appendix B). Discharge across the bottom boundary is plotted for each column in the SWIFT and MSTS cross section models (Figure 5-2). The discharge calculated by both models is approximately equal to the recharge value of 7.5 in/yr except in a few areas. These areas include: column 1 where a higher recharge value was specified to simulate leakage from Paddys Run; column 6 where a column of sandy soil provides a conduit for increased downward vertical flow; and columns 18 and 19 where discharge is less than recharge because of water leaving the model through the drain. Discharge was not significantly affected by the window feature in column 23. Agreement in bottom discharge (Figure 5-2) between SWIFT and MSTS is excellent everywhere except for columns 4, 6, 7, 14, and 15. These columns contain coarser-grained soils with the highest potential for lateral flux. The higher variability in bottom flux calculated by SWIFT indicates that the model redistributed some of the vertical flux laterally. Thus, Figure 5-2 shows that where lateral transport occurs SWIFT conservatively overpredicts the magnitude of it. Where flow is predominantly vertical, SWIFT predicts the same amount of bottom flux as MSTS.

The comparison of SWIFT and MSTS model results indicates that the SWIFT model is capable of reasonably simulating the movement of groundwater through the GO/UGMAS. In cases where the amounts of lateral flow and transport are of concern, the SWIFT GO/UGMAS Model will produce conservative estimates. Therefore, only the SWIFT code was utilized in further 3-D GO/UGMAS model development with the results of the field hydraulic studies. The following sections describe the final

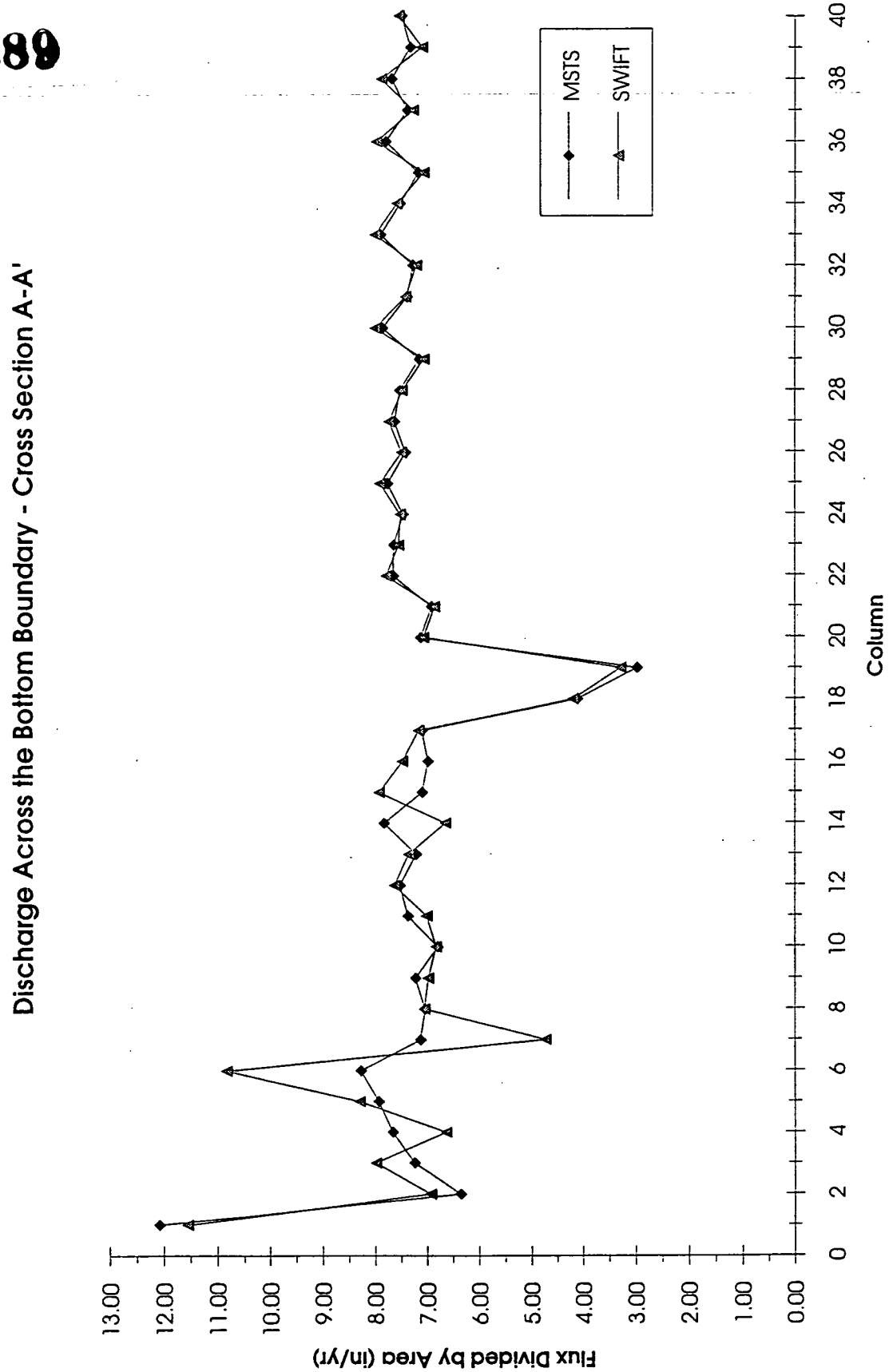

Figure 5-2 - Discharge Across the Bottom Boundary - Cross-Section A-A'

Phase I development and the first application of the 3-D GO/UGMAS model to support the CRU-5 RI/FS.

SECTION 6

PRIMARY MODEL FINAL STEADY-STATE FLOW CALIBRATION

6.1 Approach

The final steady-state flow calibration of the 3-D GO/UGMAS model was initiated when results of the field hydraulic study in the glacial overburden were available. As stated in Subsection 4.1 (Preliminary Development of the Primary 3-D Flow Model), the specified pressures at the bottom surface of the model cannot be physically realistic. Therefore a typical calibration (specify boundary conditions, vary conductivities, and/or infiltration rates to match a measured water table) cannot be performed. When the measured water table is used to establish a hydrostatic condition at the bottom surface and then surface recharge is added, the calculated water table is too high. An iterative procedure (which adjusts the top surface used to define water column height) was devised so that the calculated water table converges to the measured surface.

Because there is no clear physical basis for preferring one distribution of bottom pressures over another, constraints cannot be developed to determine the "best" combination of conductivities and bottom pressures. That is, an infinite number of combinations of conductivities and bottom pressures can produce an acceptable match to the measured water table with little or no means of discriminating between a "good" and "bad" combination. In light of this, the following "calibration" procedure was developed:

1) Use the best data available to initially fix conductivities, porosities, recharge, and discharge, and initially define the bottom pressures as hydrostatic using the measured water table to determine water column height.

2) Iteratively adjust the top surface used to define water column height and bottom pressures until an acceptable match to the measured water table is produced. Each iteration is a separate SWIFT steady-state flow run.

3) If an acceptable calculated water table cannot be obtained by iteration, change conductivities and/or infiltration rates and start the iteration process over until convergence to the measured water table occurs. The conductivities and infiltration rates should be changed as little as possible from the best initial estimates.

   It should be noted that if the upper surface used to define the height of the water column is iteratively adjusted at a location overlying a specified-pressure lateral till boundary, the side pressure specification must also be changed to reflect the adjustment.

6.2 Criteria

The residual was defined as the distribution of block-by-block differences between the calculated and measured water tables over the area for which measurements are available. The distribution of residuals should not have a clear pattern which indicates insufficient calibration. The model was considered to be "calibrated" when the sum of the squared residuals divided by the number of blocks over which measurements are available converged to some suitably small value. Taking the square root of this value yields a measure of the "average" residual value. Based on the calibration results obtained during the preliminary model development and the cross-verification tasks, an overall average residual value of 2.5 feet is considered reasonable for the 3-D GO/UGMAS model. Due to the complexity of the GO/UGMAS, more restrictive calibration criteria were not considered realistic.

6.3 Results

Thirty-two steady-state flow runs were performed before the calibration criteria were considered to be satisfied. The thirty-second run was actually the sixth iteration in a series of runs. The average residual for this run was 2.33 feet. Earlier runs failed to converge due to the fact that the saturated vertical hydraulic conductivity of the gray till (the least permeable soil) was slightly lower than the steady-state net recharge specified. Initial gray till vertical conductivity was .0011 ft/day (and it was increased approximately two-fold to .00205 [7.23 x 10^{-7} cm/s]). To keep the anisotropy and the silt/gray clay conductivity ratios the same as in the initial parameter set, gray clay horizontal and all silt conductivities were multiplied by the same factor. Table 6-1 lists the final steady-state flow parameters. The recharge distribution was also changed during the calibration process. Background recharge was decreased from 7.25 to 6 in/yr (this made it the same as used in the GMA Model) and recharge in the Paddys Run/alluvium area was increased from 10.875 to 12 in/yr. Table 3C and Figure 9C in Appendix C depict the final recharge distribution.

Figure 10C in Appendix C shows the measured till perched water level, contoured from 1000 series well and boring data. The measured water level only covers a portion of the active till area, so residuals can only be calculated over this limited area. Figure 11C in Appendix C depicts Layer 1 heads which correspond to calculated water levels. Figure 12C in Appendix C is a map of the residuals. Because the iteration process yielded very small and somewhat randomly distributed residuals, no clear pattern is discernible in the residual map. The vast majority of grid blocks have a residual of less than 1 foot. Figures 13C through 17C in Appendix C are maps of head in layers 2 through 6. Within the main portion of the model area where field measurements are available, only the Plant 6 area has higher residual values due to the increased vertical hydraulic conductivities in the model used to simulate the higher infiltration rate through the degraded clay layer.

Table 6-1 - Final Steady-State Flow Parameters by Soil Type
Used in Run 3DFLOW32

Soil Type	K_h (ft/day)*	K_v (ft/day)*	Porosity	Description
1	1.0×10^{-5}	1.0×10^{-5}	.1	Inactive Block
2	.100	1.	.45	Brown Till
3	.01025	.00205	.34	Layer 2 Gray Till
4	2.30	.0230	.39	Gray Deltaic Sand
5	.01025	.00205	.34	Layer 3 Gray Till
6	.01025	.00205	.34	Layer 4 Gray Till
7	1.0×10^{-5}**	45.	.39	Upper GMA Sand
8	10.	10.	.35	Paddys Run/SSOD Alluvium
9	10.	10.	.35	Paddys Run/SSOD Streambed
10	.466	.00466	.35	Gray Lacustrine Silt
11	5.00	.0500	.39	Brown Deltaic Sand
12	.522	.00522	.35	Brown Lacustrine Silt

* Multiply by 3.5278×10^{-4} to convert to cm/s

** Low conductivity used to restrict horizontal flow in the unsaturated GMA

Figure 18C in Appendix C is a map of the overall vertical hydraulic gradient. This was calculated at each block by differencing Layer 1 and Layer 6 heads and dividing by the distance between the Layer 1 and 6 centroids. In the areas to the south and east of the FEMP production area where thicker sequences of till predominate, the vertical hydraulic gradient ranges from roughly .2 to .5. If predominantly vertical flow is assumed in these areas, flux out the bottom of the model would be expected to be roughly equal to recharge (6 in/yr) in the area. These hydraulic gradients would then translate to equivalent vertical conductivities from .0027 to .0068 ft/day.

For a specific example, grid block (67,78) falls between the vertical hydraulic gradient contours of .2 and .3. These translate into equivalent hydraulic conductivities from .0046 to .0068 ft/day. The vertical sequence at grid block (67,78) consists of 16.57 feet of brown clay, 26.63 feet of gray clay and 37.02 feet of unsaturated GMA sand. Using the final vertical hydraulic conductivities from Table 6-1, the equivalent vertical hydraulic conductivity (calculated as the harmonic mean of the conductivities of the

three layers) is .0061 ft/day, well within the range expected. This indicates not only that the overall vertical hydraulic gradients depicted in Figure 18C of Appendix C are correct, but also that predominantly vertical flow occurs in the areas where the layer of coarser-grained material is absent and the low-permeability till sequence is thick. It is also important to note that localized lows in the overall vertical hydraulic gradient occur in areas of higher permeability silts and sands due to increased lateral flow in these materials.

Finally, Table 4C in Appendix C lists the water budget for the "calibrated" steady-state flow run. The mass flow of water to the discharges is listed in the well summary total production category.

SECTION 7

URANIUM-238 TRANSPORT SIMULATION

7.1 Uranium-238 Transport Parameters

To assess lateral plume migration and determine the optimal modeling approach for CPC screening, simulating baseline conditions, and PRG development in the CRU-5 RI/FS, a 3-D flow run and 1,000-year uranium-238 transport run were performed using the 3-D GO/UGMAS Model. The flow results are from the final calibrated primary model. All the transport parameters are selected so that the model can produce conservative estimates of the extent of uranium-238 migration in both the vertical and lateral directions.

In typical cases of low molecular diffusion, the ratio of lateral to vertical transport is dependent mainly upon mechanical properties of the porous medium (dispersivity and pore velocity) rather than constituent-dependent parameters. This means that the ratio of lateral to vertical transport seen in the uranium run is indicative of the ratio that would be seen for other constituents from the same source area. Therefore, no other constituent was simulated during the Phase I model development and application.

Table 7-1 lists the parameters used for the uranium-238 1,000-year transport runs. The parameters listed were the same for each of the 12 soil types. The K_d value of .24 cubic feet per pound (15 l/kg), which is representative of the more soluble and therefore mobile uranium in the production area, yields retardation factors in the 70 to 80 range. The dispersivities (lateral = 15 feet, longitudinal = 62.5 feet) were chosen to be the lowest allowable without violating constraints (imposed to avoid numerical dispersion) on the grid Peclet number. The grid Peclet number is a dimensionless parameter which measures the ratio of advection to dispersion. To avoid numerical dispersion, SWIFT requires that the grid Peclet number be no greater than 2. The values of dispersivities listed in Table 7-1 are higher than would normally be used for transport through till, but they should result in a conservatively large amount of plume migration for the 1,000-year run.

Table 7-1 - Transport Properties Specified in Flow Run
3DFLOW32/U238 Transport Run 3DTRAN01

Transport Parameter	Value	Unit
Solid-Liquid Partition Coefficient (K_d)	15	L/Kg
Lateral Dispersivity	15	ft
Longitudinal Dispersivity	62.5	ft
Molecular Diffusion	0.00065	ft^2/day
U-238 Decay Constant	0.0	day^{-1}

7.2 Uranium-238 Initial Conditions

The 1,000-year uranium-238 transport run was started with specified initial concentrations as depicted in figures 1D through 4D in Appendix D for layers 1 through 4 respectively. These initial plumes represent current measured uranium-238 concentrations beneath Plants 2/3, 6, and 9 at the FEMP. No additional mass loading from the ground surface was included in the simulation. These plumes have the highest measured perched groundwater concentrations of uranium-238 in the GO/UGMAS. The initial plumes in the Plant 2/3 area are located near the center of the FEMP production area, overlying sand and silt bodies contained in the glacial overburden. These coarser-grained soils provide the highest potential for lateral migration. The clay underlying Plants 6 and 9 is degraded and is not an effective barrier layer. Therefore, these initial plumes represent sources of the highest potential future impacts from contaminated perched groundwater to the GMA and surface water bodies. The southeasternmost of the three drainage areas included in the flow model lies between the two major plumes depicted in figures 2D and 3D in Appendix D.

7.3 Uranium-238 Transport Run Results

Figures 5D through 10D in Appendix D show the position of the plumes by layer at 1,000 years. Figure 5D in Appendix D shows that the western plume has dispersed upward into Layer 1 from its initial position in layers 2 and 3. Dispersivity is apparently high enough to overcome the small downward and localized lateral components of advection. The areal sizes of the initial plumes increase 2 to 3 times at the end of the simulation. However, despite the high dispersion, the western plume still does not reach the westernmost discharge and thus has no path to Paddys Run or the Pilot Plant drainage ditch. The lack of plume migration on a large scale in the 1,000-year period is due to the high retardation factors (about 70 to 80) for uranium-238, a relatively small lateral hydraulic gradient (i.e., about 0.0054 from measured perched groundwater table), and mass loss due to more significant vertical downward migration.

Table 7-2 lists total dissolved uranium-238 mass by layer through time, as well as the dissolved mass rate of change. The same data is plotted in figures 11D through 22D in Appendix D. Finally, Table 1E in Appendix E is a material balance summary for uranium-238 at each of the 50-year time steps from year zero to 1000. The amount listed under the heading "IN-PLACE" is the total dissolved and adsorbed uranium-238 mass, which is listed in further detail in the section "SUMMARY OF RADIONUCLIDE MASS BY LAYER." Mass lost to the discharge is listed under "SINKS," and mass exiting through the bottom to the GMA is listed under "E-FLUX."

From the final distribution of the mass presented in Appendix E, it can be shown that 77.4 percent of the initial uranium mass remains in the GO/UGMAS while 21.3 percent migrates vertically into the GMA and 1.3 percent exits through the drainage pipe located at the center of the production area. As shown in figures 1D to 10D, the initial maximum dissolved uranium concentration is 10 mg/L in Model Layer 3 within the glacial overburden and the final maximum concentration is 2.2 mg/L, which occurs in the unsaturated GMA. All of these results indicate the greater significance of the vertical contaminant migration relative to the lateral migration from the simulated source areas.

Table 7-2 - Flow/Transport Run 32 - Total Dissolved U-238 Mass by Layer vs. Time and Dissolved U-238 Mass Rate of Change by Layer vs. Time

FLOW/TRANSPORT RUN 32 – TOTAL DISSOLVED U238 MASS BY LAYER VS TIME AND DISSOLVED U238 MASS RATE OF CHANGE BY LAYER VS TIME

TIME (YR)	TOTAL DISSOLVED U238 MASS (LB)					
	LAYER 1	LAYER 2	LAYER 3	LAYER 4	LAYER 5	LAYER 6
0	15.47	116.83	150.46	22.71	0.00	0.00
50	44.25	78.54	98.73	55.73	27.29	1.24
100	37.42	67.27	84.95	60.52	49.45	2.74
150	32.25	59.27	75.71	61.99	65.95	3.95
200	28.40	53.42	68.89	61.74	78.53	4.92
250	25.48	48.97	63.59	60.61	88.25	5.69
300	23.20	45.43	59.32	59.06	95.84	6.33
350	21.39	42.52	55.77	57.34	101.79	6.84
400	19.91	40.07	52.73	55.58	106.48	7.27
450	18.69	37.95	50.08	53.84	110.16	7.61
500	17.66	36.09	47.74	52.17	113.02	7.90
550	16.76	34.44	45.65	50.56	115.21	8.13
600	16.02	32.95	43.75	49.04	116.86	8.31
650	15.35	31.59	42.02	47.59	118.06	8.45
700	14.76	30.36	40.43	46.21	118.87	8.57
750	14.22	29.22	38.96	44.91	119.37	8.65
800	13.74	28.16	37.60	43.67	119.60	8.71
850	13.29	27.18	36.33	42.49	119.60	8.74
900	12.88	26.26	35.14	41.36	119.40	8.76
950	12.50	25.41	34.02	40.28	119.03	8.77
1000	12.14	24.60	32.97	39.25	118.52	8.76

TIME (YR)	DISSOLVED U238 MASS RATE OF CHANGE (LB/YR)					
	LAYER 1	LAYER 2	LAYER 3	LAYER 4	LAYER 5	LAYER 6
25	0.5756	−0.7658	−1.0346	0.6604	0.5458	0.0248
75	−0.1366	−0.2254	−0.2756	0.0958	0.4432	0.0300
125	−0.1034	−0.1600	−0.1848	0.0294	0.3300	0.0242
175	−0.0770	−0.1170	−0.1364	−0.0050	0.2516	0.0194
225	−0.0584	−0.0890	−0.1060	−0.0226	0.1944	0.0154
275	−0.0456	−0.0708	−0.0854	−0.0310	0.1518	0.0128
325	−0.0362	−0.0582	−0.0710	−0.0344	0.1190	0.0102
375	−0.0296	−0.0490	−0.0608	−0.0352	0.0938	0.0086
425	−0.0244	−0.0424	−0.0530	−0.0348	0.0736	0.0068
475	−0.0206	−0.0372	−0.0468	−0.0334	0.0572	0.0058
525	−0.0180	−0.0330	−0.0418	−0.0322	0.0438	0.0046
575	−0.0148	−0.0298	−0.0380	−0.0304	0.0330	0.0036
625	−0.0134	−0.0272	−0.0346	−0.0290	0.0240	0.0028
675	−0.0118	−0.0246	−0.0318	−0.0276	0.0162	0.0024
725	−0.0108	−0.0228	−0.0294	−0.0260	0.0100	0.0016
775	−0.0096	−0.0212	−0.0272	−0.0248	0.0046	0.0012
825	−0.0090	−0.0196	−0.0254	−0.0236	0.0000	0.0006
875	−0.0082	−0.0184	−0.0238	−0.0226	−0.0040	0.0004
925	−0.0076	−0.0170	−0.0224	−0.0216	−0.0074	0.0002
975	−0.0072	−0.0162	−0.0210	−0.0206	−0.0102	−0.0002

SECTION 8

CONCLUSIONS AND RECOMMENDATIONS

The model development and runs detailed in this report show that the saturated 3-D GO/UGMAS Model can be used to reasonably assess contaminant plume migration in the variably saturated glacial overburden and upper GMA. More specifically, the model yields answers as to the relative significance of the vertical and lateral migration of contaminants from the two major contaminated perched groundwater sources. This information supports the selection of the optimal approach to glacial overburden modeling for CPC screening, simulation of baseline conditions, and PRG development in the CRU-5 RI/FS. The model is also available as the basis for further improvements to simulate any glacial overburden remedial designs with perched groundwater recovery wells in which impacts of lateral plume migration under induced flow and loading from multiple source areas are important.

The foregoing model development results and discussion have shown that the GO/UGMAS Model provides a level of conservatism that is appropriate for a Comprehensive Environmental Response, Compensation, and Liability Act (CERCLA) Risk Assessment. Use of GO/UGMAS will not underestimate transport or risk under the current site conditions. First and foremost, conservatism is achieved simply by using conservative flow and transport parameters with the model. It has also been shown, however, that several features unique to the model lead to conservative estimates of transport. Among these are assumption of a highly permeable top layer (i.e., weathered till) and fully saturated bottom layer (i.e., unsaturated GMA). In instances where lateral transport is of concern, it was shown in Subsection 5.4 that the GO/UGMAS Model (assuming full saturation) produces conservatively higher estimates of lateral flux than an unsaturated auxiliary model.

8.1 Recommendations for the CRU-5 RI/FS Glacial Overburden Modeling

The results of the GO/UGMAS uranium transport simulation indicate that lateral plume migration from the major contaminated perched groundwater source areas is not significant in relation to vertical transport. As mentioned above, in comparisons with the unsaturated auxiliary code MSTS, the SWIFT GO/UGMAS Model predicts conservatively higher degrees of lateral Darcy flux. In addition, unrealistically high dispersivities were used for the 1,000-year uranium simulation to assure that numerical dispersion would not corrupt the solution. The combined effect is to spread the plume further laterally than would be the case with less lateral flow and more realistic dispersion, yet the 1,000-year plots still show only relatively minor lateral migration. It is therefore logical to recommend that a one-dimensional vertical model of contaminant transport (e.g., ODAST) be used as the main modeling tool for CPC screening, simulating baseline conditions, and PRG development in the glacial overburden.

Although uranium in perched groundwater under the Plant 2/3 and Plant 6 areas can not reach the surface water exposure points west of the production area in 1,000 years through lateral migration routes, certain more mobile perched groundwater contaminants or contaminants from other source areas closer to the surface water bodies (i.e., Paddys Run and Pilot Plant drainage ditch) may still impact these surface water exposure points within the same time frame. To screen and evaluate the impact due to lateral (as well as vertical) migration of these contaminants in the perched groundwater zone, it is recommended that simple analytical transport models (e.g., the ECTran model, DOE 1993b) be used to supplement the main 1-D vertical transport model. Conservative assumptions (such as assuming that all the mass of contaminant migrates laterally) can be made to simplify the modeling of lateral migration. For each source area or plume in the major perched zone, groundwater travel time to the closest surface water exposure point can be estimated based on the measured lateral hydraulic gradient, conductivity, and travel distance. Chemical-specific retardation factors and the source-area-specific perched groundwater travel times can be used to select contaminants that may reach the surface water exposure points in the perched zone within 1,000 years. For each source area, 1-D or 2-D analytical transport models (accounting for adsorption/desorption and decay effects) can be applied for these constituents to compile a final area-specific CPC list in the lateral migration pathway and to estimate conservative maximum exposure point concentrations of CPCs. Cumulative impacts at any exposure point can also be determined by superposition of modeling results from all the individual source areas. Based on the results of 3-D GO/UGMAS modeling results (i.e., relatively insignificant impacts due to lateral migration of the major contaminants), this simplified modeling approach is considered sufficient for incorporating the lateral migration pathway into the CPC screening, baseline condition simulation, and PRG development processes in the CRU-5 RI/FS.

SECTION 9

REFERENCES

(Bradbury and Muldoon 1990) Bradbury, K.R. and M.A. Muldoon, 1990. "Hydraulic Conductivity Determinations in Unlithified Glacial and Fluvial Materials, Groundwater and Vadose Zone Monitoring," *ASTM STP 1053*, D.M. Nielson and A.I. Johnsons, Eds. Philadelphia, PA: American Society for Testing and Materials.

(Brooks and Corey 1966) Brooks, R.H., and A.T. Corey, 1966. "Properties of Porous Media Affecting Fluid Flow." *Journal of Irrigation and Drainage Division*. 93(3):61-88.

(Burdine 1953) Burdine, N.T., 1953. "Relative Permeability Calculations from Pore-Size Distribution Data." *Petroleum Trans*. 198:71-77.

(Dell and Fetch 1985) Dell, K.S., and J.S. Fetch, 1985. "Heat and Mass Transfer in Capillary Porous Media Considering Evaporation, Condensation, and Non-Condensible Gas Effects. Presented at the 23rd ASME/AIChE National Heat Transfer Conference, Denver, August 1985.

(DOE 1993) United States Department of Energy, 1993. "Development and Application of the ECTran Model to Support RI/FS at the FEMP," Prepared by Halliburton NUS.

(DOE 1994) United States Department of Energy, 1994. Fernald Environmental Management Project Industrial Workshop On Characterization of the Vadose Zone (Glacial Tills), a workshop to address issues at the Fernald Environmental Management Project (FEMP), April 15-16, 1993, Sponsored by Office of Technology Development, U.S. Department of Energy, Coordinated by the University of Cincinnati, College of Engineering.

(Everett et al. 1984) Everett, L.G., L.G. Wilson, and E.W. Holyman, 1984. "Vadose Zone Monitoring for Hazardous Waste Sites," *Pollution Technology Review*. No. 112. Park Ridge, NJ: Noyes Data Corporation.

(Fatt and Klikoff 1959) Fatt, I., and W.A. Klikoff, 1959. "Effect of Fractional Wettability on Multiphase Flow Through Porous Media." AIME Transactions. 216:246.

(Fetter 1988) Fetter, C.W., 1988. "Applied Hydrology." New York: MacMillan Publishing Company.

(Freeze and Cherry 1979) Freeze, R.A. and J.A. Cherry, 1979. *Groundwater*. Englewood Cliffs, NJ: Prentice-Hall, Inc.

(Johnson, et al. 1983) Johnson, T.M., T.H. Larson, B.L. Herzog, K. Cartwright, C.J. Stohr, and S.J. Klein, 1983. "A Study of Trench Covers to Minimize Infiltration at Waste Disposal Sites." Prepared for U.S. Nuclear Regulatory Commission. ISGS Contract/Grant Report:1983-3. Champaign, Illinois: Illinois Geological Survey.

(Haverkamp, et al. 1977) Haverkamp, R., M. Vauclin, J. Touma, P. Wierenga, and G. Vachaud, 1977. "A Comparison of Numerical Simulation Models for One-Dimensional Infiltration." *Soil Sciences America Journal*. 41:285-294.

(Klavetter and Peters 1986) Klavetter, E.A., and R.R. Peters, 1986. "Estimation of Hydrologic Properties of Unsaturated, Fractured Rock Mass. Albuquerque, New Mexico: Sandia National Laboratories. SAND84-2642.

(Leverett 1941) Leverett, M.C., 1941. "Capillary Behavior in Porous Solids." AIME Transactions 142:152.

(McCay et al. 1993) McCay, L.D., J.A. Cherry, R.W. Gillham, April 1993. "Hydraulic Conductivity and Fracture Aperture," *Water Resources Research*, Volume 29, No. 4.

(Mualem 1976) Mualem, Y., 1976. "A New Model for Predicting the Hydraulic Conductivity of Unsaturated Porous Media." *Water Resources Research*. 12:513-522.

(Nichols and White 1993) Nichols, W.E., and M.D. White, 1993. *MSTS, Multiphase Subsurface Transport Simulator: User's Guide and Reference*. Richland, Washington: Pacific Northwest Laboratory. PNL-8637.

(Nitao 1988) Nitao, J.J., 1988. *Numerical Modeling of the Thermal and Hydrological Environment around a Nuclear Waste Package Using the Equivalent Continuum Approximation: Horizontal Emplacement*. Livermore, California: Lawrence Livermore National Laboratory. UCID-2144.

(PARSONS 1993a) PARSONS, 1993a. *Glacial Overburden/Upper Great Miami Aquifer Modeling Improvement Technical Approach/Work Plan*, Revision 3. Fairfield: PARSONS.

(PARSONS 1993b) ----------, 1993b. *Fate and Transport Modeling Transition Report*, Revision A. Fairfield: PARSONS.

(Pruess 1987) Pruess, K., 1987. *TOUGH User's Guide*. Berkeley, California: Lawrence Berkeley Laboratory. LBL-20700.

(Schroeder, et al. 1988) Schroeder, P.R., R.L. Peyton, B.M. McEnroe, and J.W. Sjostrom, October 1988. "The Hydrologic Evaluation of Landfill Performance (HELP) Model," User's Guide for Version 2, Author's Draft. US EPA, Cincinnati, OH.

(Touma and Vauclin 1986) Touma, J. and M. Vauclin, 1986. "Experimental and Numerical Analysis of Two-Phase Infiltration in a Partially Saturated Soil." *Transport in Porous Media*. (1986):27-55.

(van Genuchten 1980) van Genuchten, M.T., 1980. "A Closed Form Equation for Predicting the Hydraulic Conductivity of Unsaturated Soils." *Soil Sciences America Journal*. 44:982-998.

(White and Nichols 1993) White, M.D., and W.E. Nichols, 1993. *MSTS: Multiphase Subsurface Transport Simulator Theory Manual*. Richland, Washington: Pacific Northwest Laboratory. PNL-8636.

APPENDIX A

MSTS SOIL CHARACTERISTIC CURVE PARAMETERS

APPENDIX A
MSTS Soil Characteristic Curve Parameters

The soil hydraulic conductivity values that were determined through the calibration of the Multiphase Subsurface Transport Simulator (MSTS) model are dependent upon the functional relations that were specified in the MSTS model to define the water-retention and relative permeability characteristics of each soil type. Functions are available in the MSTS code to describe the following liquid saturation and liquid-relative permeability relations, including: van Genuchten (1980), Brooks and Corey (1966), Mualem (1976), Burdine (1953), Corey (Pruess 1987), Fatt and Klikoff (1959), Leverett (Leverett 1941; Dell and Fetch 1985), Haverkamp (Haverkamp et al. 1977), Touma and Vauclin (1986), and the Dual-Porosity Model with van Genuchten relations (Klavetter and Peters 1986; Nitao 1988). The van Genuchten relation with Mualem's equation was chosen to describe the liquid saturation and liquid-relative permeability relations for this investigation. For this functional description, effective liquid saturation (S_l^*) is defined as a function of tension head (ψ) as:

$$S_l^* = [1+(\alpha\psi)^n]^{-m} \qquad \psi<0$$

$$S_l^* = 1 \qquad \psi\geq 0$$

The parameters α and n are empirically determined van Genuchten fitting parameters (α has the dimension L^{-1} and n is dimensionless) and m is a function of n:

$$m = 1 - \frac{1}{n}$$

These parameters are determined by fitting curves defining a soil's water retention (i.e., soil moisture vs. pressure) and/or unsaturated hydraulic conductivity characteristics to the van Genuchten function. With Mualem's equation specified, the relative permeability (k_{rl}) is defined as:

$$k_{rl}(S_l^*) = (S_l^*)^{\frac{1}{2}}[1-(1-(S_l^*)^{\frac{1}{m}})^m]^2$$

To model the movement of groundwater through the GO/UGMAS, the water-retention and liquid relative permeability characteristics of the soils should be known. However, these properties have not been determined for the soils at the Fernald site, therefore, the values of the parameters α, n, and m were estimated for the purpose of modeling the GO/UGMAS with MSTS.

The parameters α and n were estimated by fitting curves defining the moisture vs. pressure relationship for soil types similar to those at the Fernald site to the van Genuchten function using non-linear least

squares regression analysis. An α value of 0.019 1/cm and an n value of 2.0 was used for the coarse soils including the unsaturated GMA, Paddys Run alluvium, and the sands. These values were determined from water retention data for a medium sand (the HT-1 sand) described by Johnson et al. (1983). An α value of 0.0035 1/cm and an n value of 1.43 was used for the fine-grained soils in the model. These parameters were determined from water retention data for a loess soil (Peoria Loess) described by Johnson et al. (1983). The model is rather insensitive to the value of these parameters if the soil is saturated, as is the case with the soils in the glacial overburden above the unsaturated GMA, since the relative permeability does not change if the soil is fully saturated. However, the model is sensitive to the value of the parameters if the soil is unsaturated, as is the case with the upper GMA, because the relative permeability of the soil decreases with decreasing saturation. Therefore, calibration results obtained with the MSTS model should be considered estimated values because of the fact that data are not available to describe the soil-moisture retention and liquid-relative permeability characteristics of the soils at the Fernald site.

APPENDIX B

CROSS-SECTIONAL STEADY-STATE FLOW FIGURES AND TABLES

Table 1B - Initial Steady-State Flow Parameters Used for MSTS Row 80 Cross-Section Model

Soil Type		K_h (ft/day)*	K_v (ft/day)*	Porosity
1	Inactive Nodes	1.00E-05	1.00E-05	0.1
2	Brown Till	0.25	2.5	0.45
3	Gray Till - Layer 2	0.25	0.025	0.34
4	Gray Sand	450	4.5	0.365
5	Gray Till - Layer 3	0.14	0.014	0.335
6	Gray Till - Layer 4	0.079	0.0079	0.33
7	GMA	1.00E-05	45	0.39
8	Paddys Run/SSOD Alluvium	450	45	0.39
9	Paddys Run/SSOD Streambed	450	45	0.39

*Multiply by 3.5278 x 10^{-4} to convert to cm/s

Table 2B - Final "Calibrated" Steady-State Flow Parameters Used for MSTS Row 80 Cross-Section Model

Soil type	K_h (ft/day)*	K_v (ft/day)*	Porosity
1	---	---	---
2	0.25	2.5	0.45
3	0.25	0.025	0.34
4	2.5	0.25	0.365
5	0.14	0.014	0.335
6	0.079	0.00088	0.33
7	450	45	0.39
8	450	45	0.39
9	450	45	0.39

*Multiply by 3.5278 x 10^{-4} to convert to cm/s

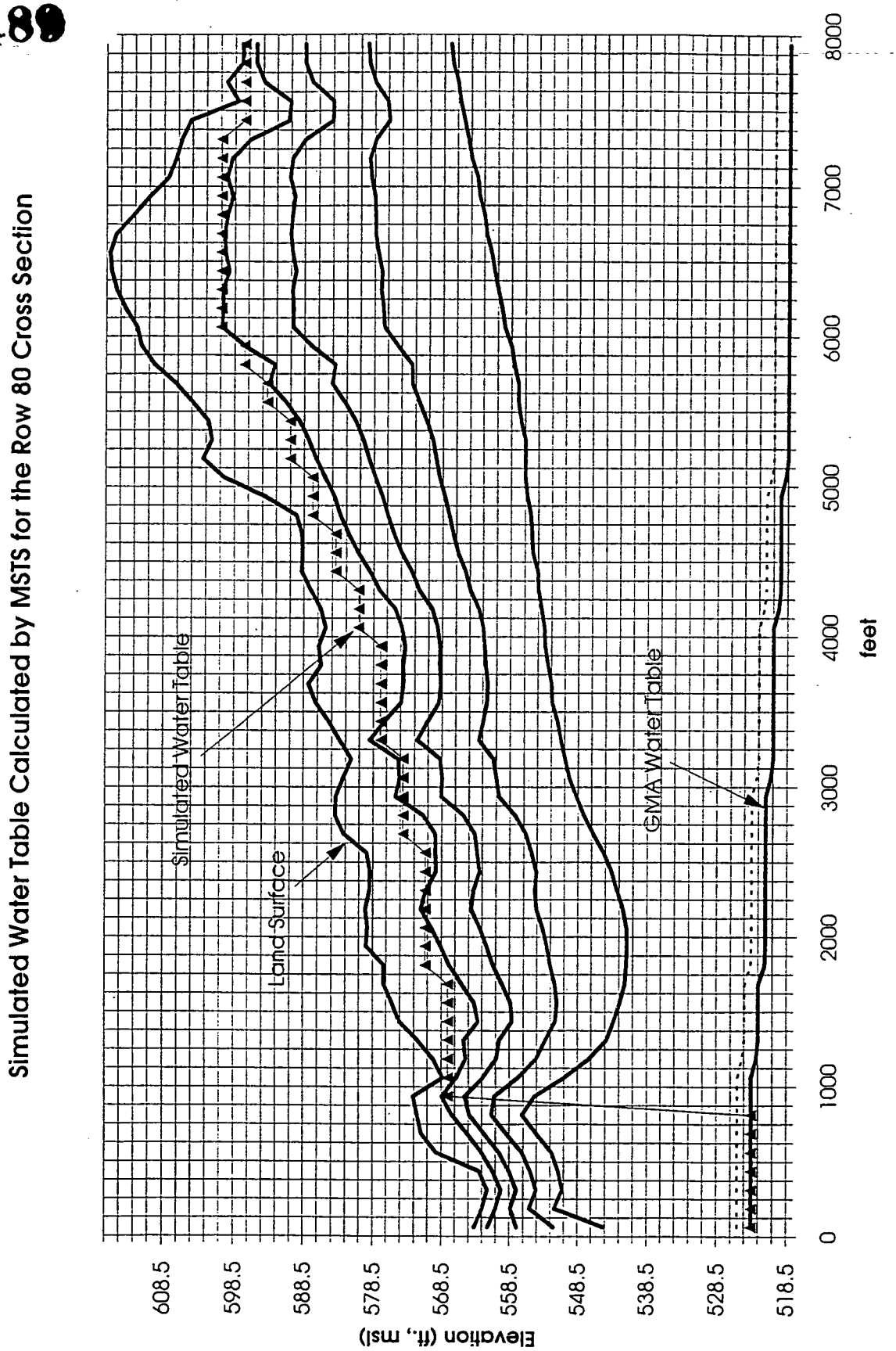

Figure 1B - Simulated Water Table Calculated by MSTS for the Row 80 Cross-Section

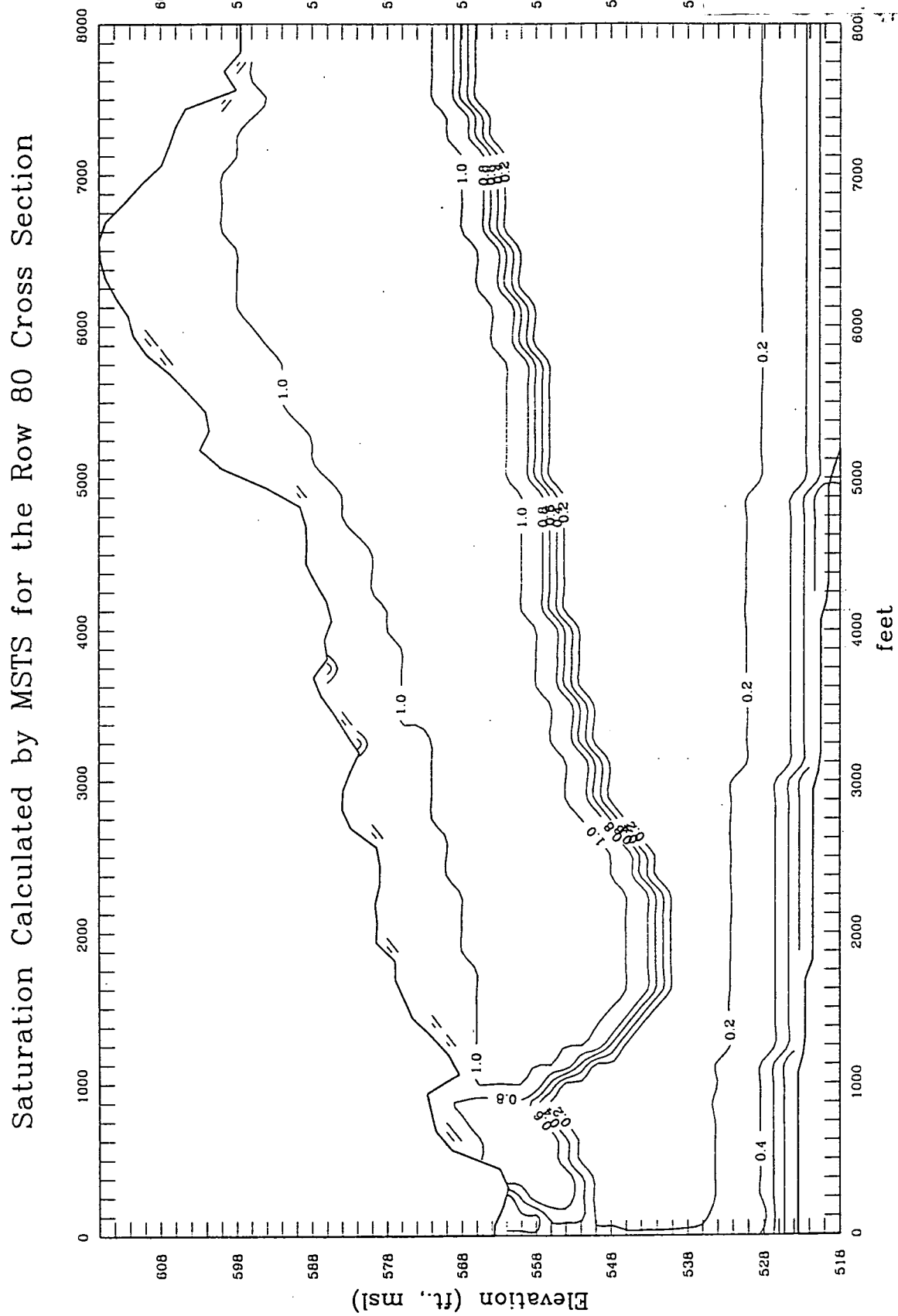

Figure 2B - Saturation Calculated by MSTS for the Row 80 Cross-Section

5489

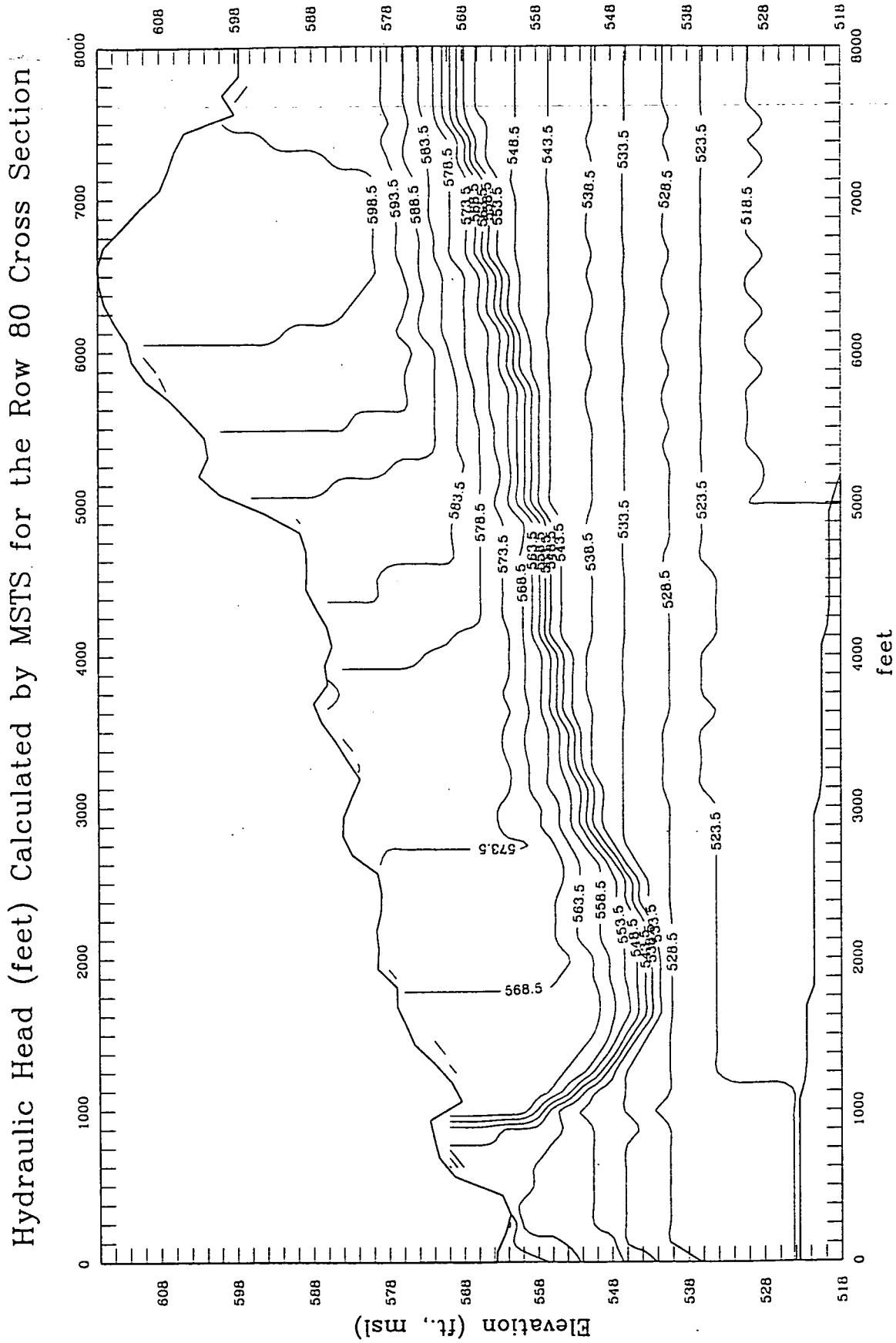

Figure 3B - Hydraulic Head (feet) Calculated by MSTS for the Row 80 Cross-Section

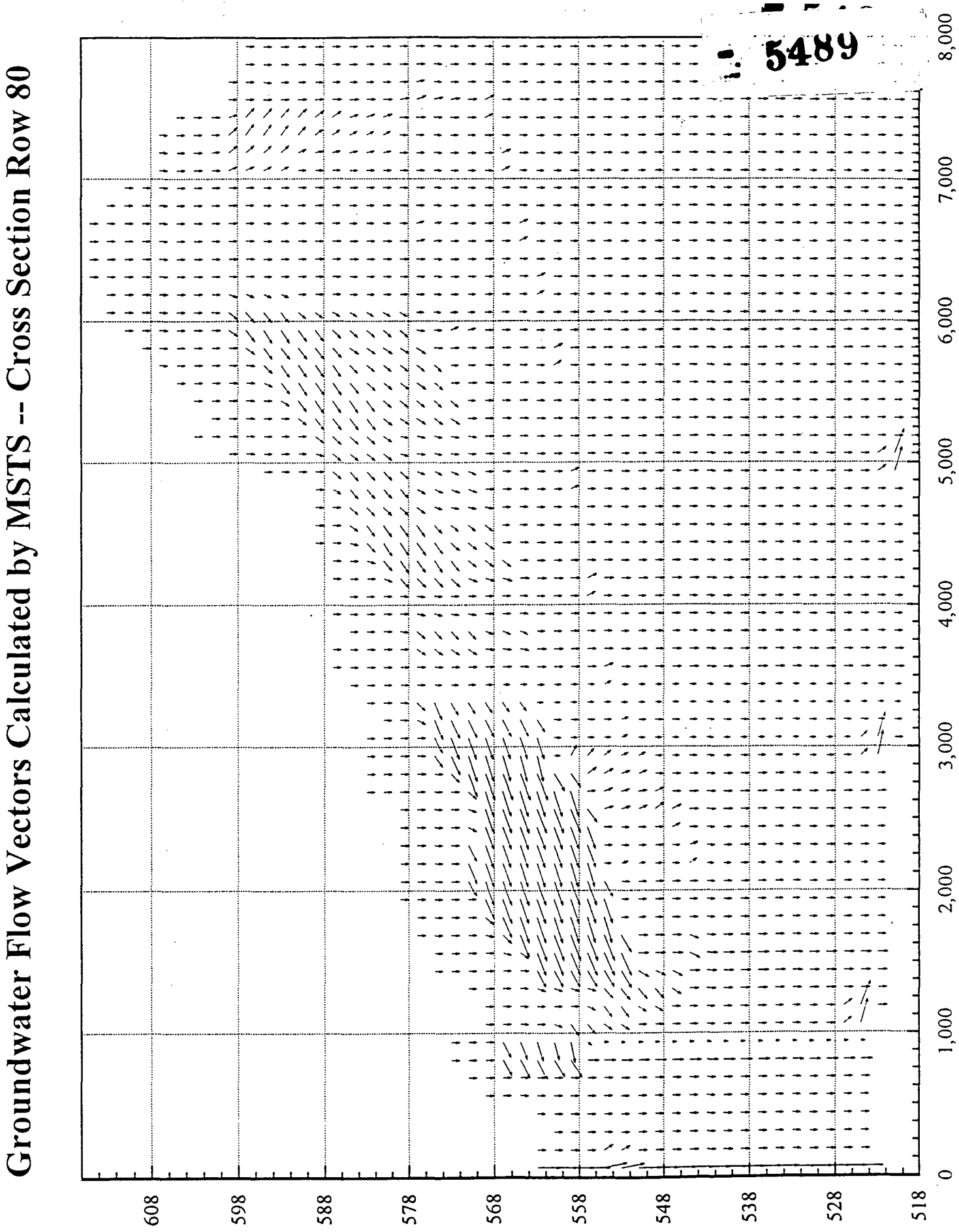

Figure 4B - Groundwater Flow Vectors Calculated by MSTS - Cross-Section Row 80

Table 3B - Initially Used Site Characterization Data and Values Determined from Calibration of the MSTS Cross-Section A-A' Model

Initially Used Site Characterization Data					Parameters Determined from Calibration of MSTS Model - Cross-Section A-A'			
Soil Type		K_h (ft/day)*	K_v (ft/day)*	Porosity	Soil Type	K_h (ft/day)*	K_v (ft/day)*	Porosity
1	Inactive	1.00E-05	1.00E-05	0.1	1	---	---	---
2	Brown Till	0.1	1	0.45	2	0.1	1	0.45
3	Gray Till - Layer 2	0.0055	0.0011	0.34	3	0.055	0.011	0.34
4	Gray Sand	2.3	0.023	0.39	4	2.3	0.023	0.39
5	Gray Till - Layer 3	0.0055	0.0011	0.34	5	0.055	0.011	0.34
6	Gray Till - Layer 4	0.0055	0.0011	0.34	6	0.0055	0.0011	0.34
7	GMA	1.00E-05	45	0.39	7	45	45	0.39
8	Paddys Run/SSOD Alluvium	10	10	0.35	9	10	10	0.35
9	Paddys Run/SSOD Streambed	10	10	0.35	9	10	10	0.35
10	Gray Silt	0.25	0.0025	0.35	10	0.25	0.025	0.35
11	Brown Sand	5	0.05	0.39	11	5	0.05	0.39
12	Brown Silt	0.28	0.0028	0.35	12	0.28	0.028	0.35

*Multiply by 3.5278 x 10^{-4} to convert to cm/s

5489

000089

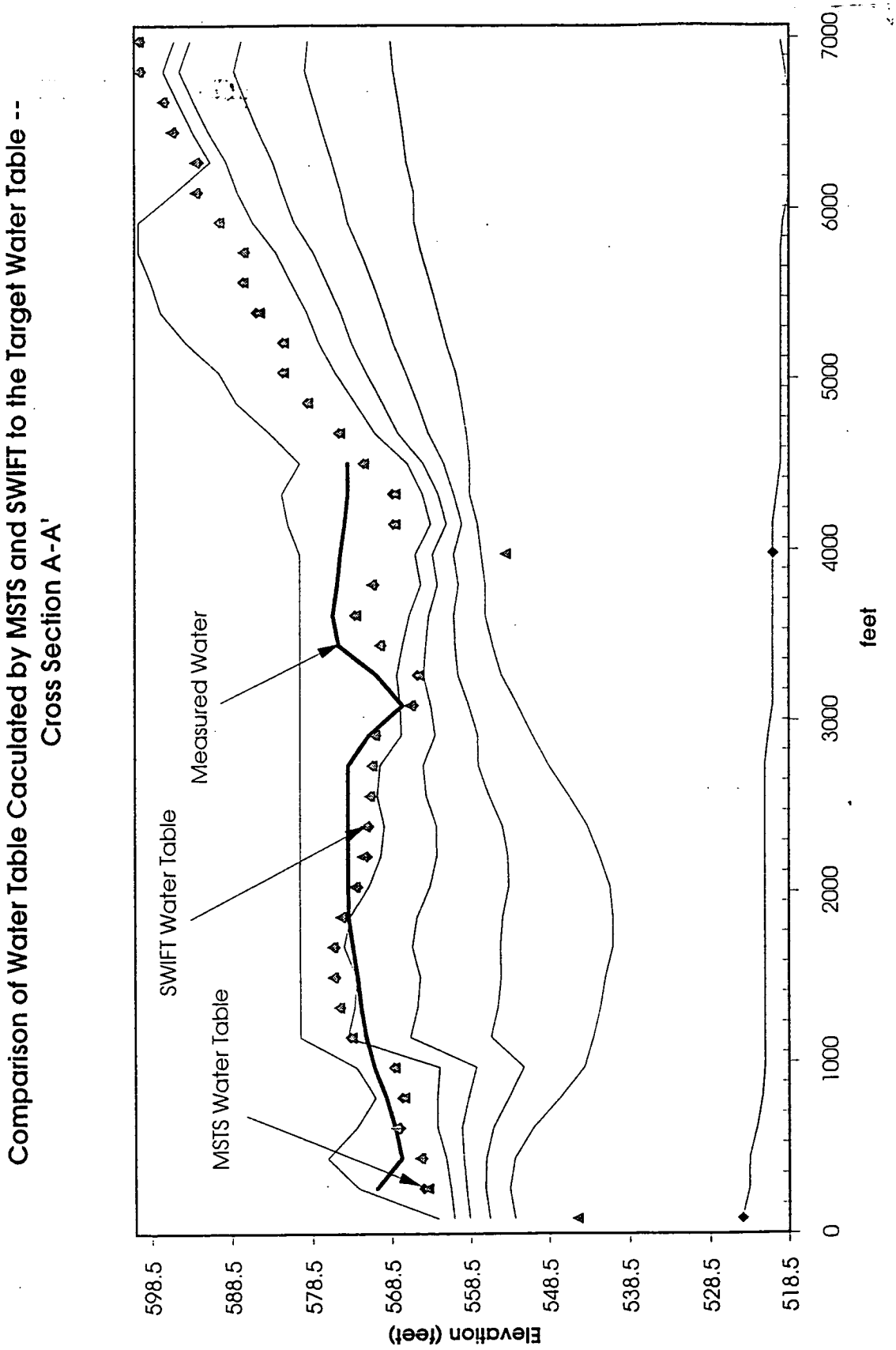

Figure 5B - Comparison of MSTS, SWIFT and Target Water Tables - Cross-Section A-A'

5489

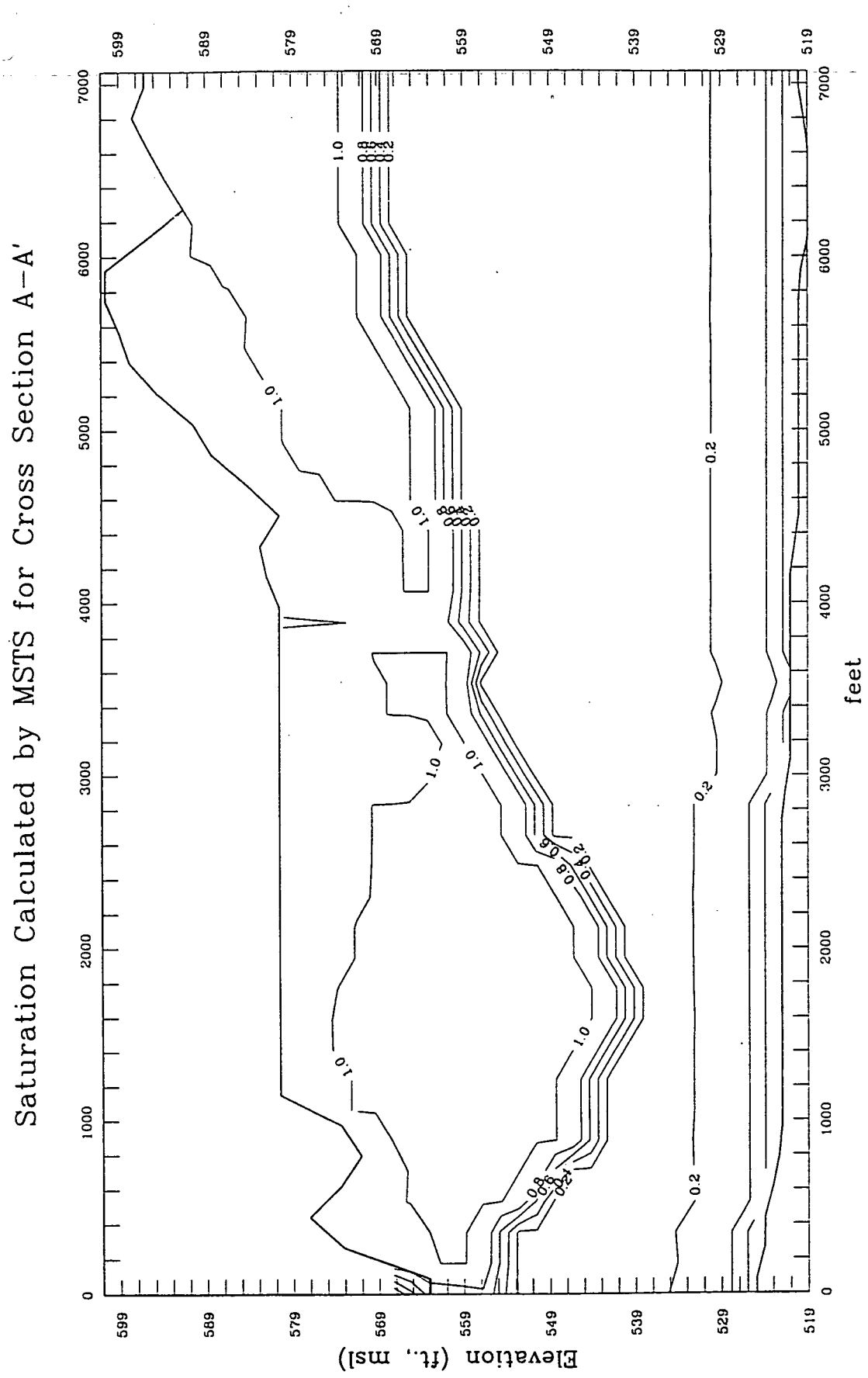

Figure 6B - Saturation Calculated by MSTS for Cross-Section A-A'

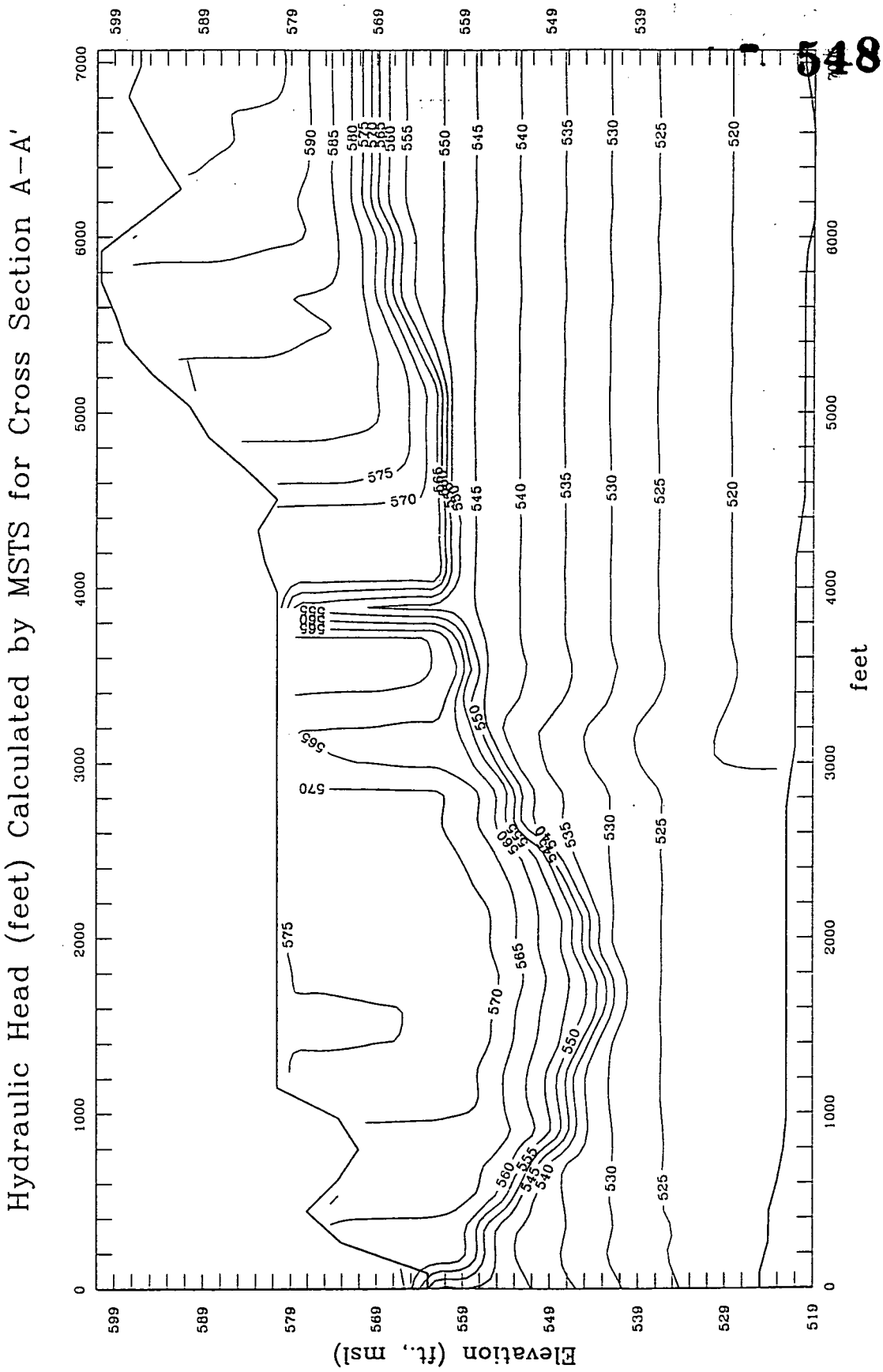

Figure 7B - Hydraulic Head (feet) Calculated by MSTS for Cross-Section A-A'

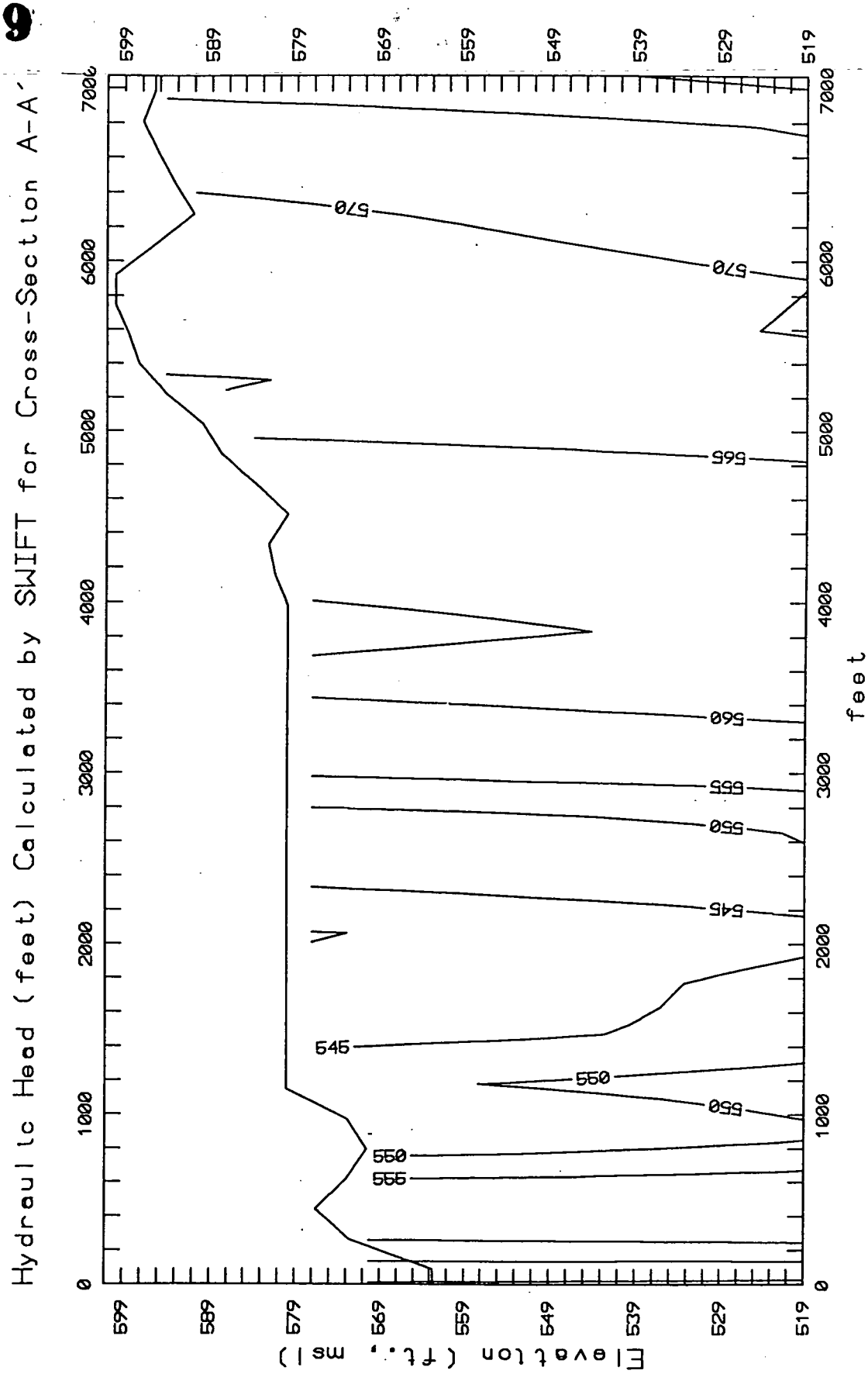

Figure 8B - Hydraulic Head (feet) Calculated by SWIFT for Cross-Section A-A'

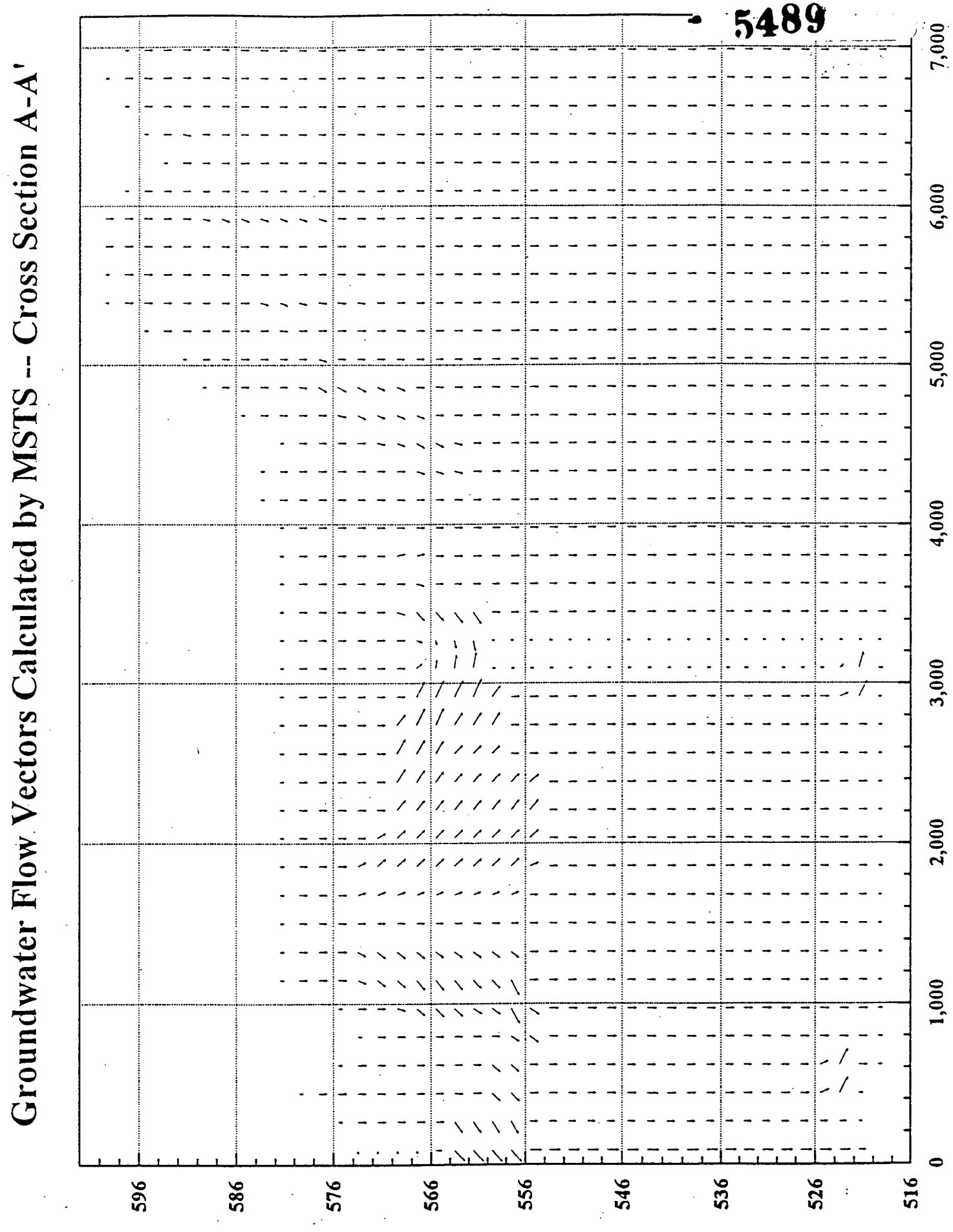

Figure 9B - Groundwater Flow Vectors Calculated by MSTS - Cross-Section A-A'

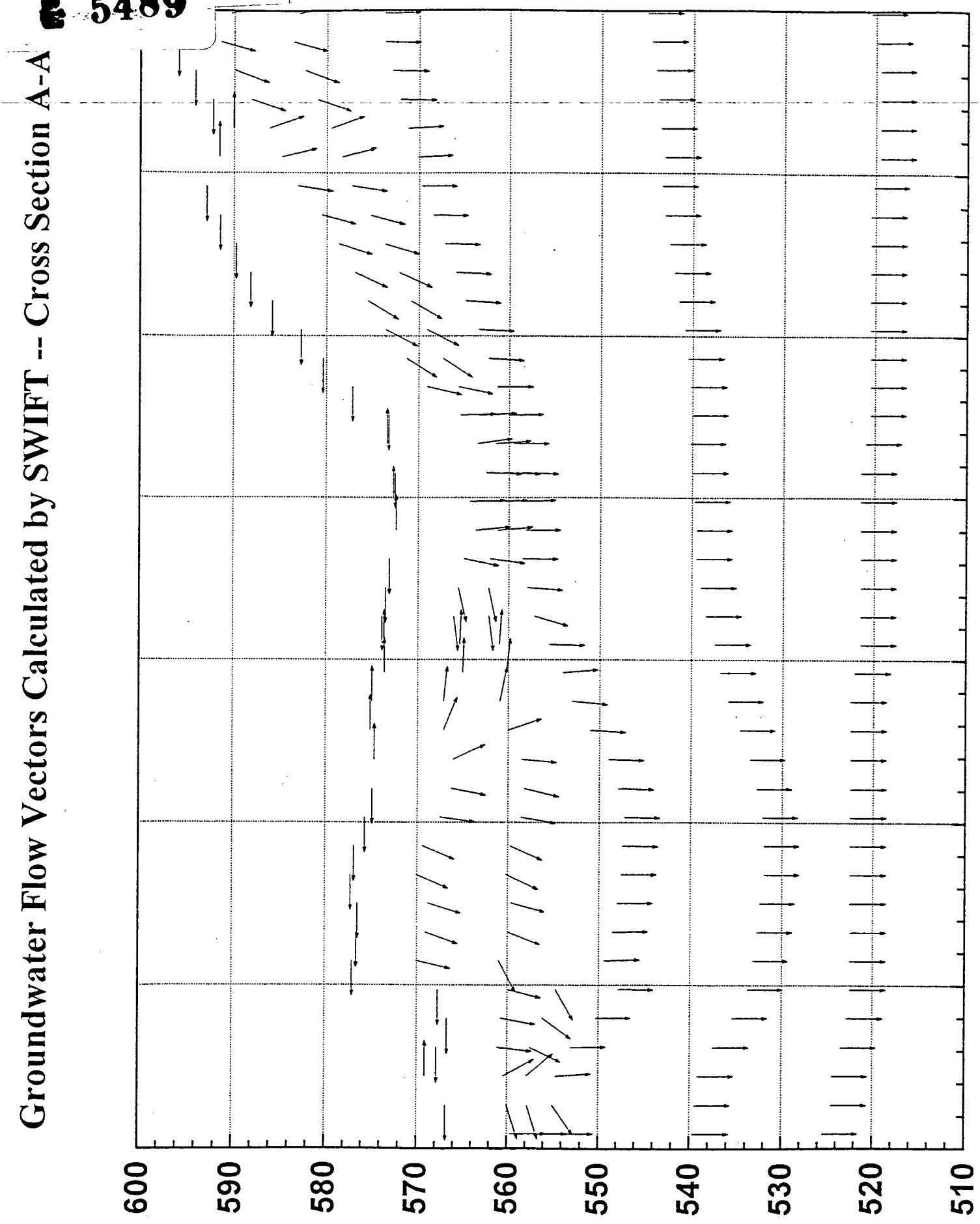

Figure 10B - Groundwater Flow Vectors Calculated by SWIFT - Cross-Section A-A'

APPENDIX C

3-D FLOW MODEL FIGURES AND TABLES

Table 1C - Key for Layer-Specific Soil Type Maps

1	=	Inactive
2	=	Brown Till
3	=	Bray Till (Layer 2)
4	=	Gray Deltaic Sand
5	=	Gray Till (Layer 3)
6	=	Gray Till (Layer 4)
7	=	Upper GMA Sand
8	=	Paddys Run/SSOD Alluvium
9	=	Paddys Run/SSOD Streambed
X	=	Gray Lacustrine Silt
0	=	Brown Deltaic Sand
*	=	Brown Lacustrine Silt

Figure 1C - Layer 1 - Rock Types

Figure 2C - Layer 2 - Rock Types

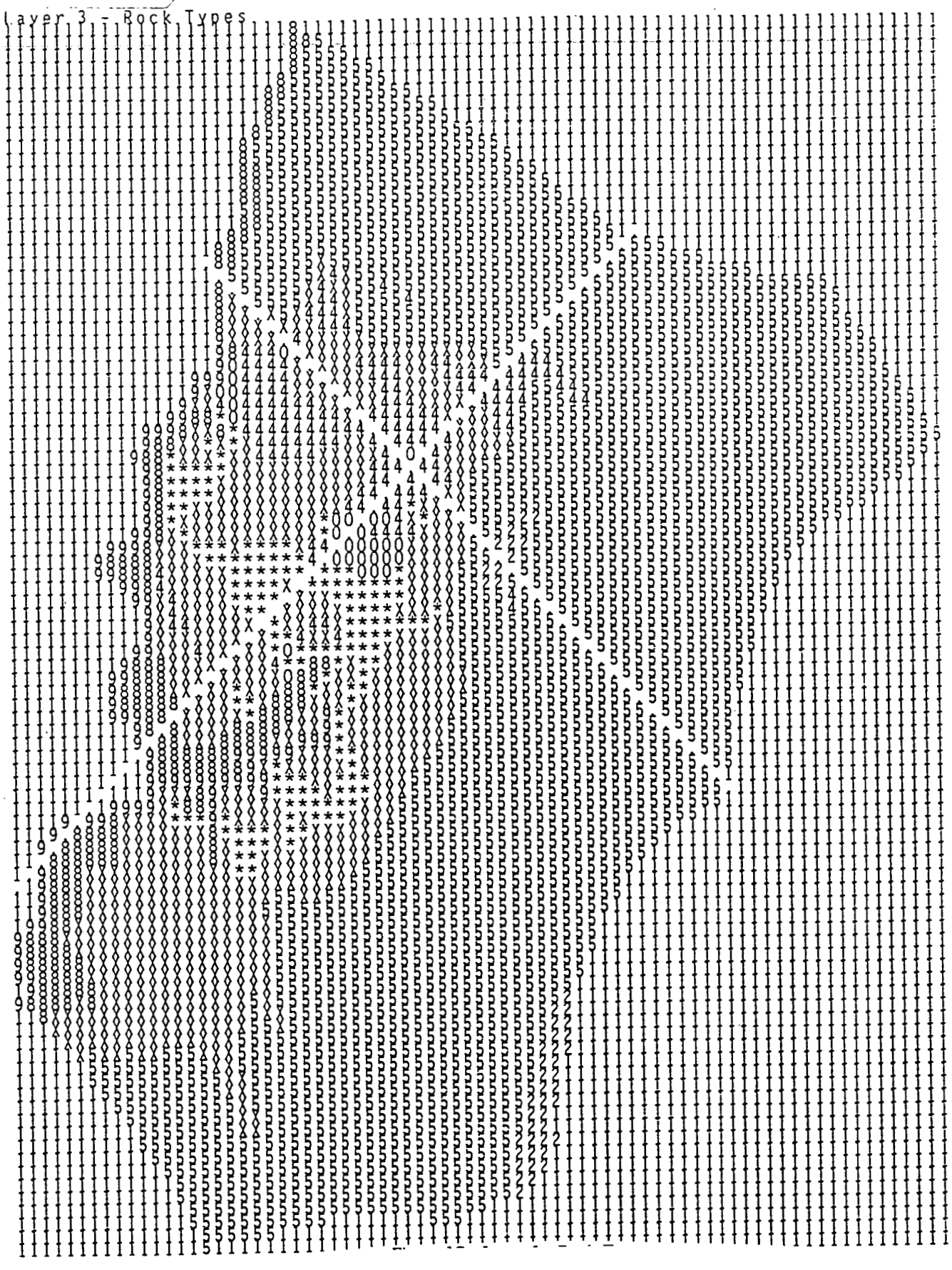

Figure 3C - Layer 3 - Rock Types

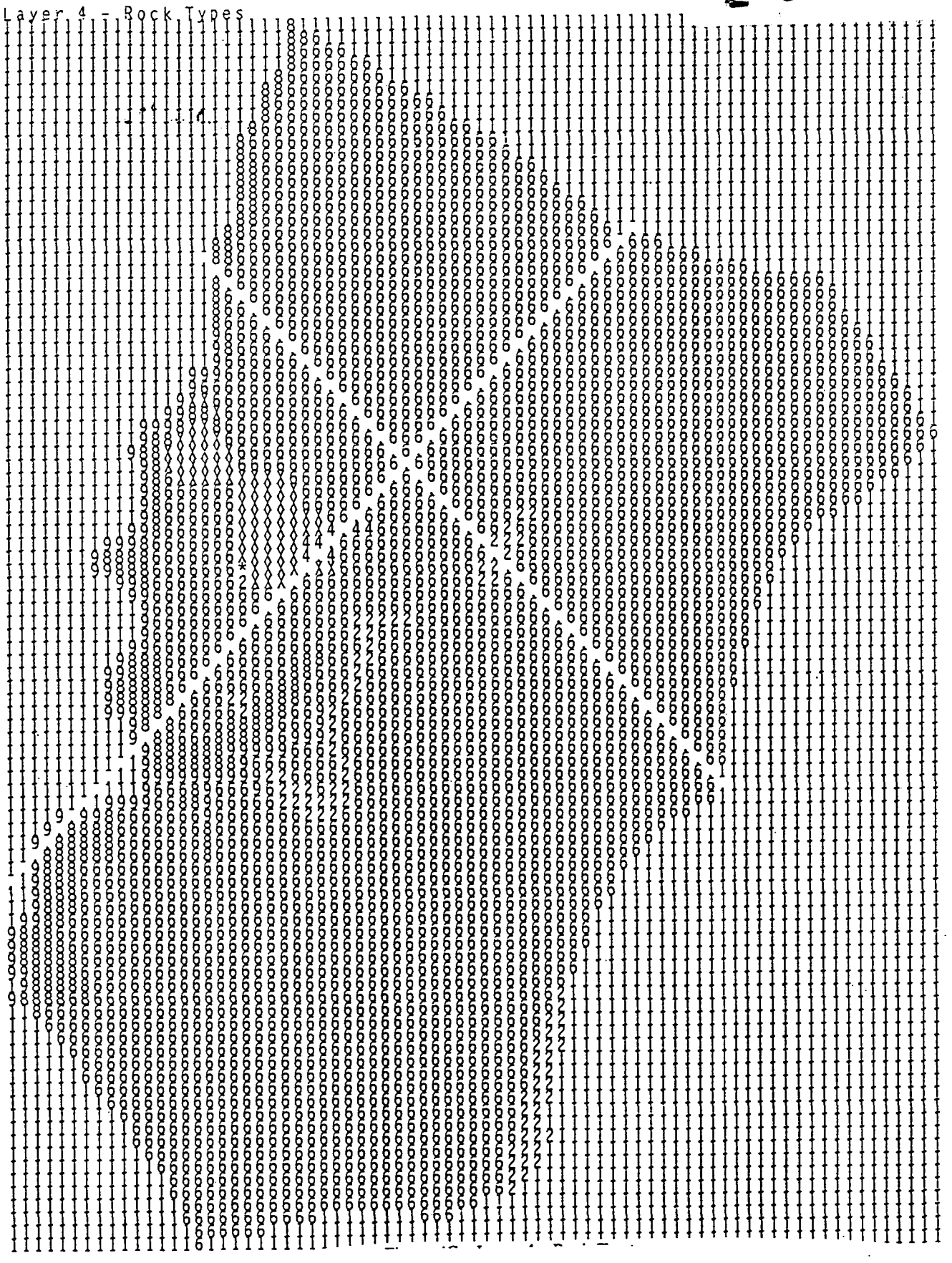

Figure 4C - Layer 4 - Rock Types

5489

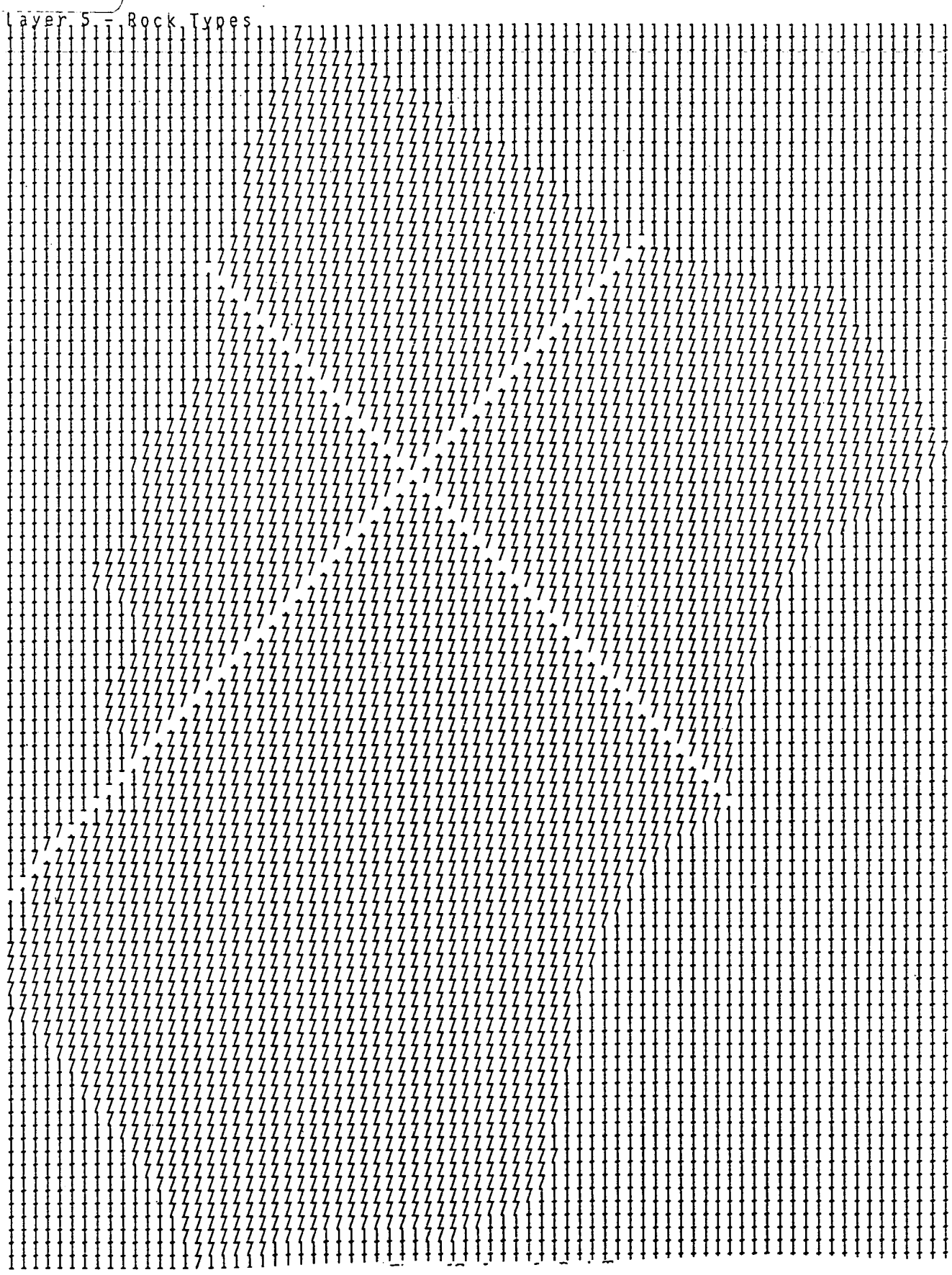

Figure 5C - Layer 5 - Rock Types

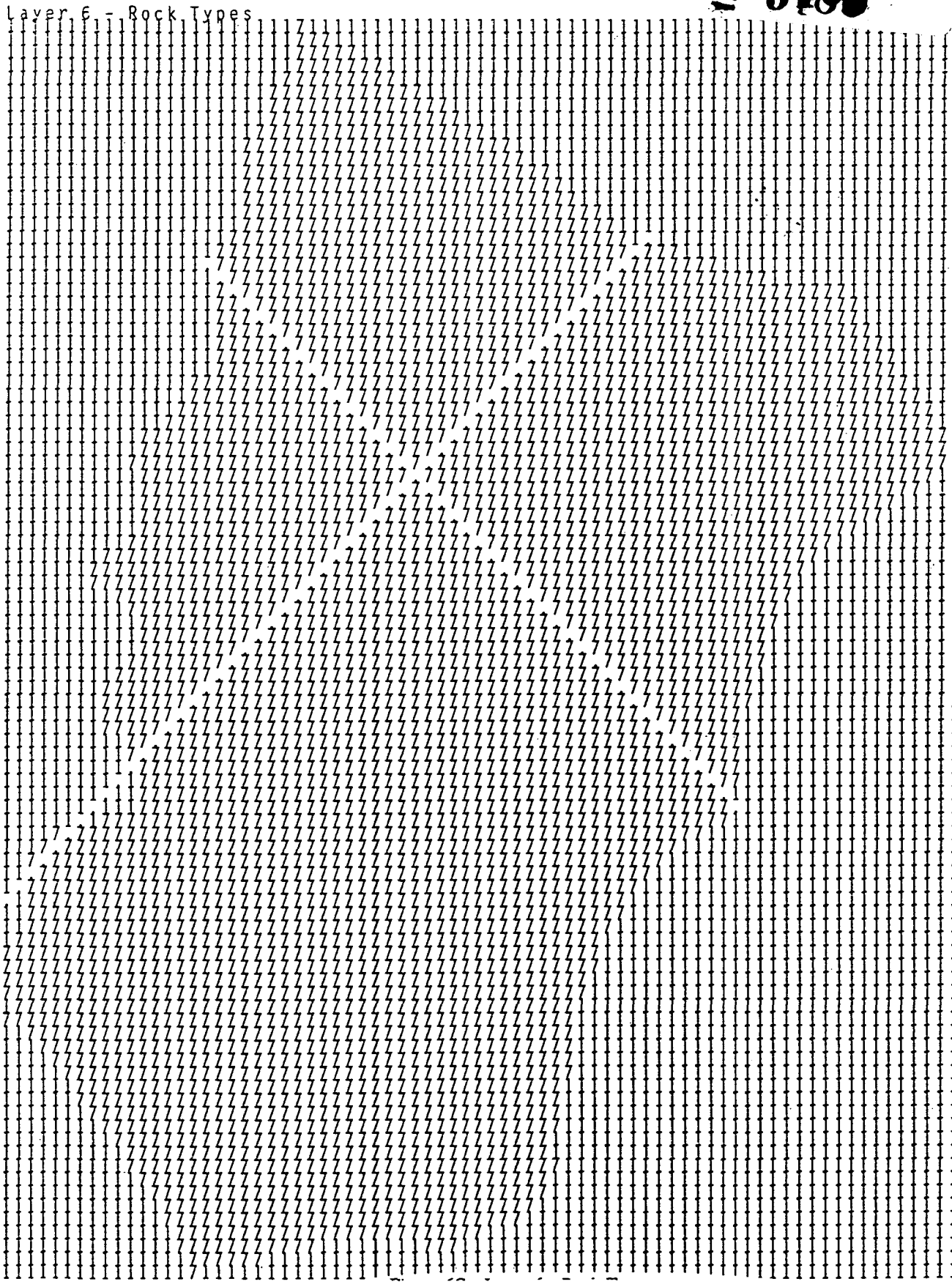

Figure 6C - Layer 6 - Rock Types

5489

Table 2C - Key for Initial Surface Recharge Distribution Map

0 = Inactive

1 = 7.25 in/yr

2 = 10.875 in/yr

Layer 1 - Recharge

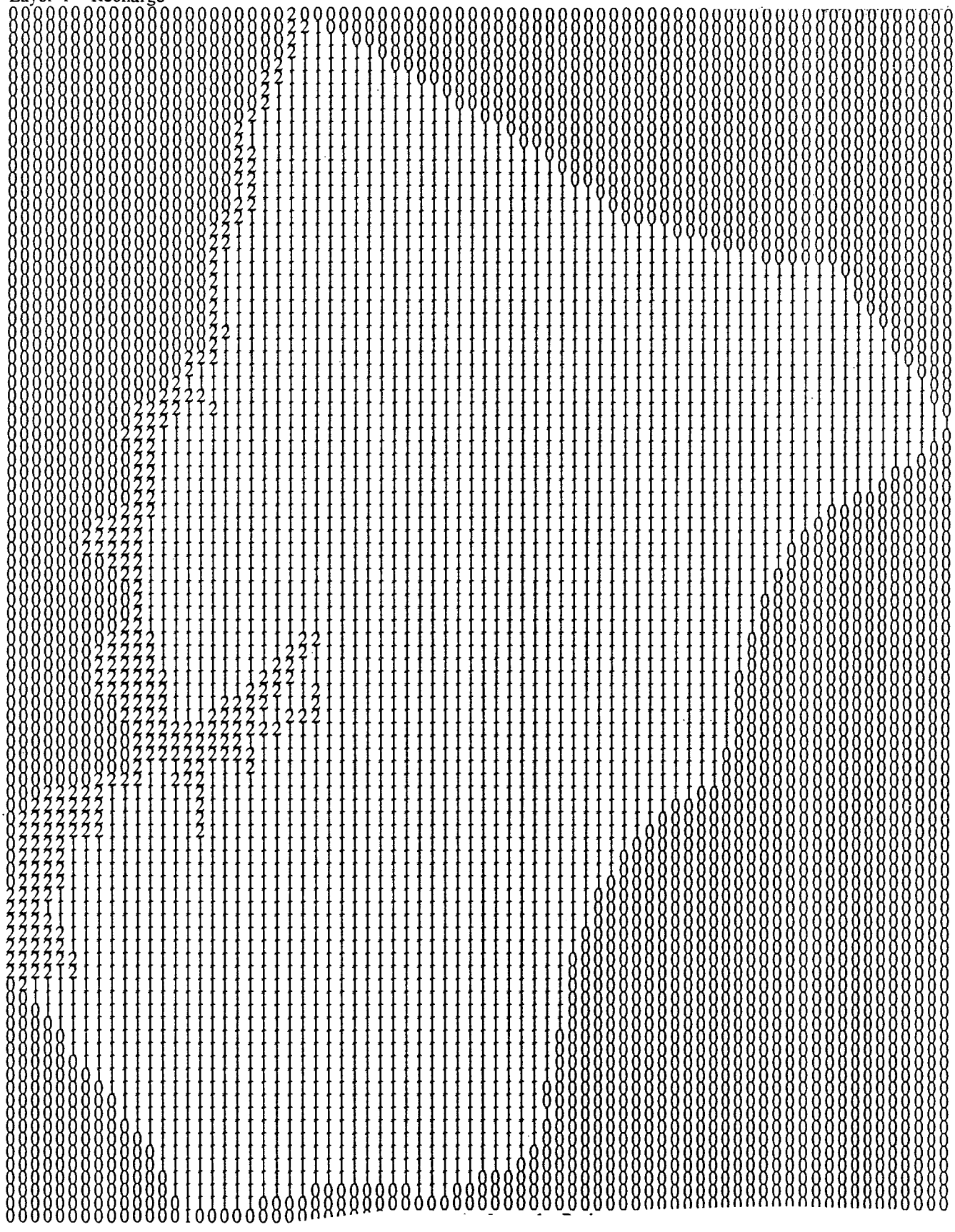

Figure 7C - Layer 1 - Recharge

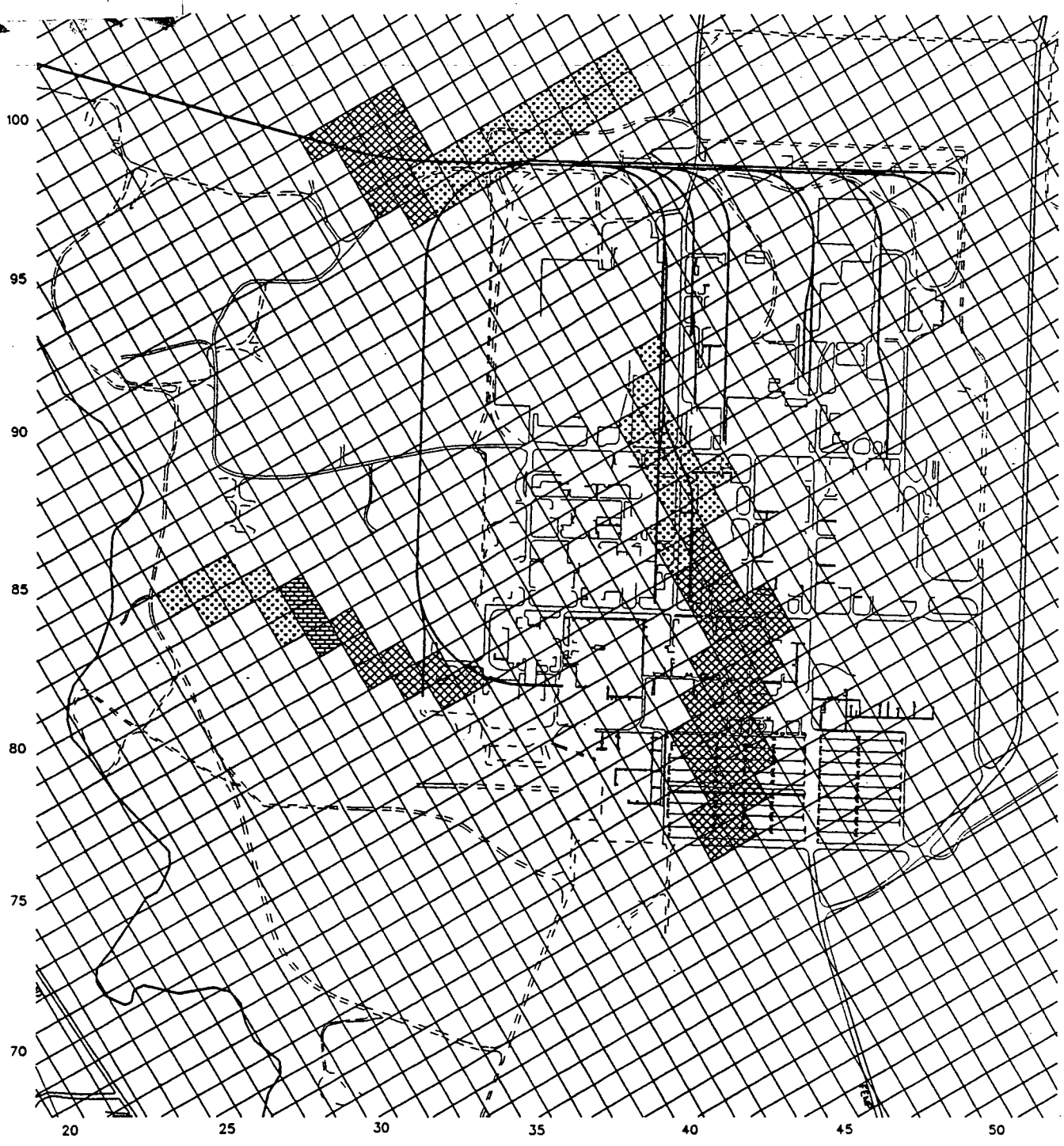

DISCHARGE

0.0926 gpm

0.0741 gpm

0.0556 gpm

MAP OF GO/UGMAS DISCHARGE MAGNITUDES AND LOCATIONS

Figure 8C - Map of GO/UGMAS Discharge Magnitudes and Locations

Table 3C - Key for Final Calibrated Surface Recharge Distribution Map

0 = Inactive

1 = 6 in/yr

2 = 12 in/yr

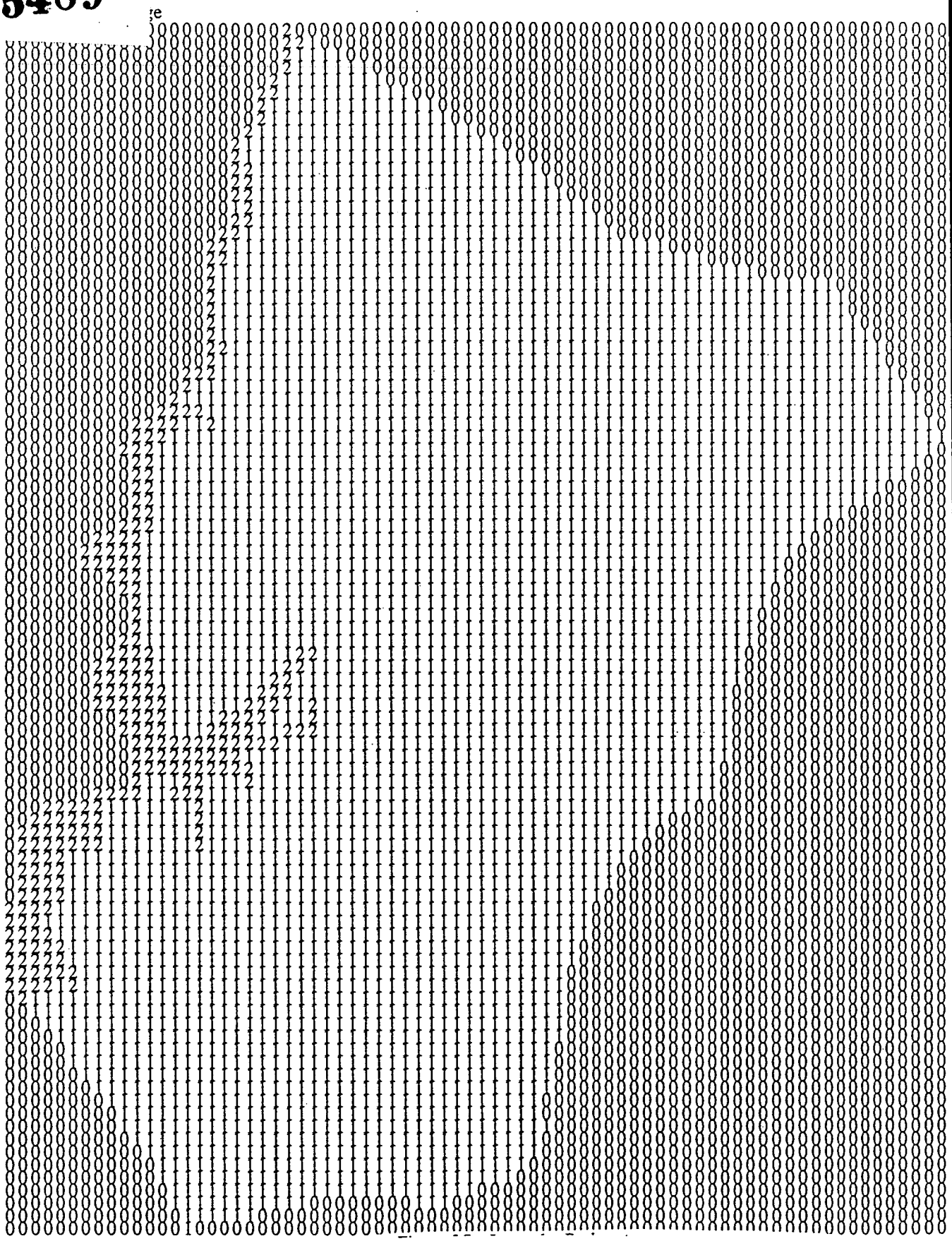

Figure 9C - Layer 1 - Recharge

TILL PERCHED WATER LEVEL

5489

CONTOURED 1000 SERIES WELL MEASUREMENTS

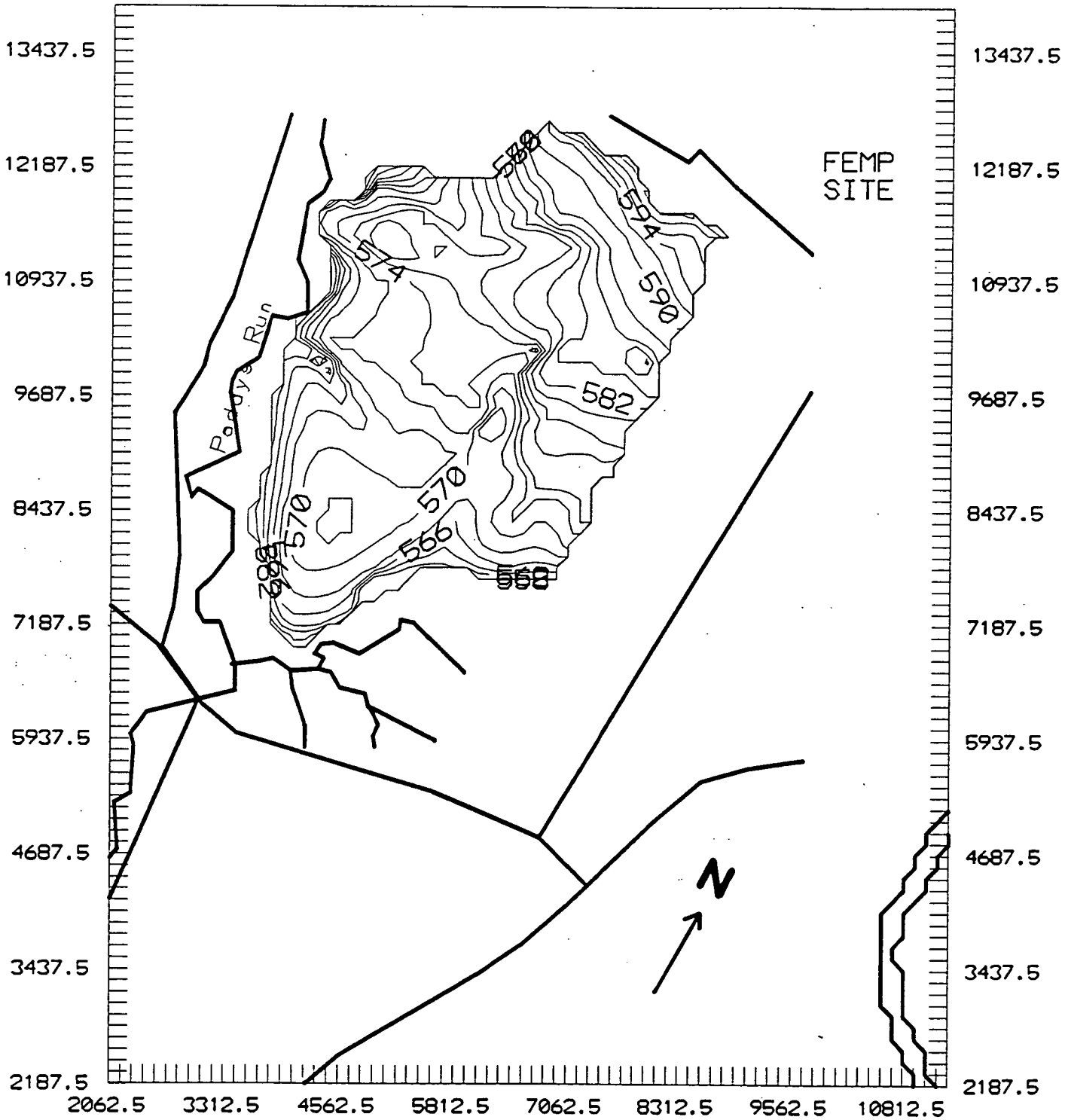

Figure 10C - Till Perched Water Level

LAYER 1 HEAD, CALIBRATED FLOW RUN

5489 BOTTOM HEADS ADJUSTED ITERATIVELY TO MATCH MEASURED TILL WATER LEVELS

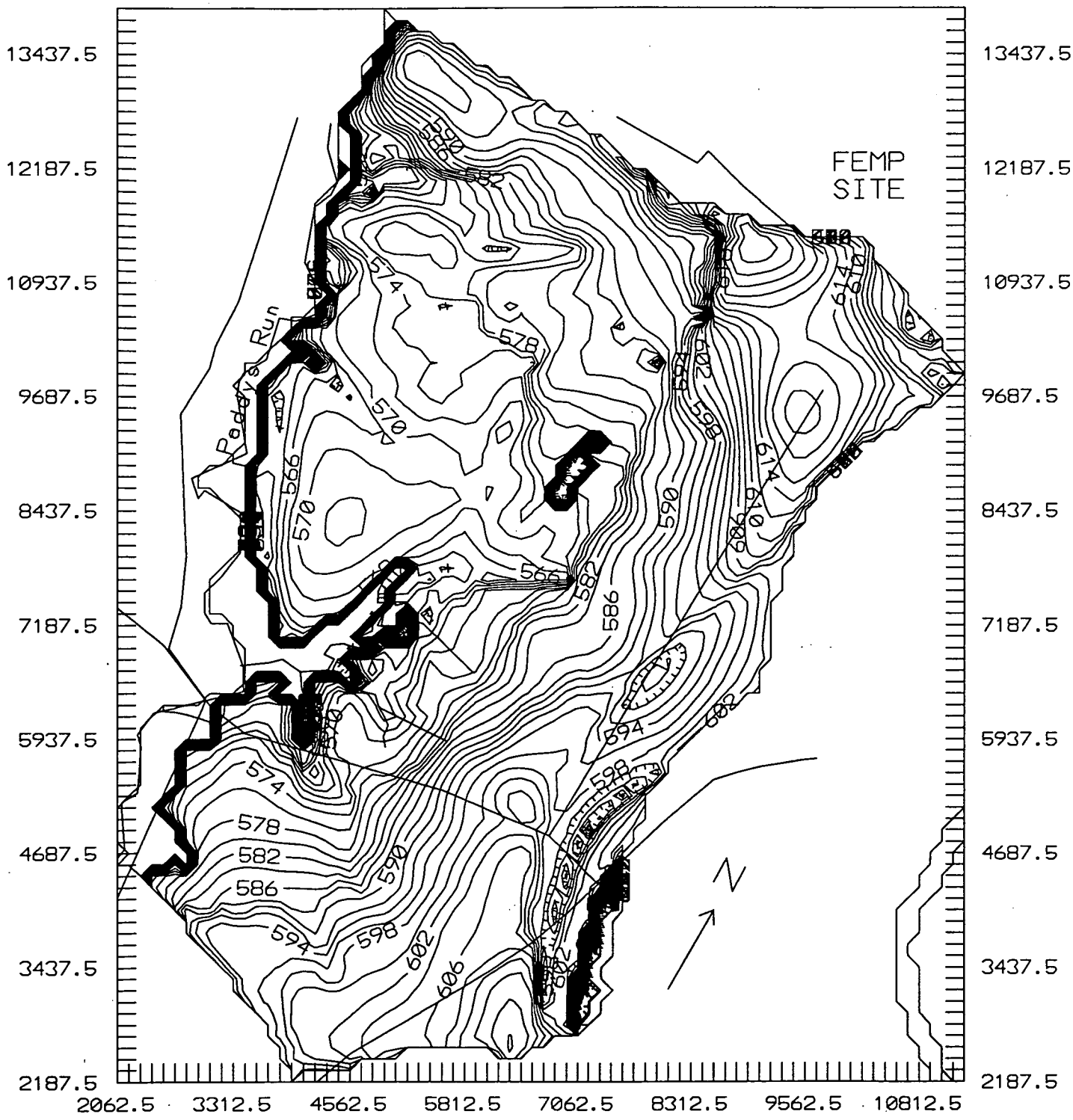

Figure 11C - Layer 1 Head, Calibrated Flow Run

RESIDUAL FOR CALIBRATED FLOW RUN

CALCULATED LAYER 1 HEAD MINUS MEASURED TILL WATER LEVEL

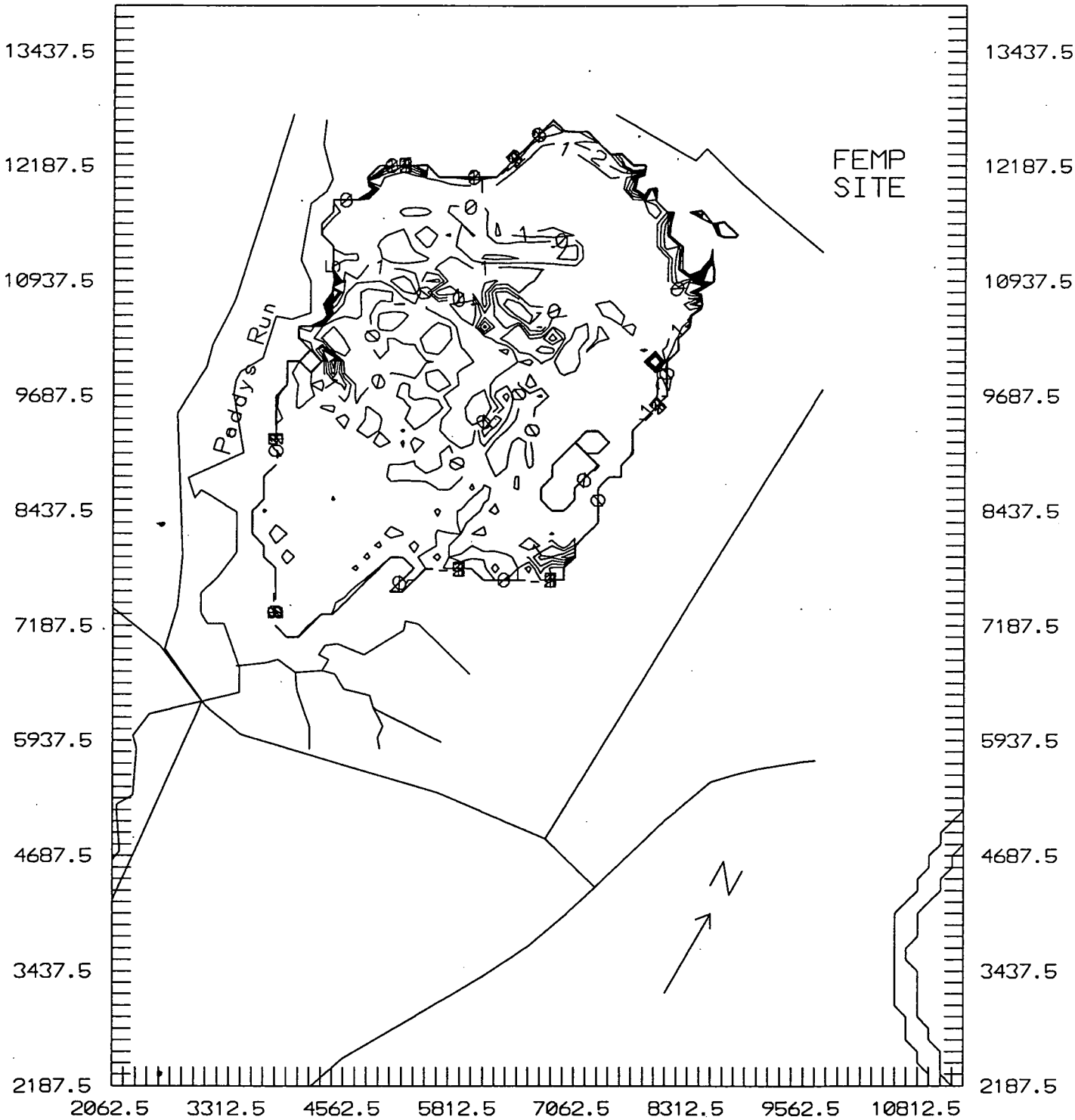

Figure 12C - Residual for Calibrated Flow Run

LAYER 2 HEAD, CALIBRATED FLOW RUN

BOTTOM HEADS ADJUSTED ITERATIVELY TO MATCH MEASURED TILL WATER LEVELS

5489

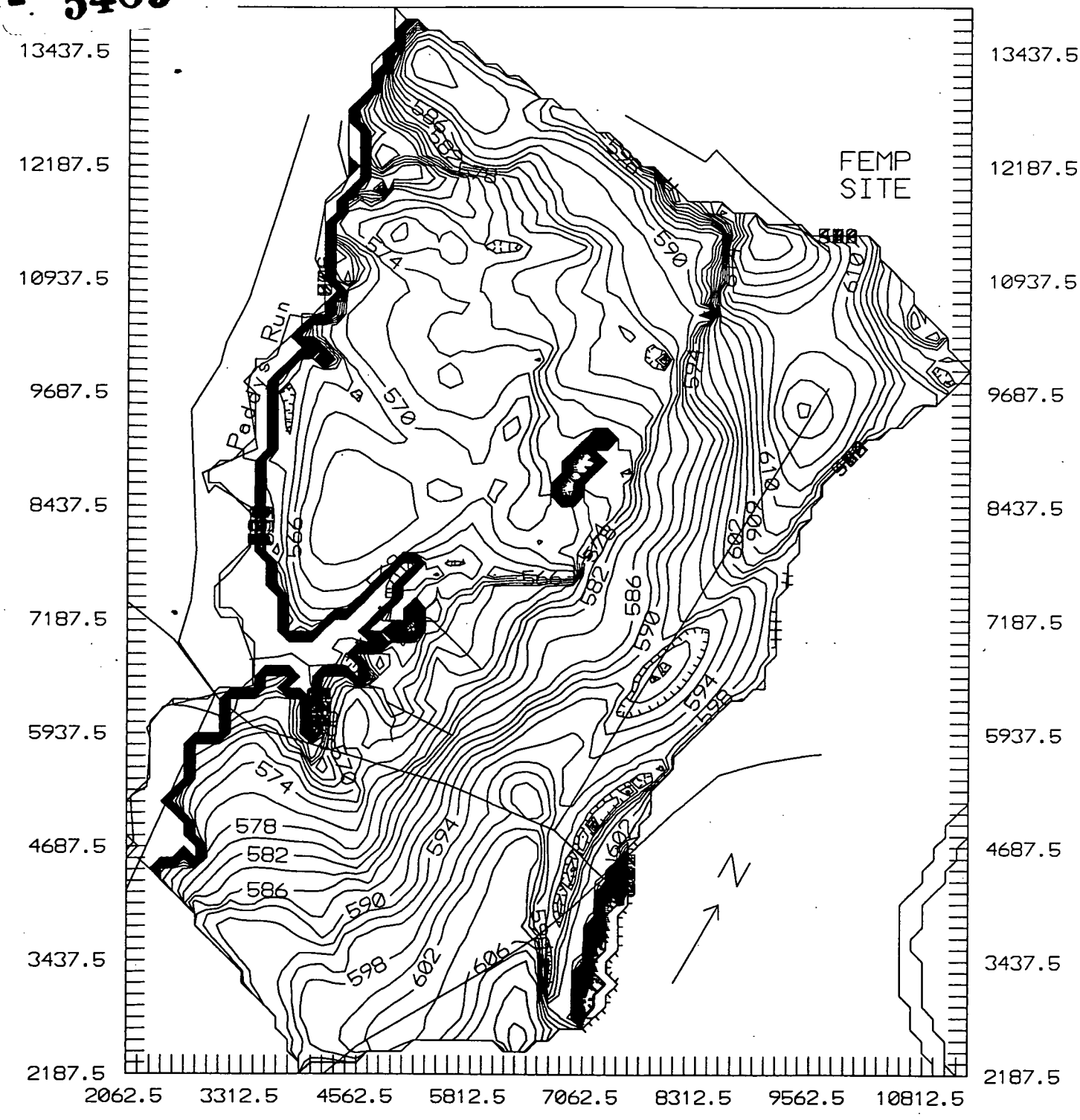

Figure 13C - Layer 2 Head, Calibrated Flow Run

LAYER 3 HEAD, CALIBRATED FLOW RUN

BOTTOM HEADS ADJUSTED ITERATIVELY TO MATCH MEASURED TILL WATER LEVELS

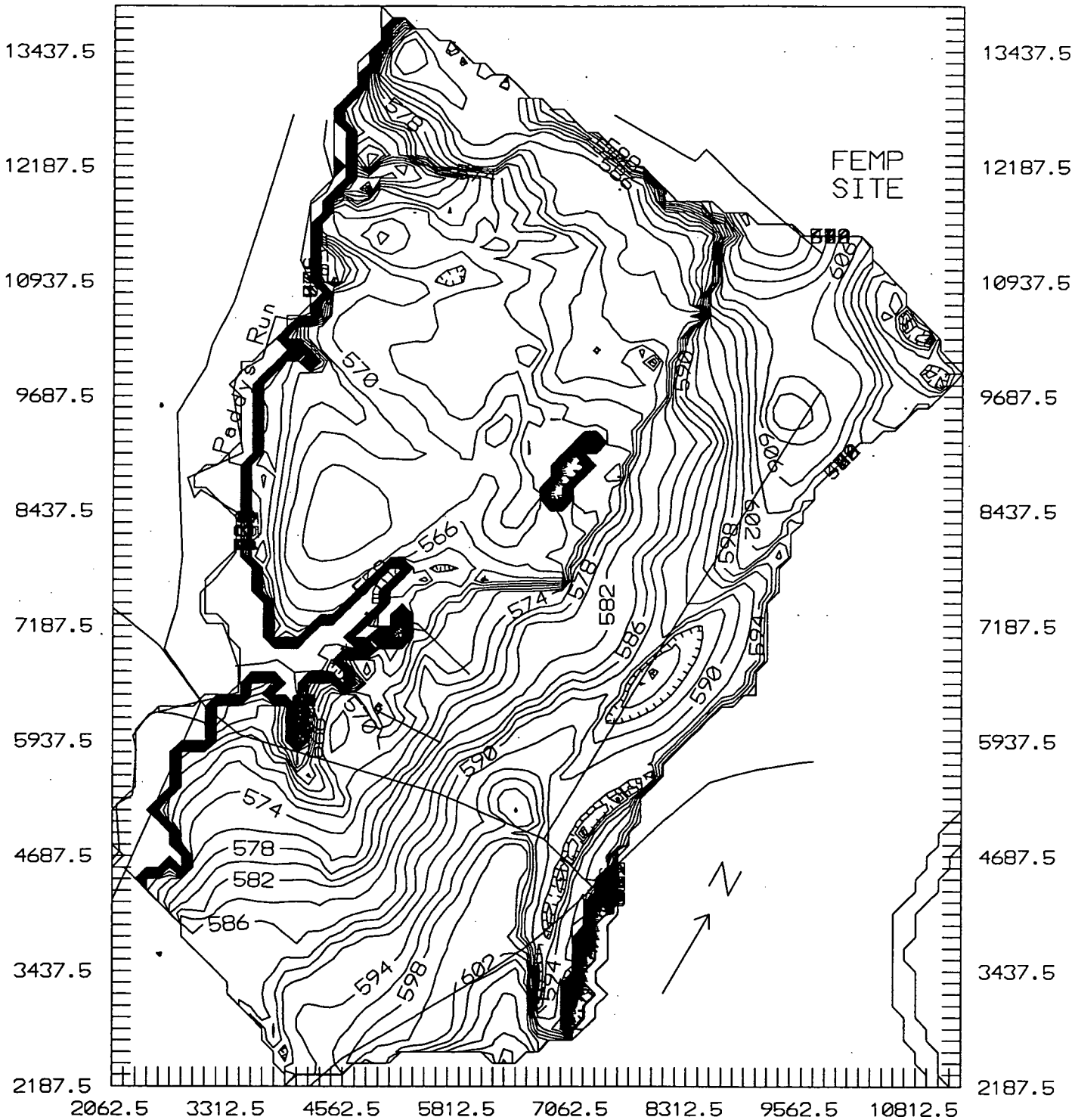

Figure 14C - Layer 3 Head, Calibrated Flow Run

ER 4 HEAD, CALIBRATED FLOW RUN

BOTTOM HEADS ADJUSTED ITERATIVELY TO MATCH MEASURED TILL WATER LEVELS

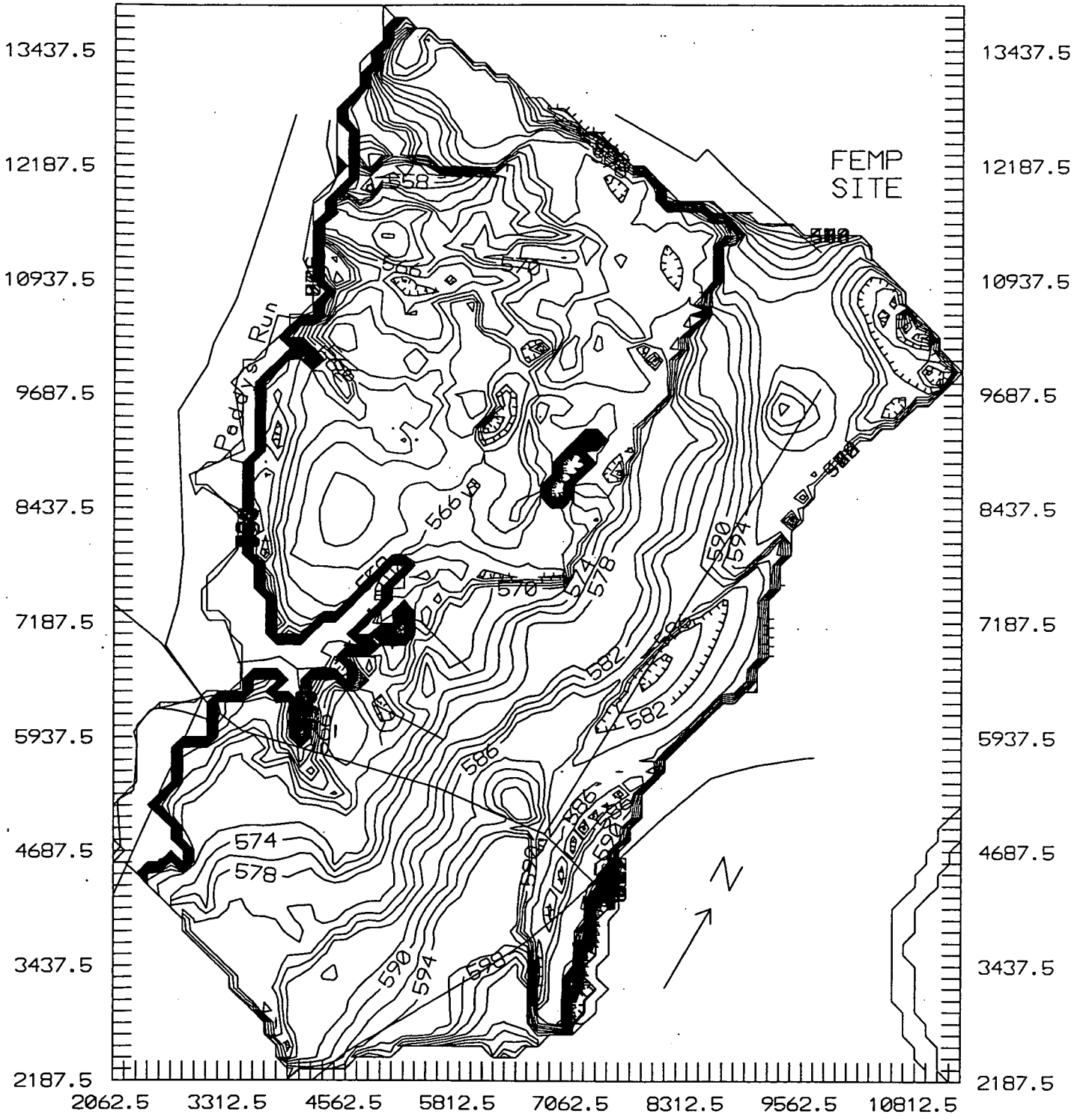

Figure 15C - Layer 4 Head, Calibrated Flow Run

LAYER 5 HEAD, CALIBRATED FLOW RUN

BOTTOM HEADS ADJUSTED ITERATIVE
MATCH MEASURED TILL WATER LEV

5489

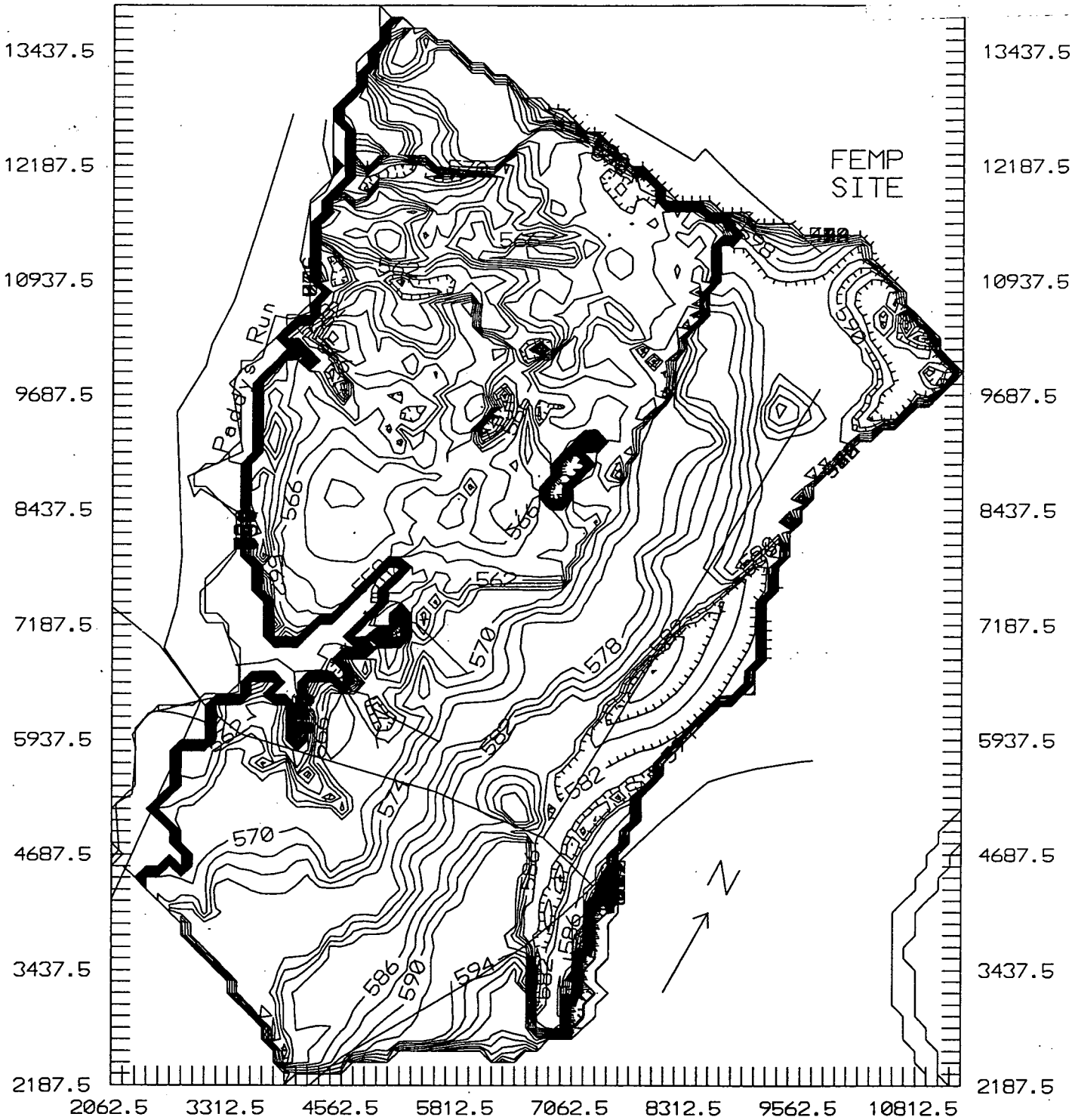

Figure 16C - Layer 5 Head, Calibrated Flow Run

5489

6 HEAD, CALIBRATED FLOW RUN

BOTTOM HEADS ADJUSTED ITERATIVELY TO MATCH MEASURED TILL WATER LEVELS

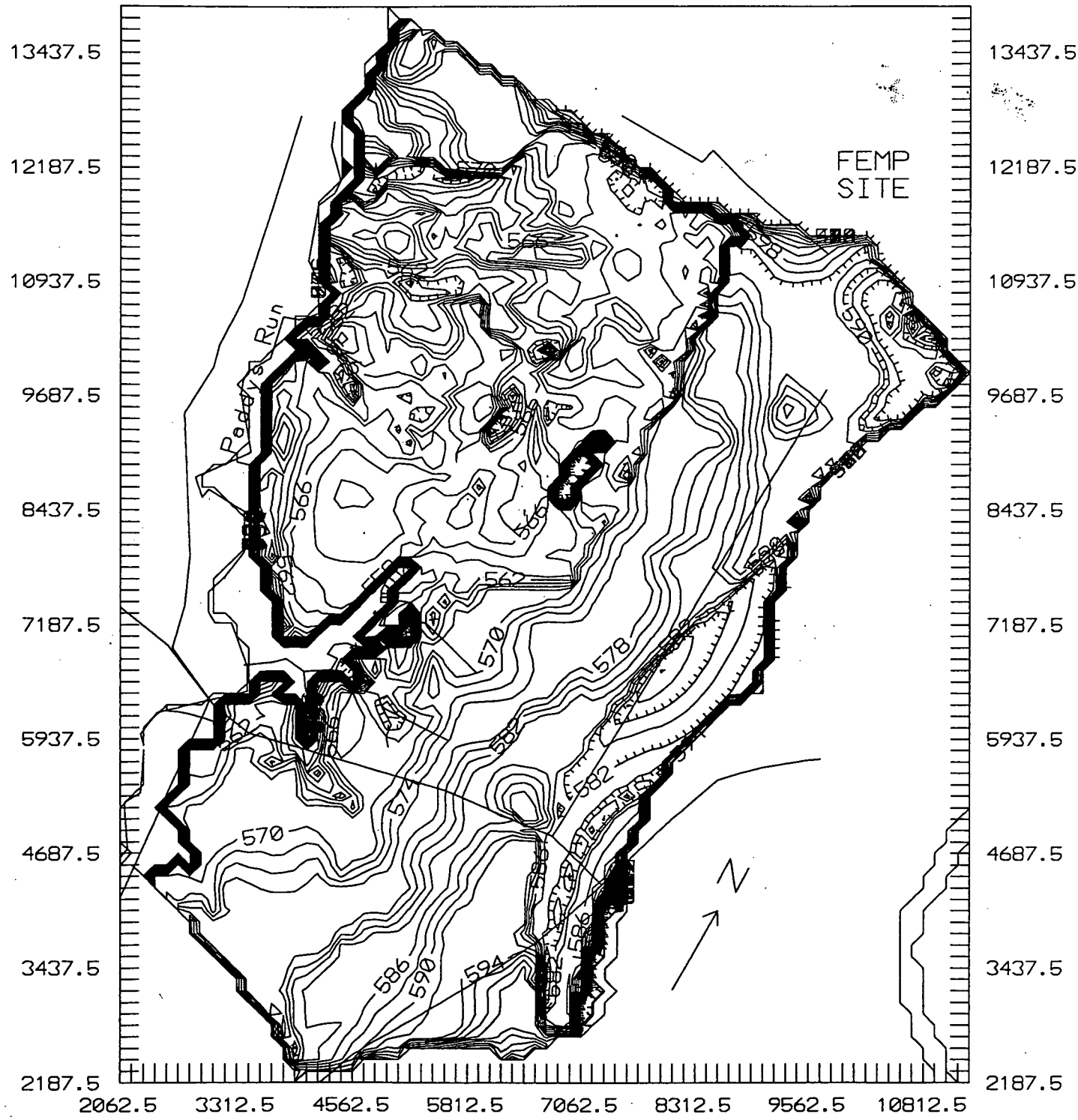

Figure 17C - Layer 6 Head, Calibrated Flow Run

OVERALL VERTICAL HYDRAULIC GRA

CALIBRATED FLOW RUN

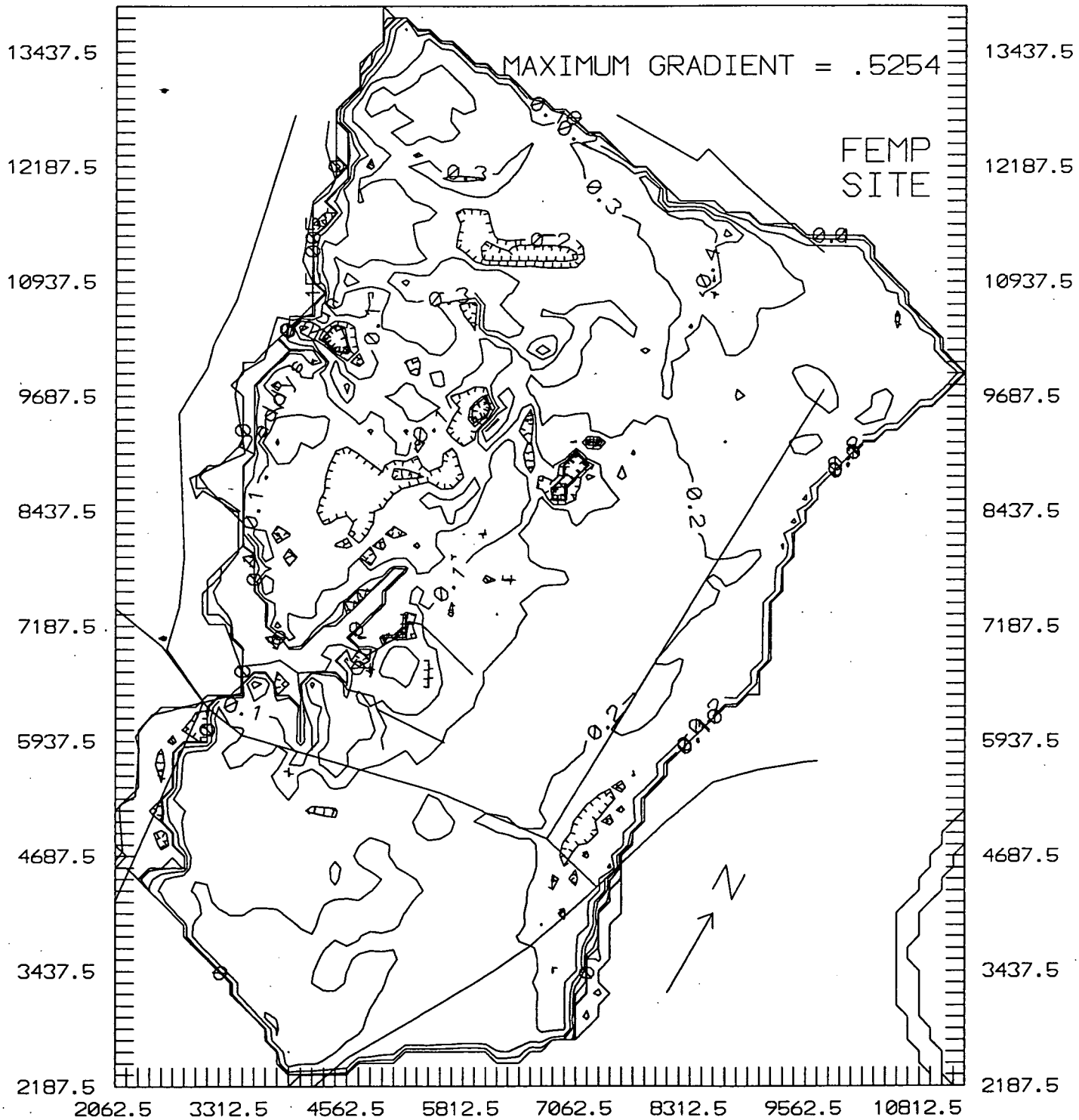

Figure 18C - Overall Vertical Hydraulic Gradient

Table 4C - Water Budget for Steady-State Flow Run 3DFLOW32

WATER BUDGET FOR STEADY-STATE FLOW RUN 3DFLOW32

ELAPSED SIMULATION TIME 0.0000E+00 DAYS (0.0000E+00 SECS , 0.0000E+00 YEARS)

TIME STEP NUMBER 1 NUMBER OF OUTER ITERATIONS 15 CURRENT TIME STEP 1.000 DAYS

	STEADY STATE	FLUID (LB/DAY)	ENERGY (BTU/DAY)	BRINE (LB/DAY)
(GLOBAL+LOCAL)	MASS OR HEAT BALANCE	1.0000	*******	*******
	WELL SUMMARY			
	TOTAL PRODUCTION	8.2946E+04	0.0000E+00	0.0000E+00
	TOTAL INJECTION	0.0000E+00	0.0000E+00	0.0000E+00
	AQUIFER-INFLUENCE FUNCTION			
	TOTAL INFLUX (+)	1.4999E+04	0.0000E+00	0.0000E+00
	TOTAL EFFLUX (-)	5.4861E+06	0.0000E+00	0.0000E+00
	CUMULATIVE FLUX	-5.4711E+06	0.0000E+00	0.0000E+00
	SURFACE RECHARGE	5.5540E+06	1.2249E+08	
	TOTAL IN PLACE	8.87778E+10 (LB)	1.95791E+12 (BTU)	0.00000E+00 (LB)

APPENDIX D

1,000-YEAR URANIUM-238 TRANSPORT RUN FIGURES AND TABLES

LAYER 1 - U238 INITIAL CONCENT

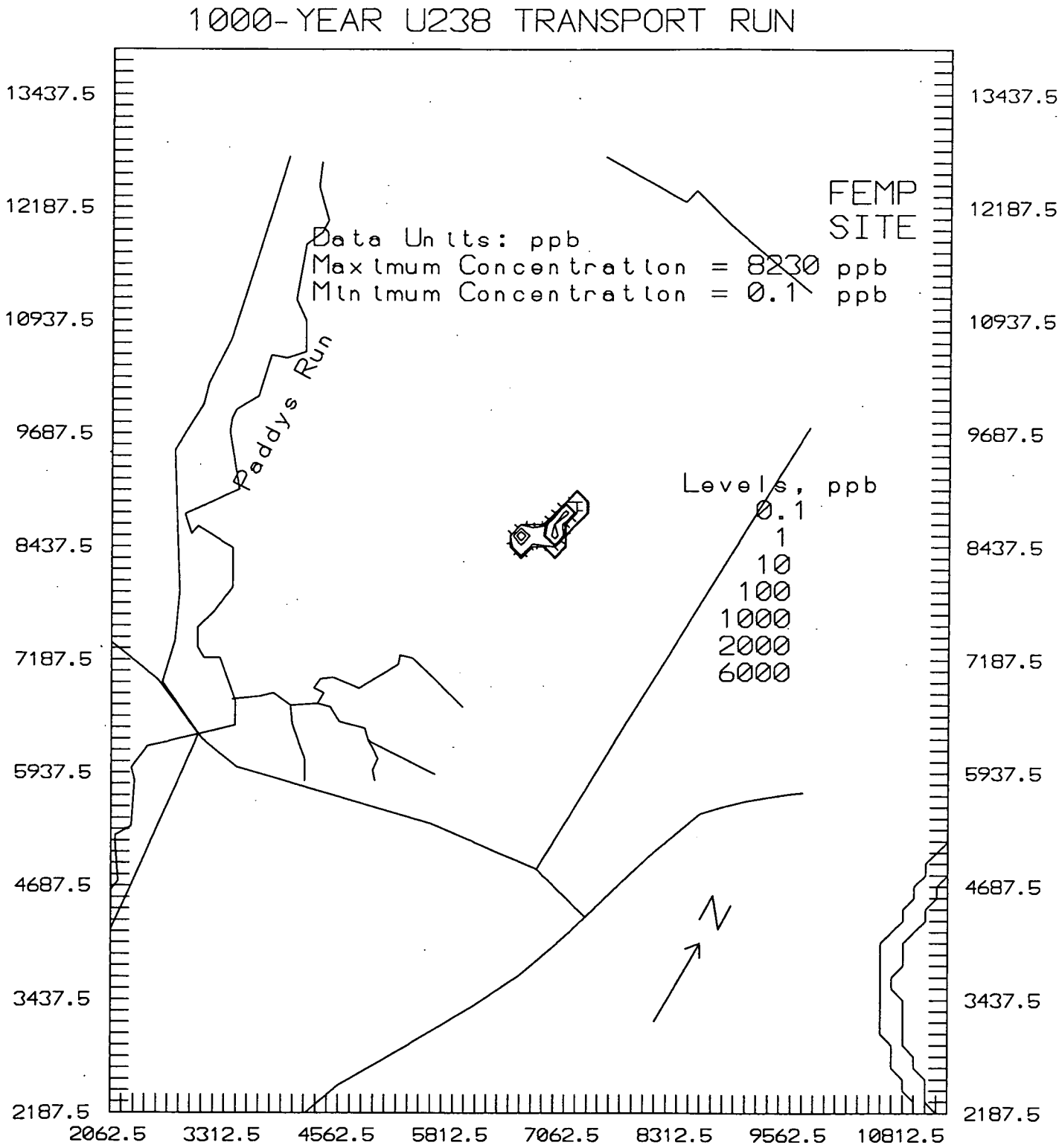

Figure 1D - Layer 1 - U238 Concentration Initial Condition

LAYER 2 - U238 INITIAL CONCENTRATION

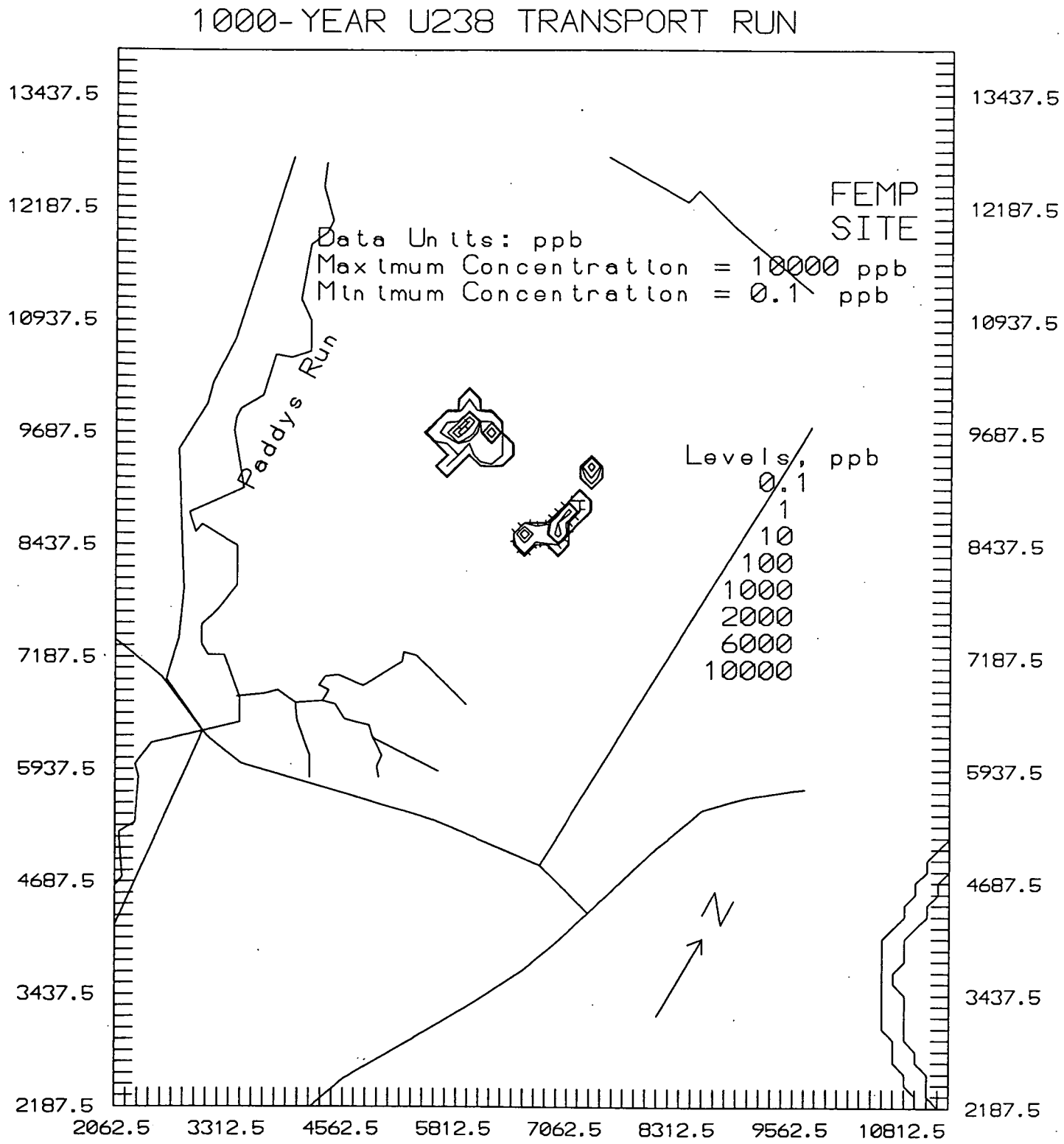

Figure 2D - Layer 2 - U238 Concentration Initial Condition

LAYER 3 - U238 INITIAL CONCENTRATION

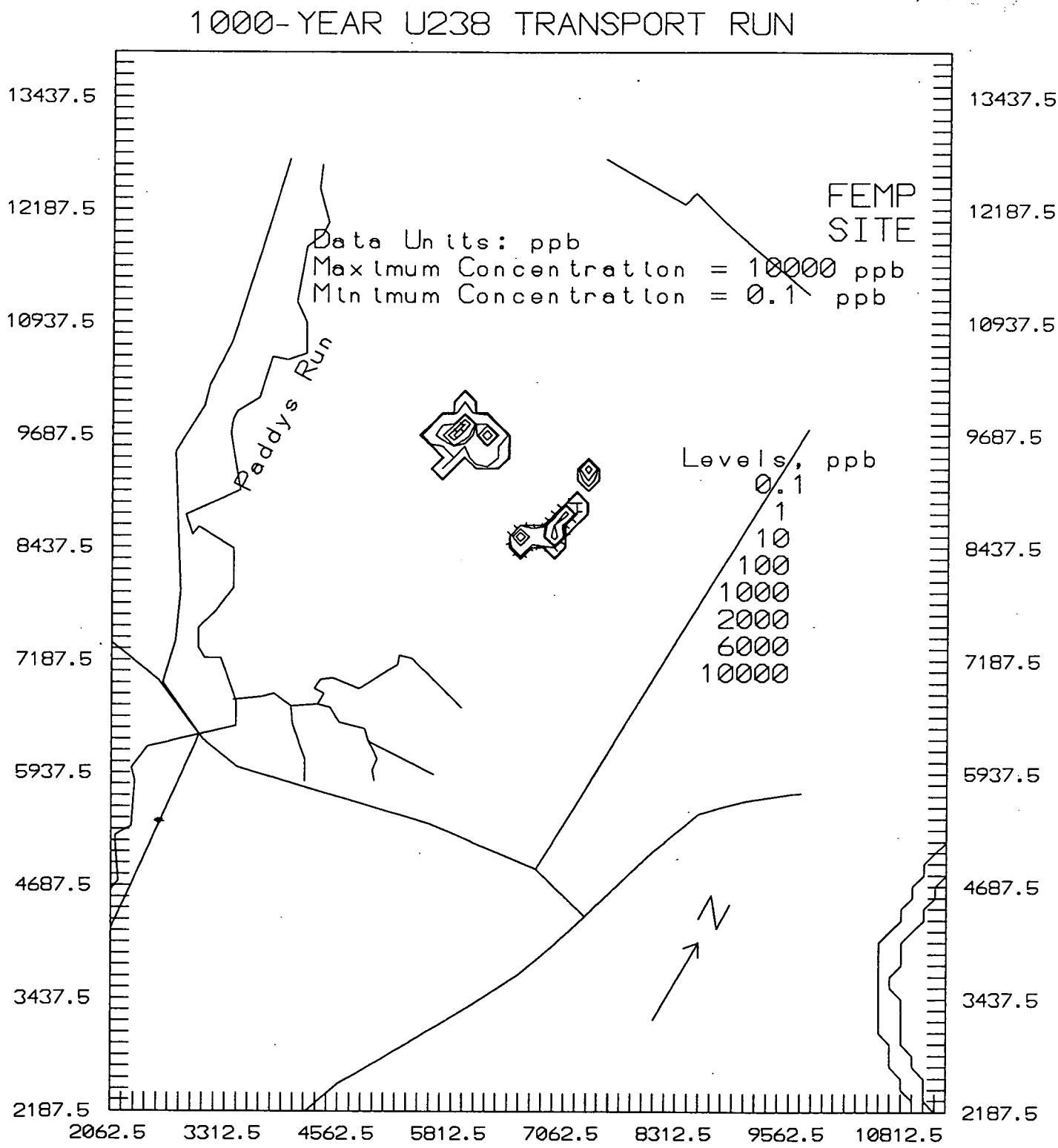

Figure 3D - Layer 3 - U238 Concentration Initial Condition

LAYER 4 - U238 INITIAL CONCENTRATION

0489

1000-YEAR U238 TRANSPORT RUN

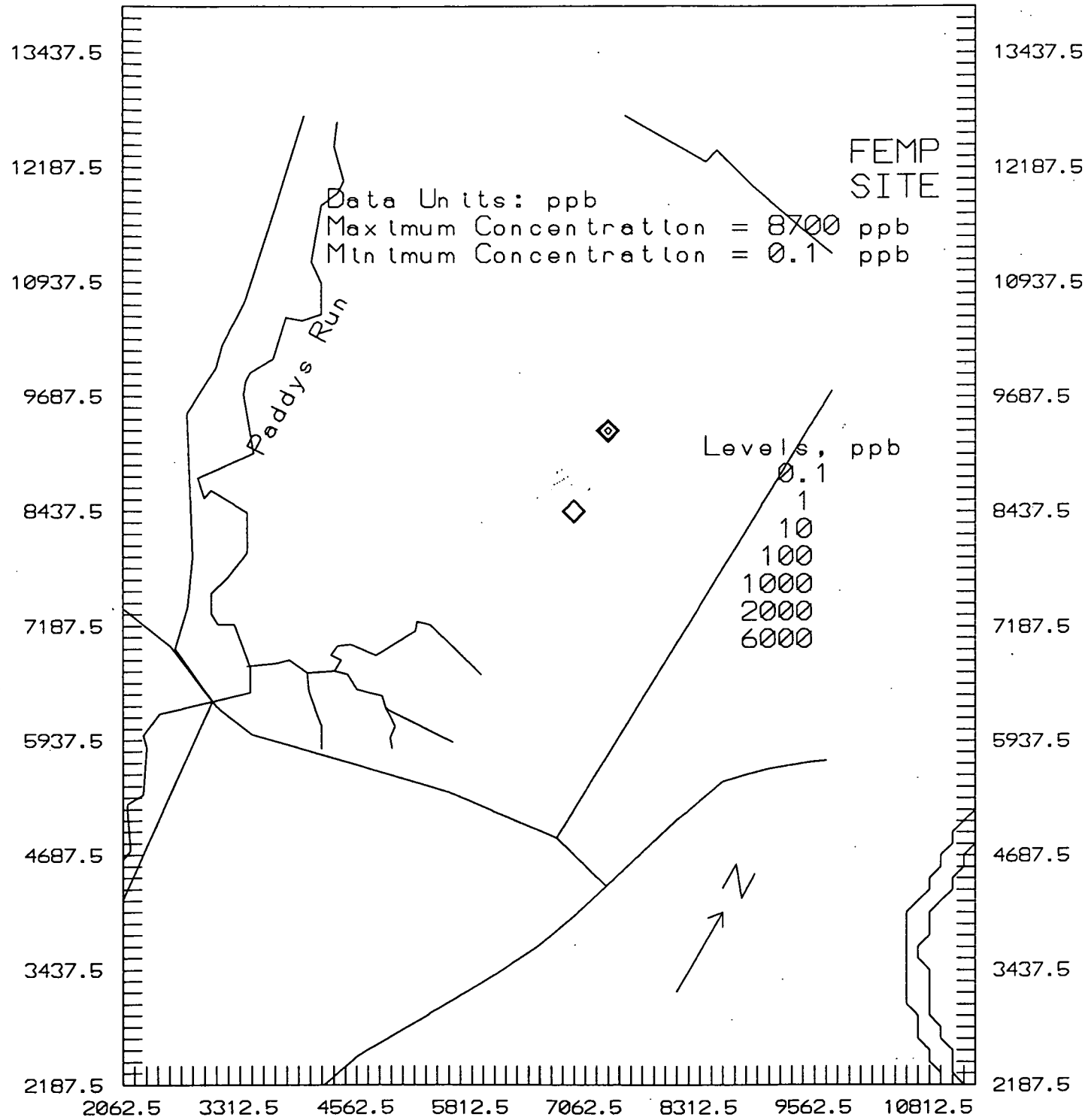

Figure 4D - Layer 4 - U238 Concentration Initial Condition

LAYER 1 - U238 CONCENTRATION AT 1000 YEARS

5489

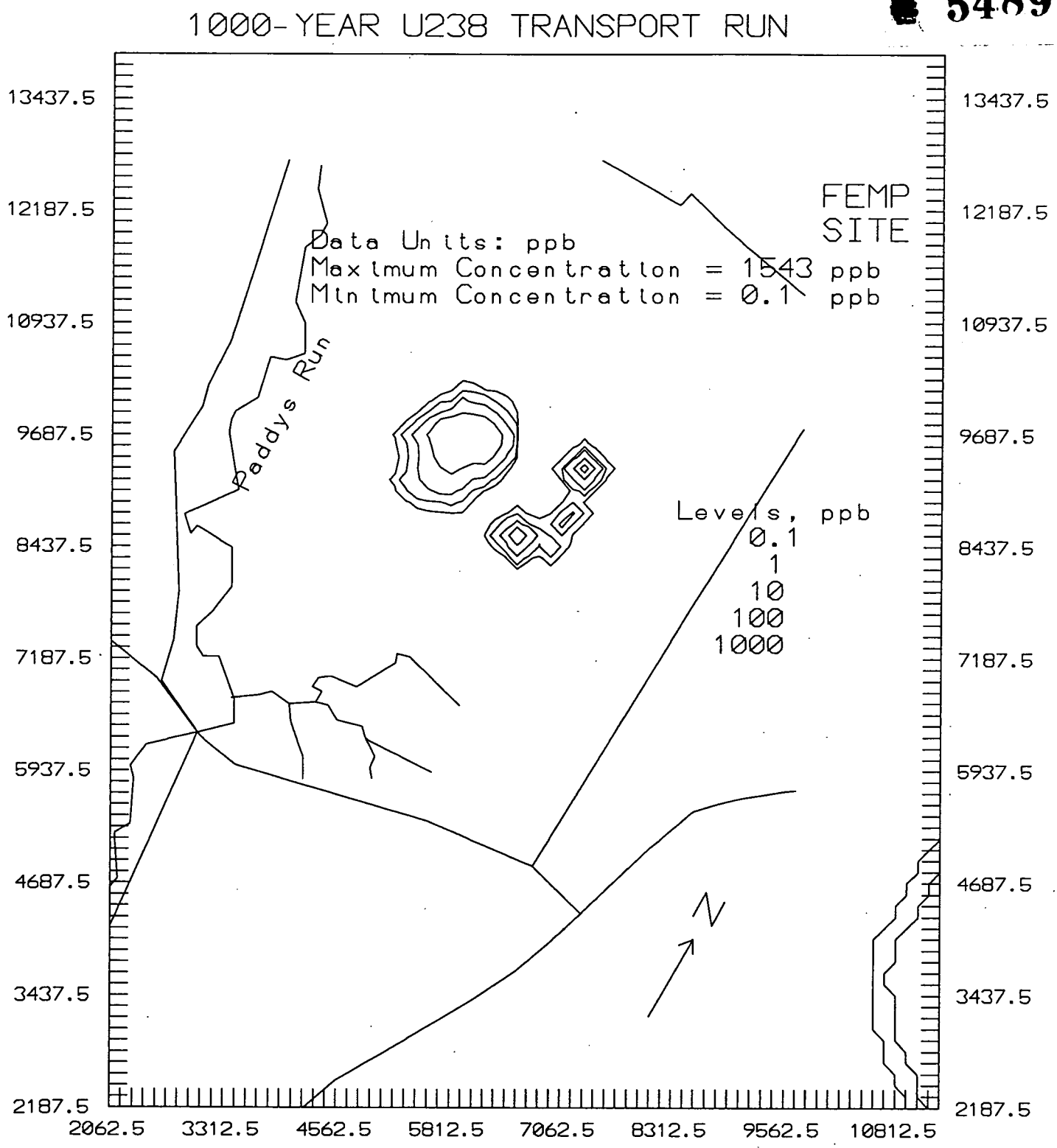

Figure 5D - Layer 1 - U238 Concentration Contours at 1,000 Years

LAYER 2 - U238 CONCENTRATION AT 1000 YEARS

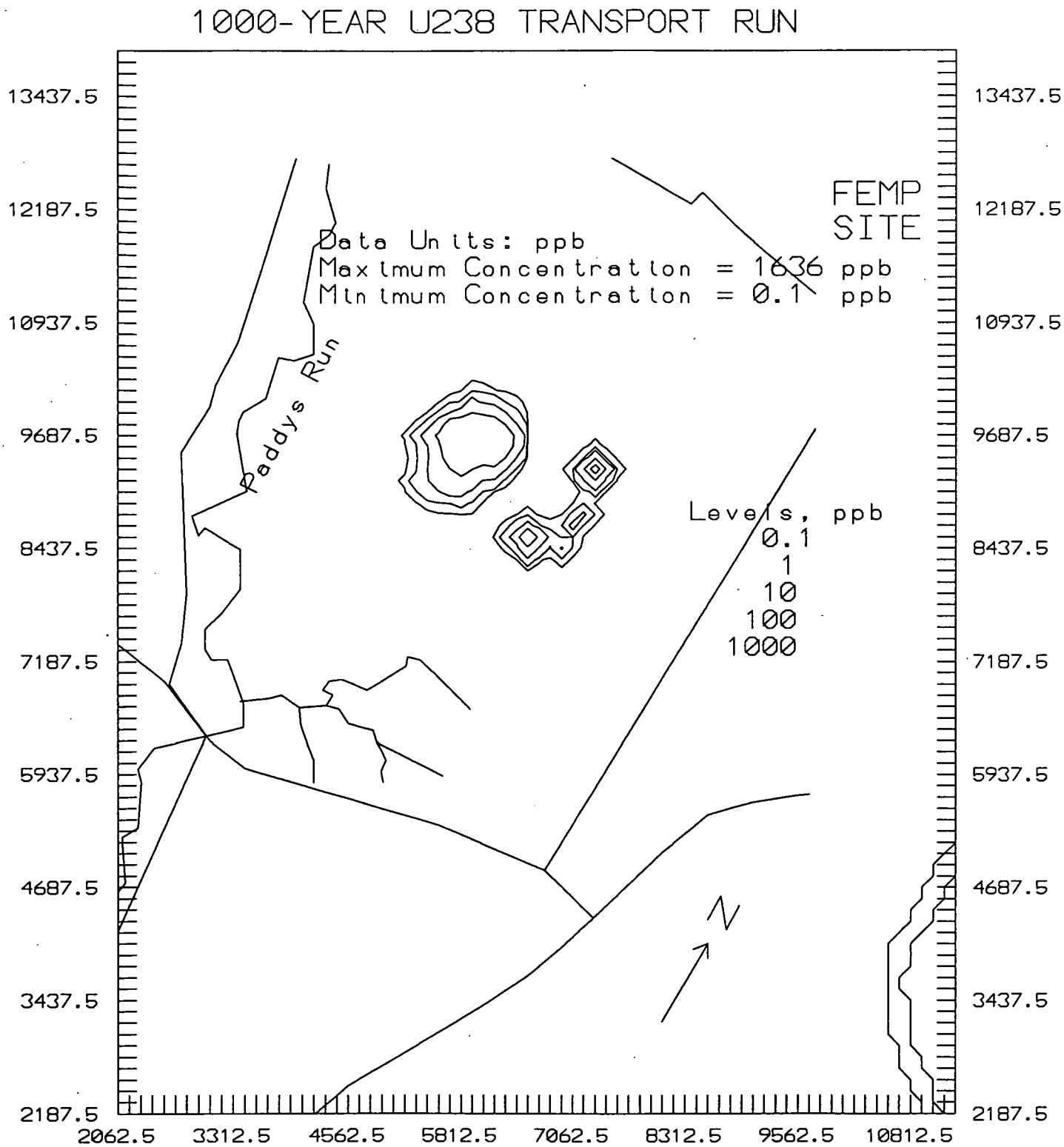

Figure 6D - Layer 2 - U238 Concentration Contours at 1,000 Years

LAYER 3 - U238 CONCENTRATION AT 1000 YEARS

5489

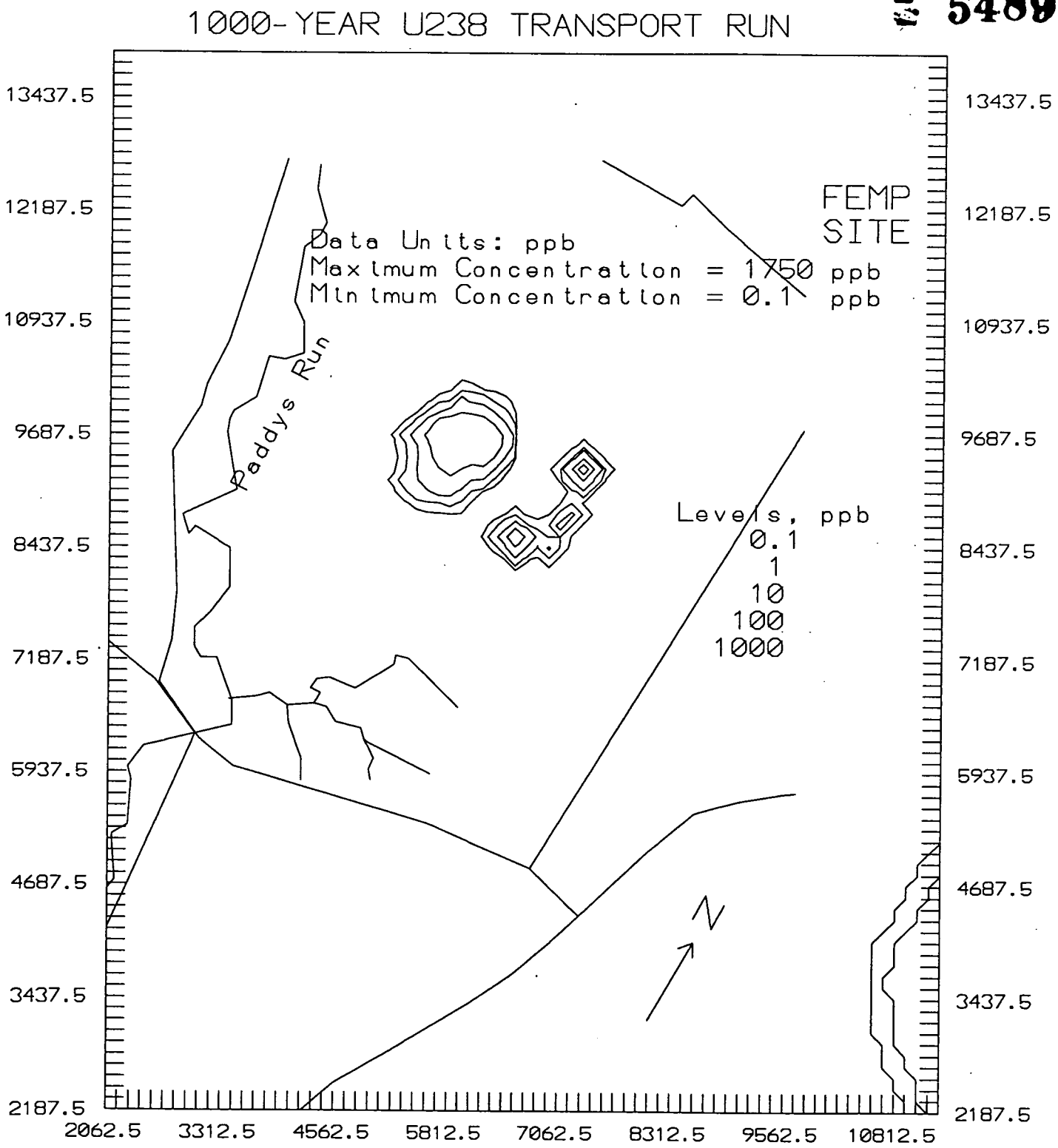

Figure 7D - Layer 3 - U238 Concentration Contours at 1,000 Years

LAYER 4 - U238 CONCENTRATION AT 1000 YEARS

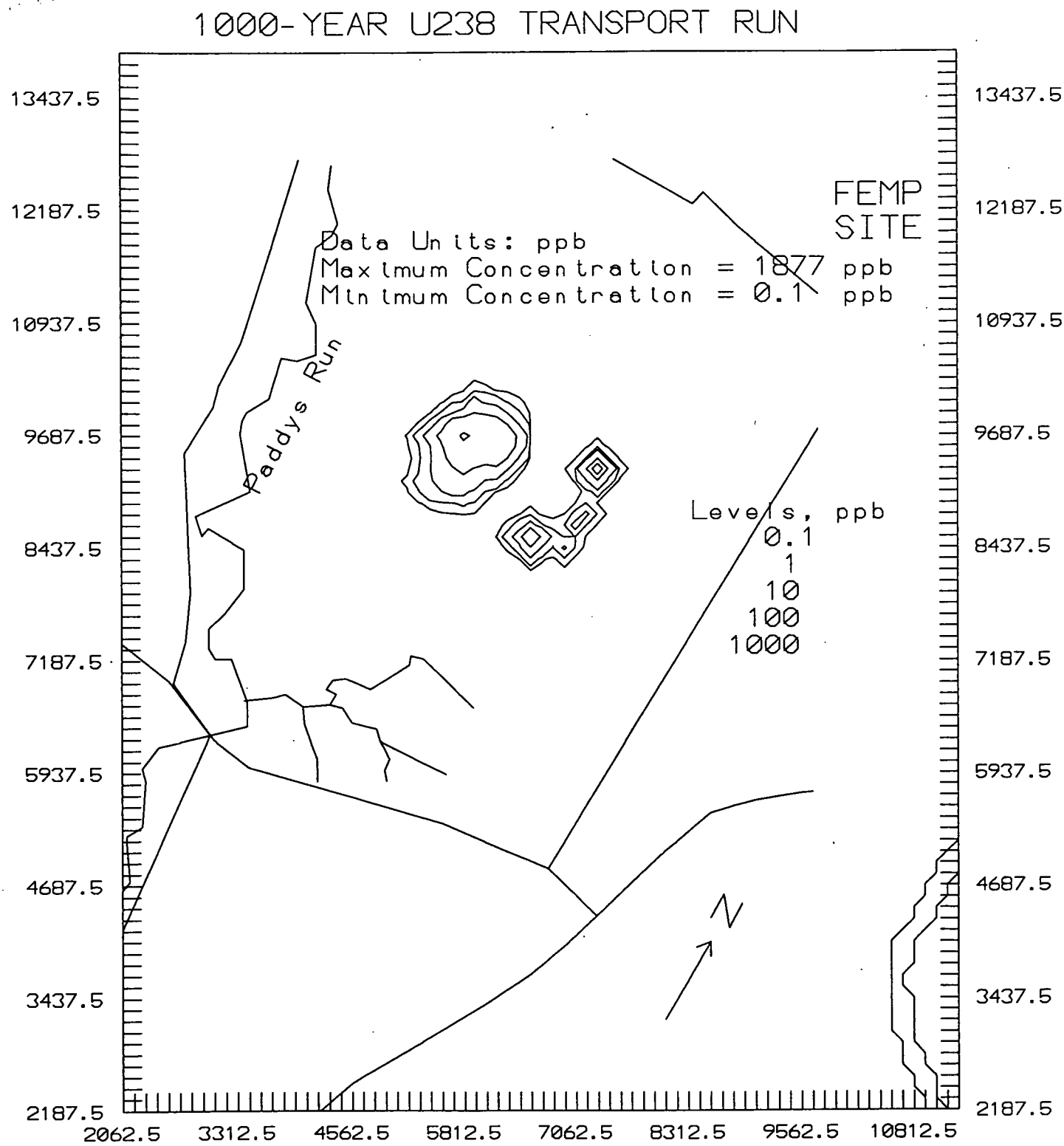

Figure 8D - Layer 4 - U238 Concentration Contours at 1,000 Years

LAYER 5 - U238 CONCENTRATION AT 1000 YEARS

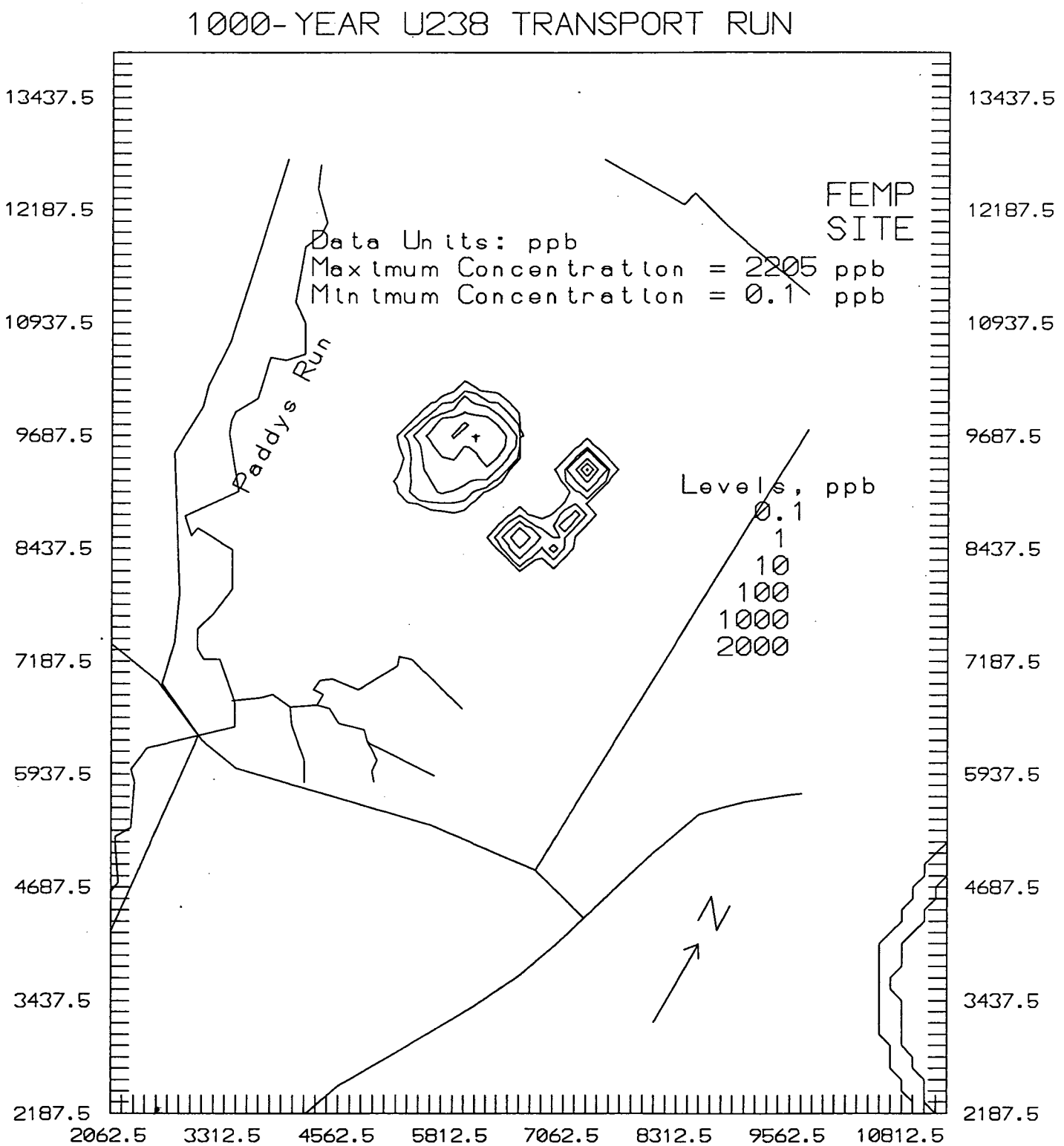

Figure 9D - Layer 5 - U238 Concentration Contours at 1,000 Years

U238 CONCENTRATION AT 1000 YEAR

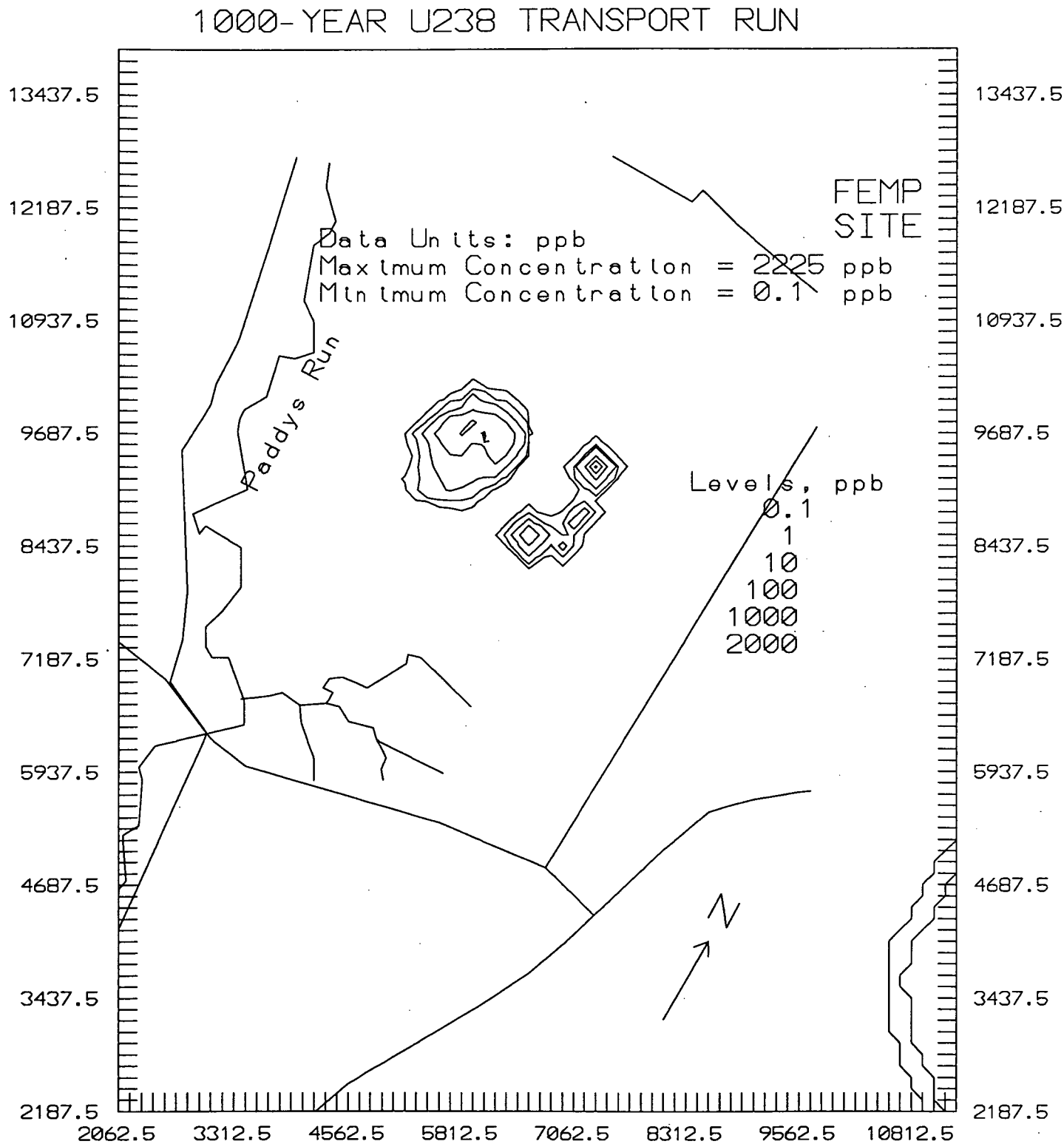

Figure 10D - Layer 6 - U238 Concentration Contours at 1,000 Years

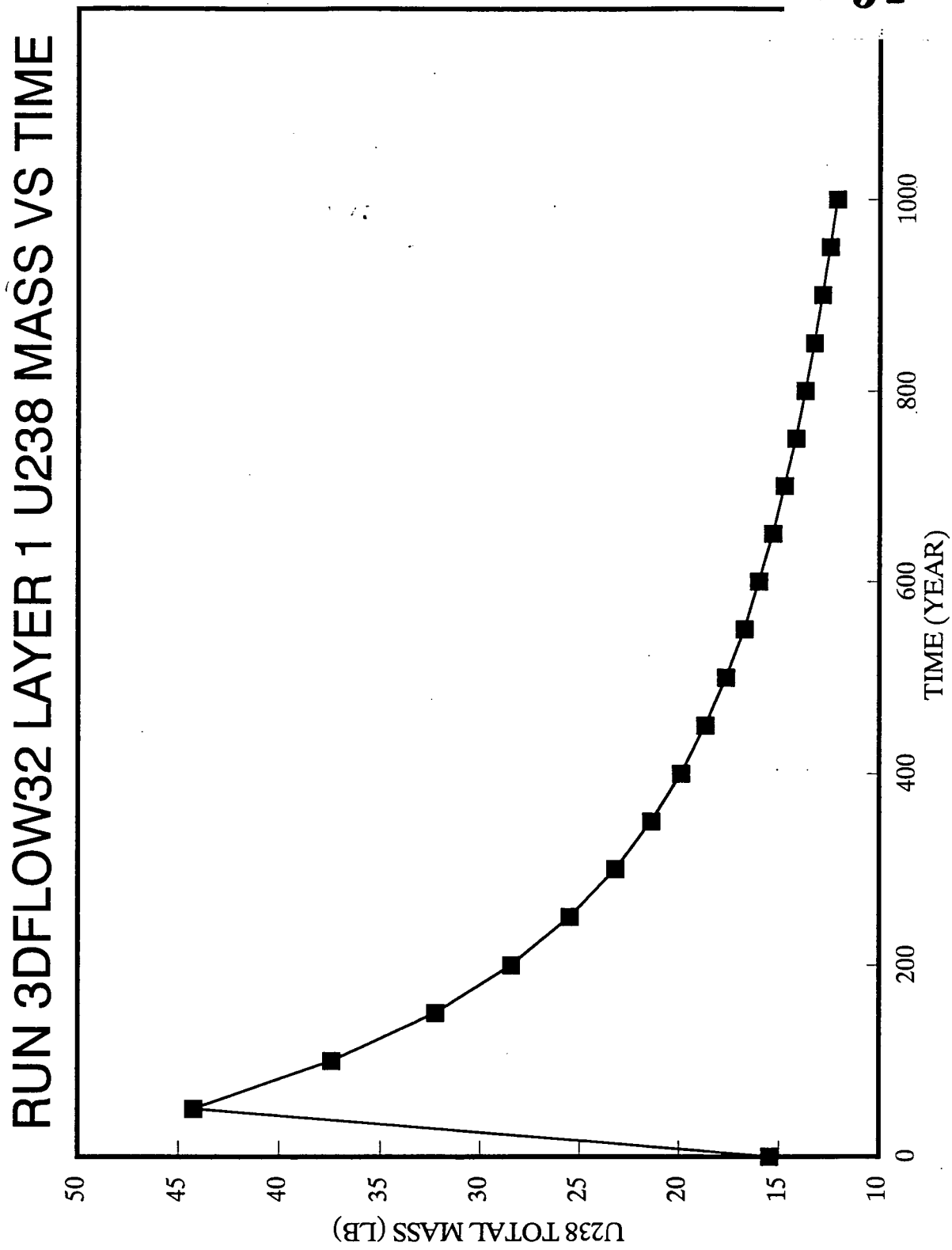

Figure 11D - Run 3DFLOW32 Layer 1 U238 Mass vs. Time

5489

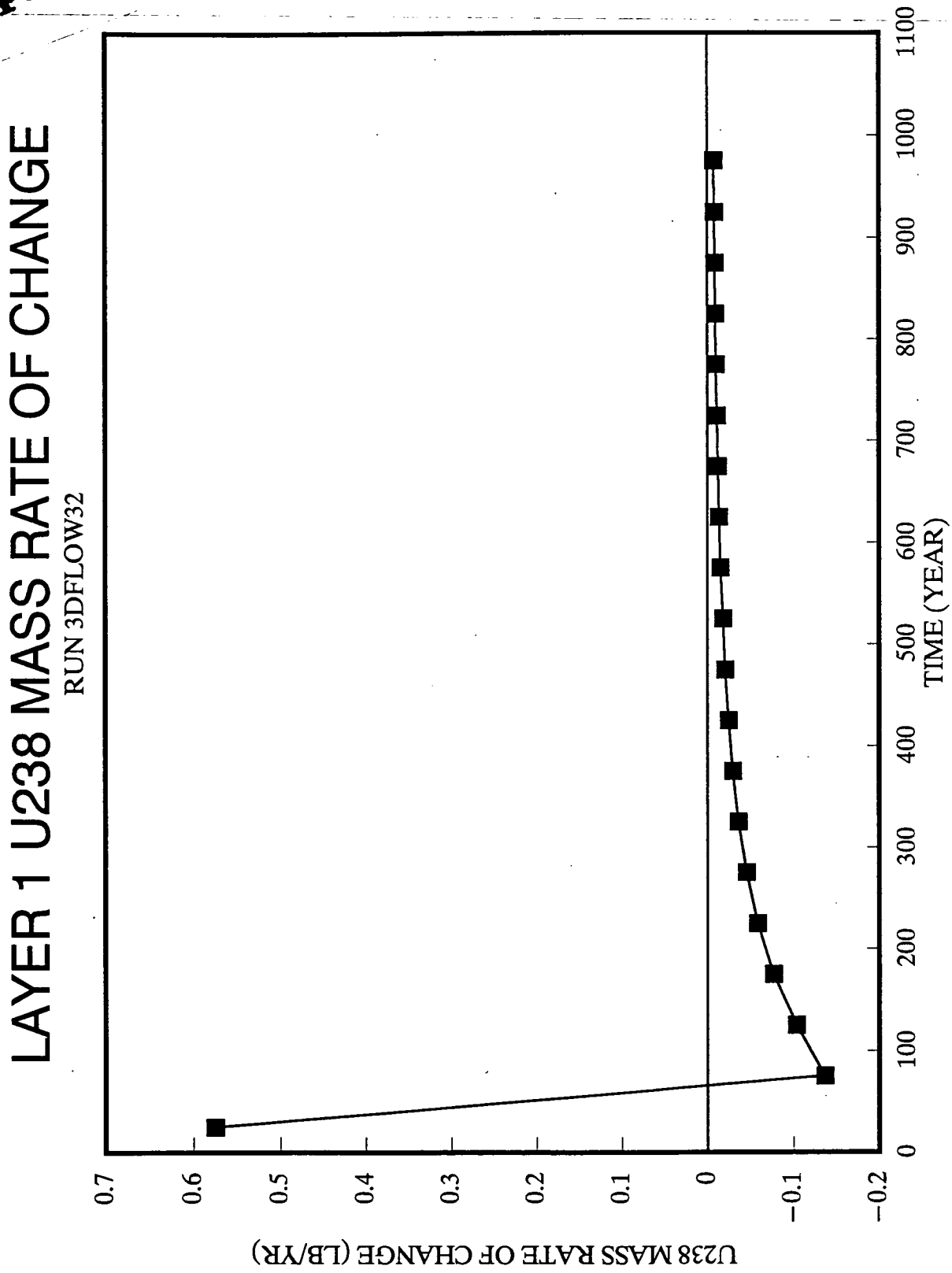

Figure 12D - Layer 1 U238 Mass Rate of Change

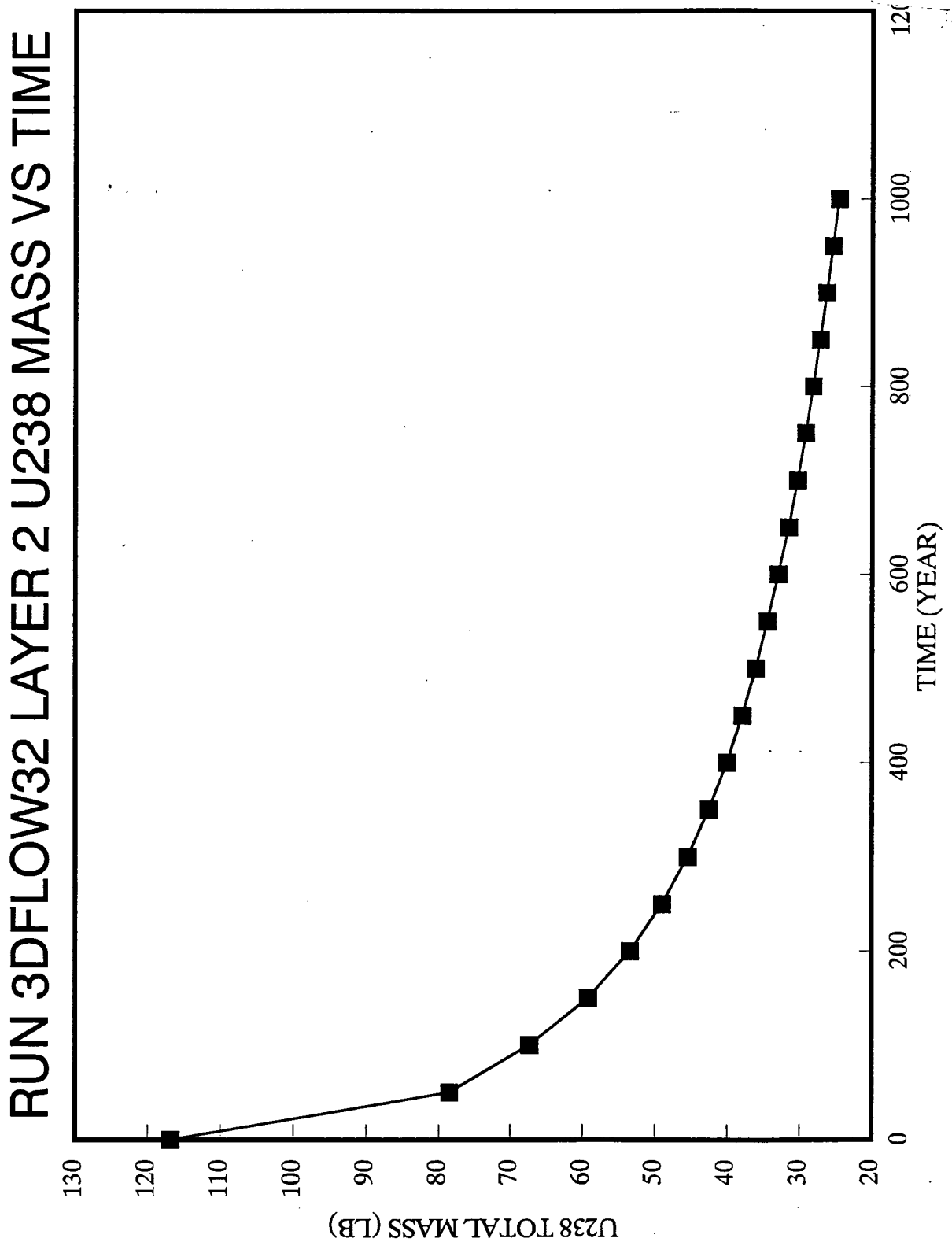

Figure 13D - Run 3DFLOW32 Layer 2 U238 Mass vs. Time

5489

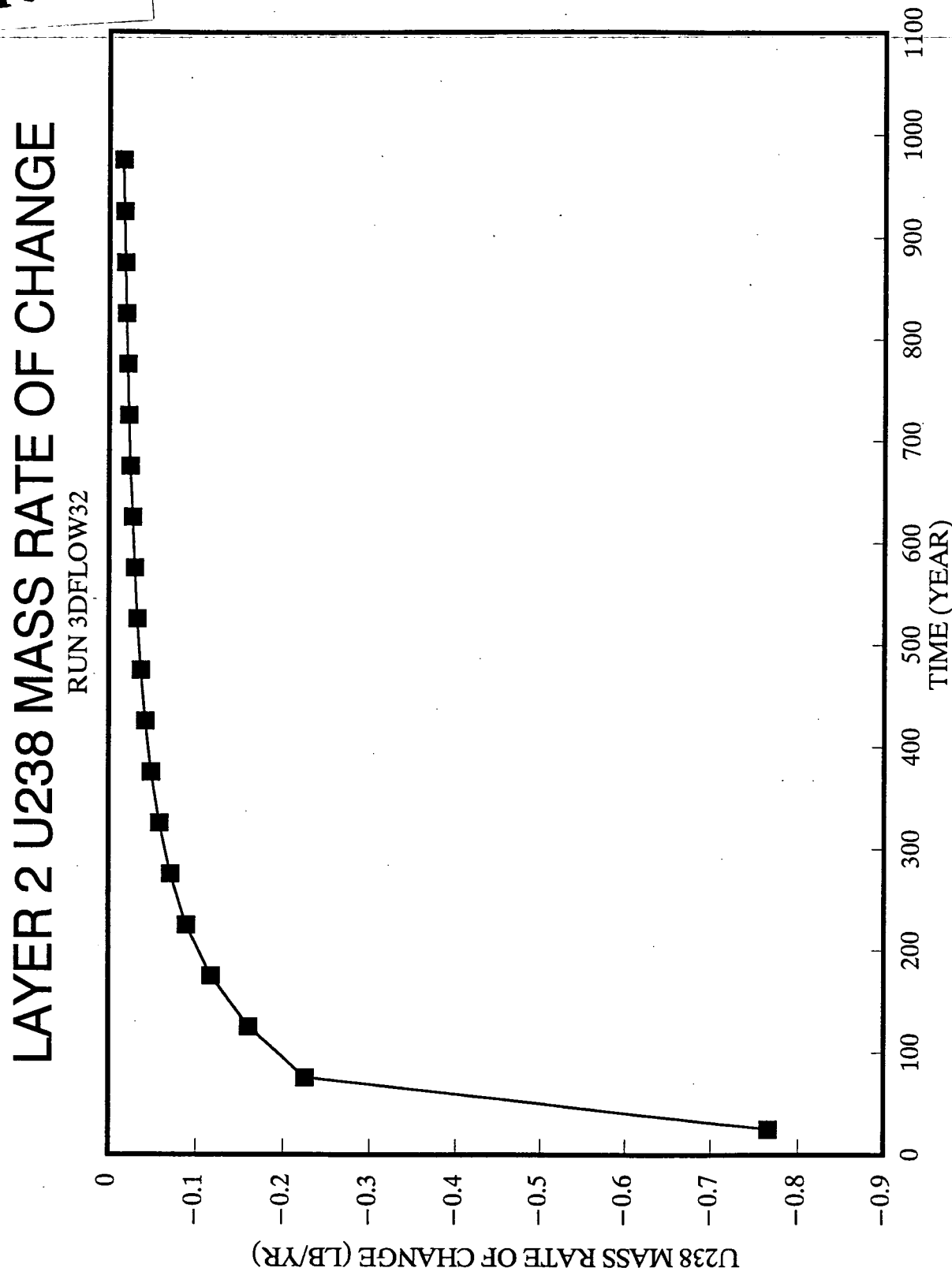

Figure 14D - Layer 2 U238 Mass Rate of Change

5489

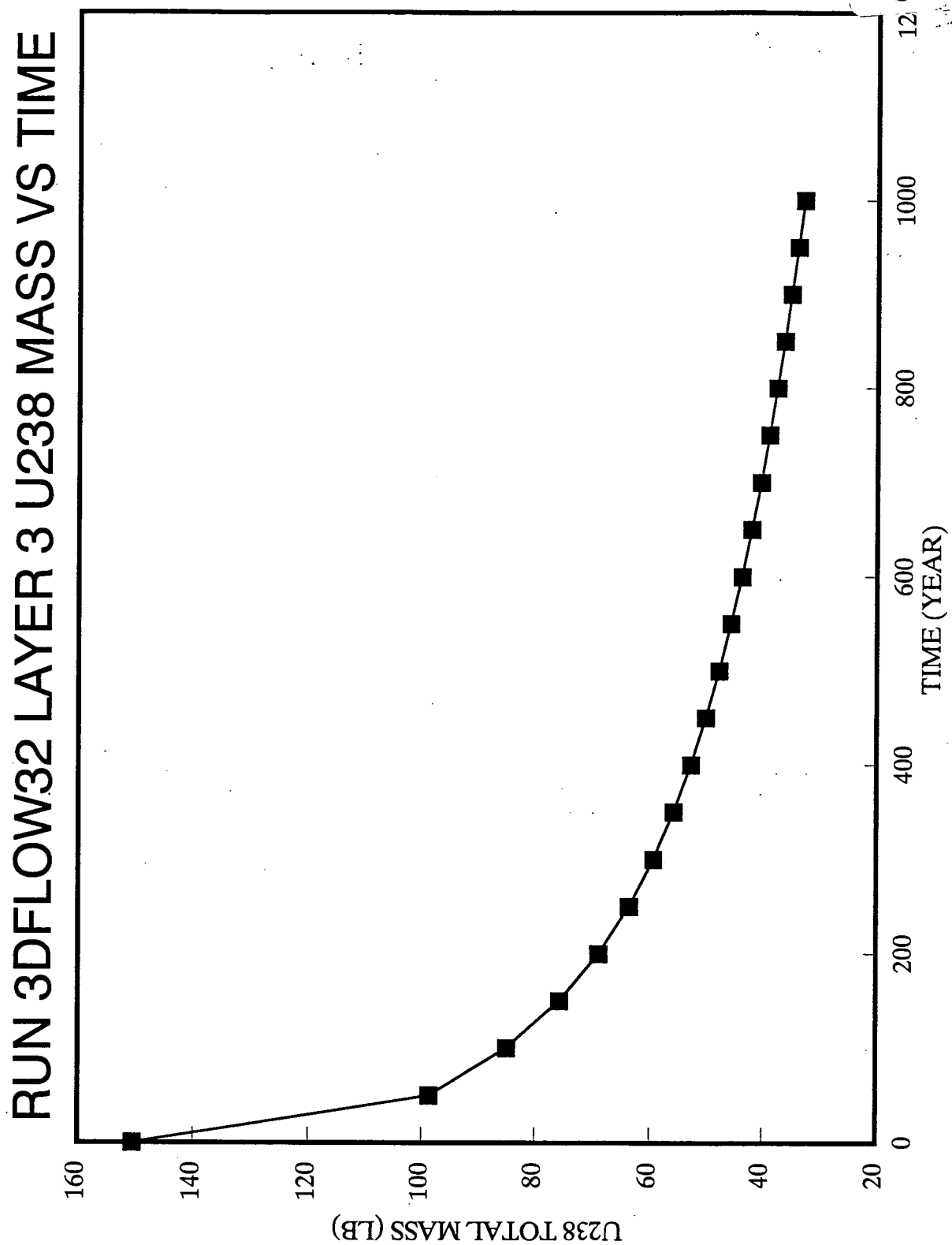

Figure 15D - Run 3DFLOW32 Layer 3 U238 Mass vs. Time

5489

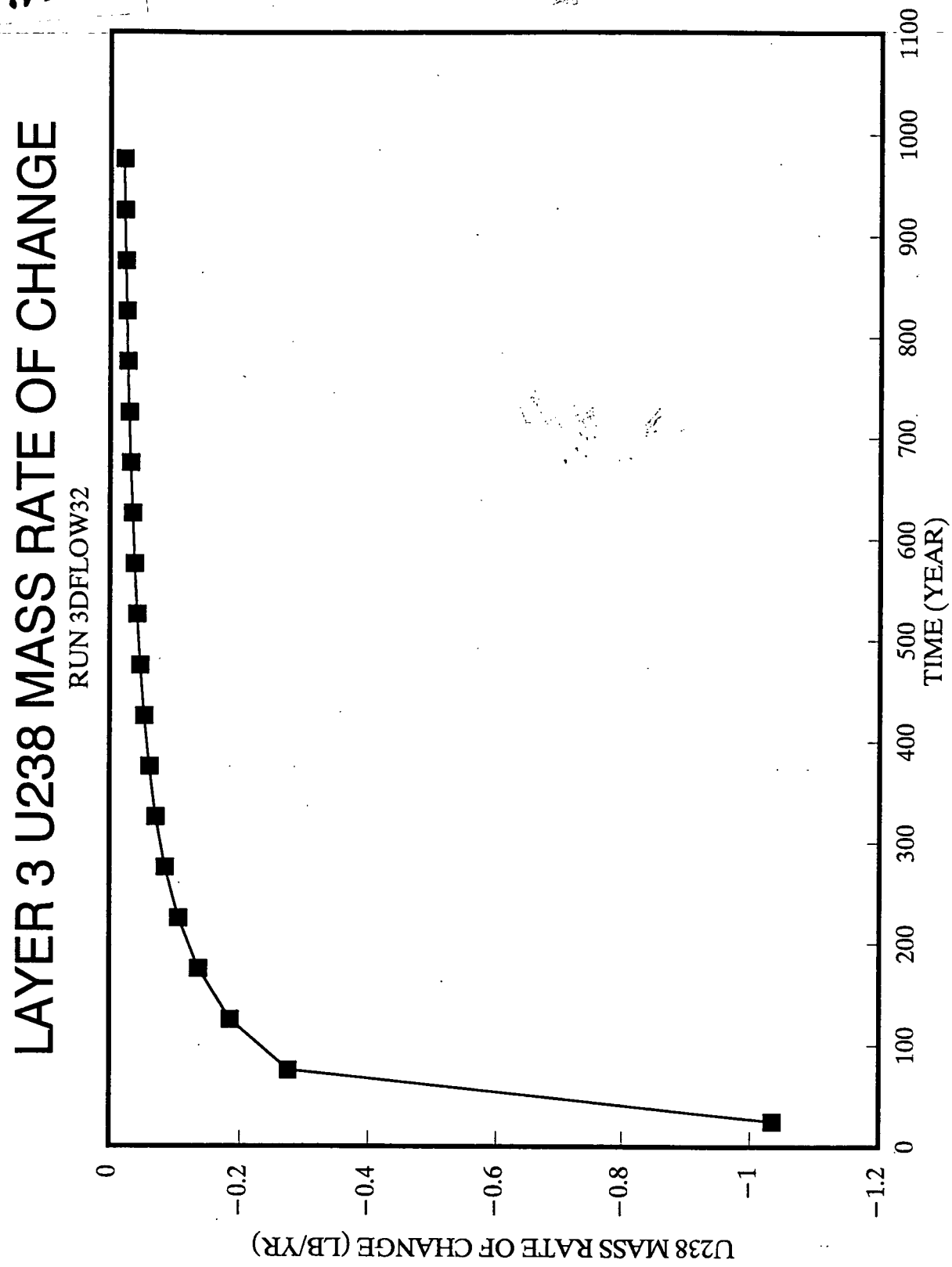

Figure 16D - Layer 3 U238 Mass Rate of Change

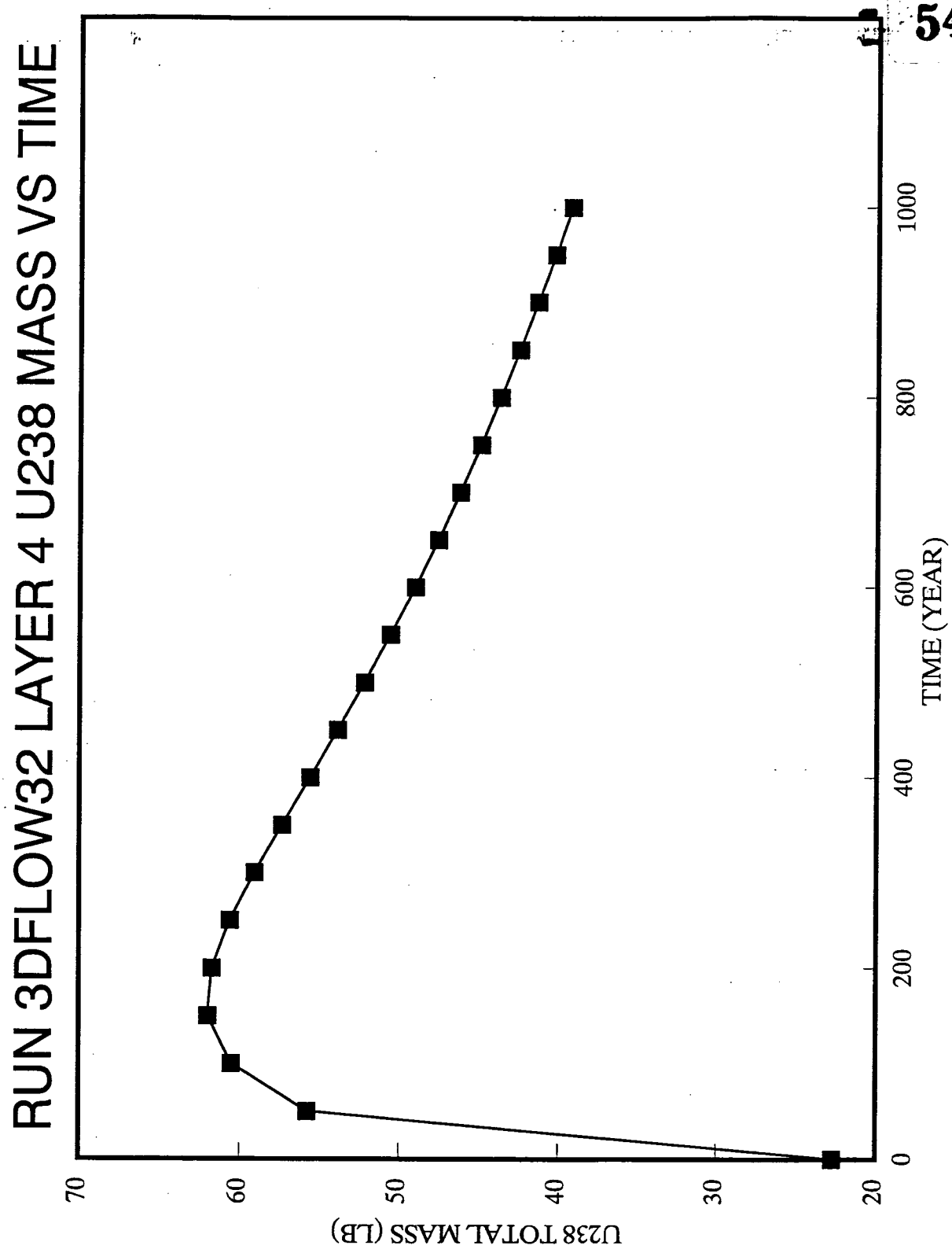

Figure 17D - Run 3DFLOW32 Layer 4 U238 Mass vs. Time

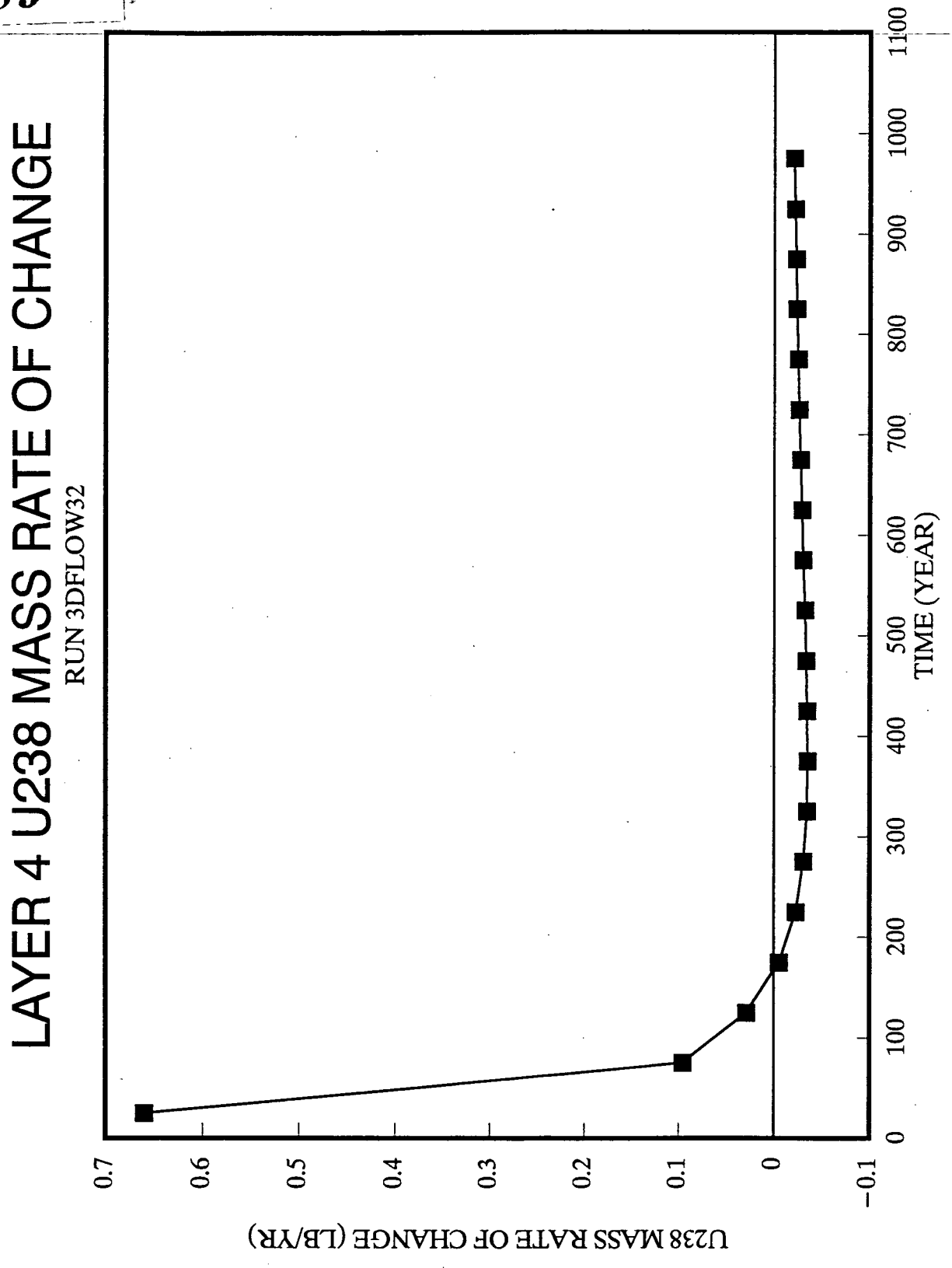

Figure 18D - Layer 4 U238 Mass Rate of Change

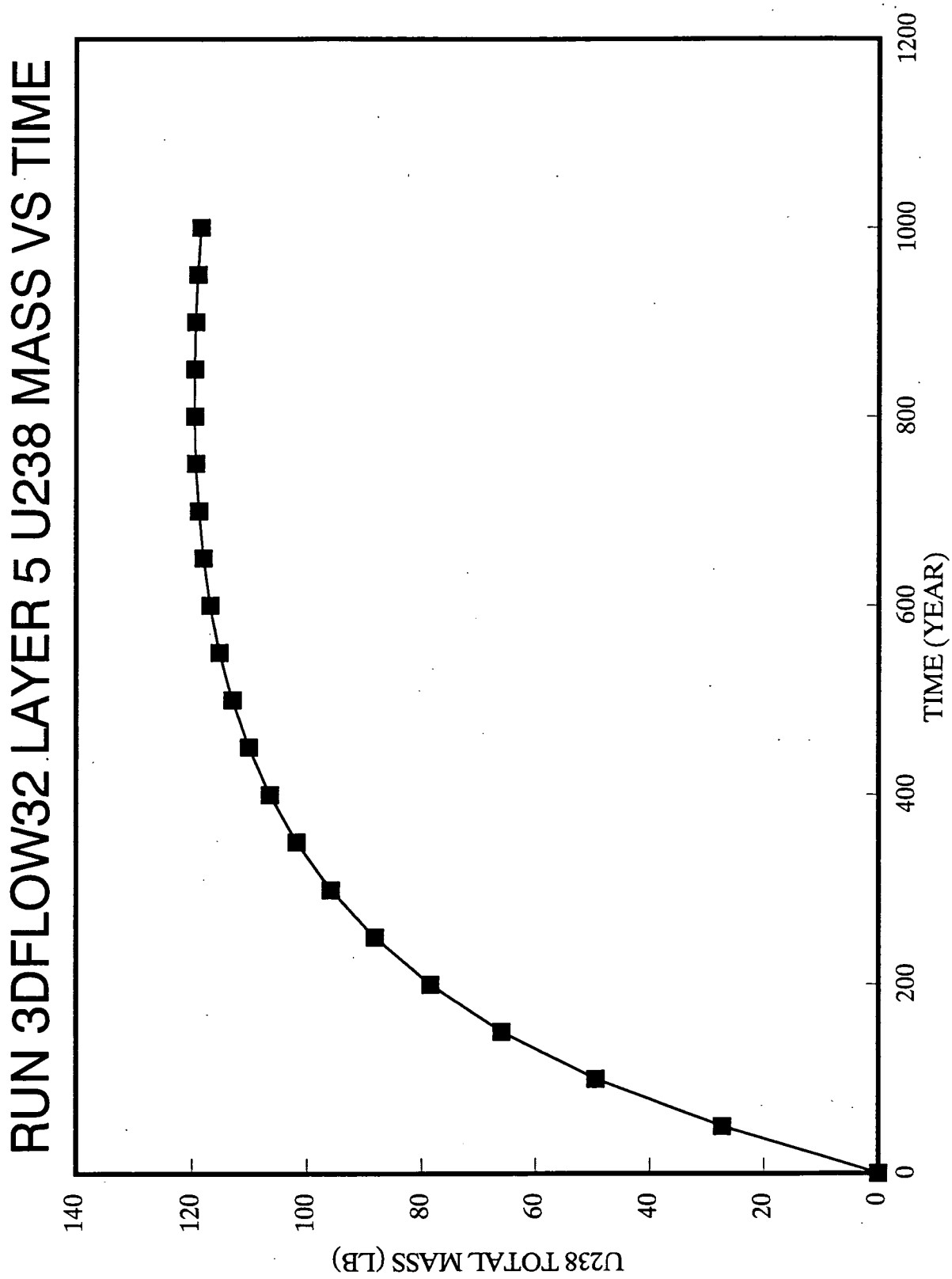

Figure 19D - Run 3DFLOW32 Layer 5 U238 Mass vs. Time

5489

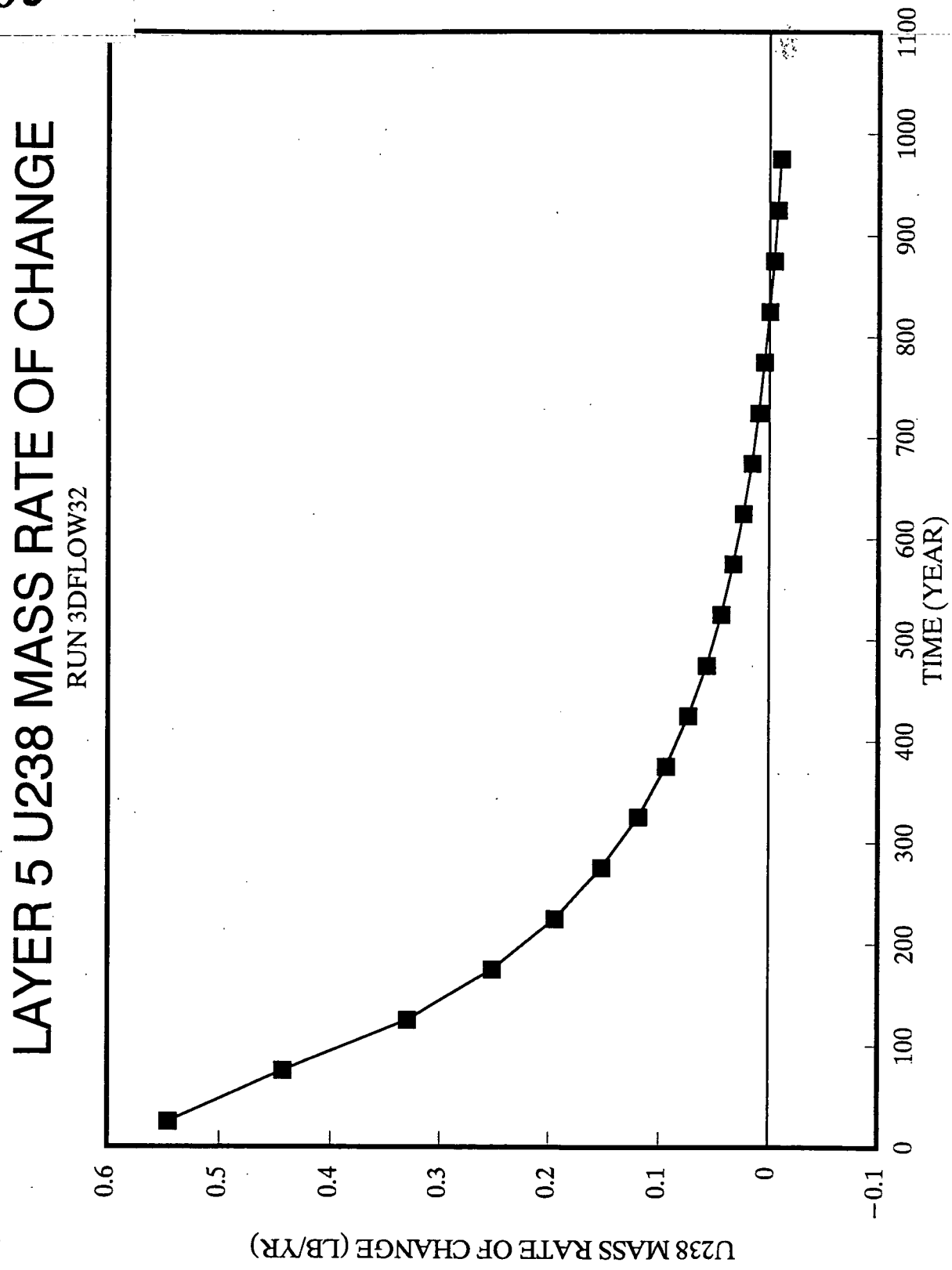

Figure 20D - Layer 5 U238 Mass Rate of Change

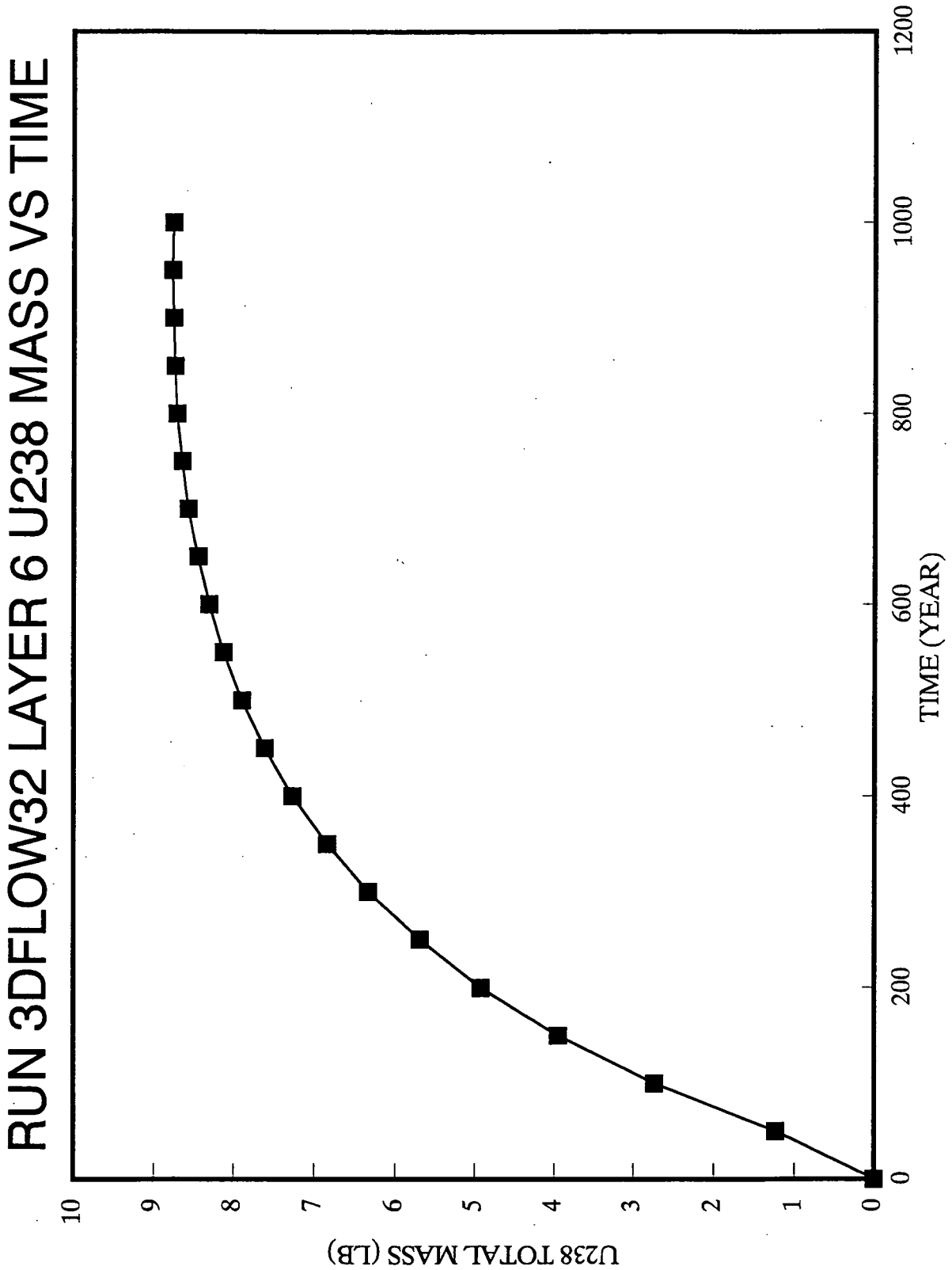

Figure 21D - Run 3DFLOW32 Layer 6 U238 Mass vs. Time

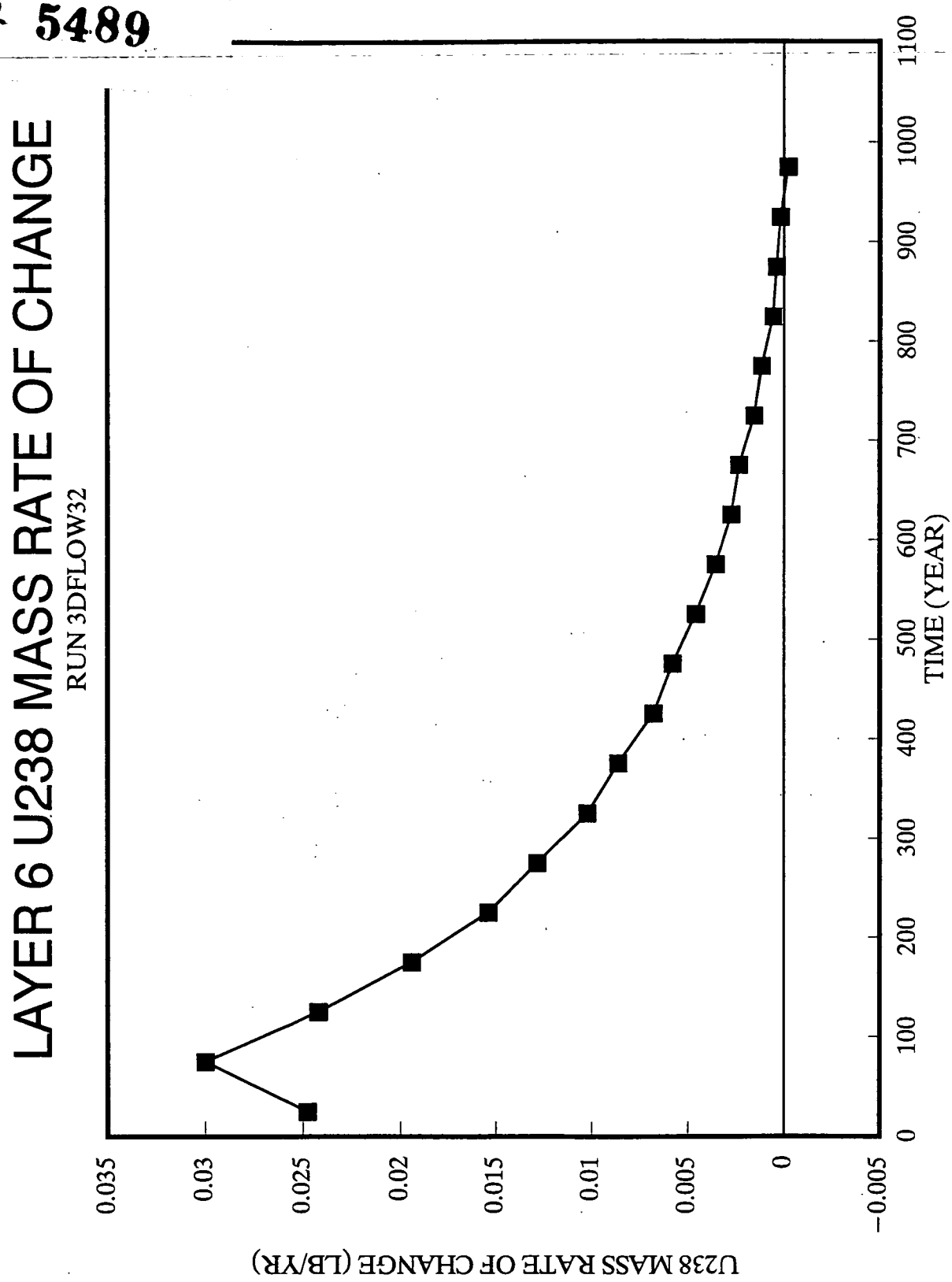

Figure 22D - Layer 6 U238 Mass Rate of Change

APPENDIX E

1,000-YEAR URANIUM RUN MATERIAL BALANCE SUMMARY

INITIAL DISTRIBUTION OF RADIONUCLIDE MASS

SUMMARY OF RADIONUCLIDE MASS BY LAYER

UPDATED FOR PARTIALLY SATURATED BLOCKS

COMPONENT 1 URANIUM

LAYER	DISSOLVED MASS(LB)	SORBED MASS(LB)
1	15.47270	750.6943
2	116.8326	7476.615
3	150.4619	9712.245
4	22.70773	1749.789
5	0.0000000E+00	0.0000000E+00
6	0.0000000E+00	0.0000000E+00

ELAPSED SIMULATION TIME 1.8250E+04 DAYS (1.5768E+09 SECS , 50.00 YEARS)

TIME STEP NUMBER 305 NUMBER OF OUTER ITERATIONS 0 CURRENT TIME STEP 70.00 DAYS

COMP. 1 NO. OF L2SOR ITERATIONS 1 CONVERGENCE-4.8327E-12

PARENT MAXIMUM CHANGE AT (40,52, 3)
OVER LAST TIME STEP 8.9135E-09

MATERIAL BALANCE SUMMARY OF DISSOLVED AND SORBED RADIOACTIVE COMPONENTS -- (LB)

NO	COMPONENT	IN-PLACE	SOURCES	SINKS	GENERATION	DECAY	E-FLUX	BALANCE
1	URANIUM	1.9957E+04	0.0000E+00	9.334	0.0000E+00	0.0000E+00	28.71	1.0000

000123

5489

SUMMARY OF RADIONUCLIDE MASS BY LAYER

COMPONENT 1 URANIUM

LAYER	DISSOLVED MASS(LB)	SORBED MASS(LB)
1	44.25201	2146.989
2	78.54346	5039.021
3	98.72595	6398.972
4	55.73284	4294.563
5	27.28930	1694.355
6	1.241646	77.09206

ELAPSED SIMULATION TIME 3.6500E+04 DAYS (3.1536E+09 SECS , 100.0 YEARS)

TIME STEP NUMBER 609 NUMBER OF OUTER ITERATIONS 0 CURRENT TIME STEP 70.00 DAYS

COMP. 1 NO. OF L2SOR ITERATIONS 1 CONVERGENCE-2.5945E-12

PARENT MAXIMUM CHANGE AT (31,61, 2)
OVER LAST TIME STEP 2.2387E-09

MATERIAL BALANCE SUMMARY OF DISSOLVED AND SORBED RADIOACTIVE COMPONENTS -- (LB)

NO	COMPONENT	IN-PLACE	SOURCES	SINKS	GENERATION	DECAY	E-FLUX	BALANCE
1	URANIUM	1.9853E+04	0.0000E+00	21.30	0.0000E+00	0.0000E+00	120.6	1.0000

SUMMARY OF RADIONUCLIDE MASS BY LAYER

COMPONENT 1 URANIUM

LAYER	DISSOLVED MASS(LB)	SORBED MASS(LB)
1	37.42376	1815.701
2	67.27158	4324.505
3	84.94726	5506.378

5489

000124

4	60.51867	4663.311
5	49.45210	3070.413
6	2.742864	170.3006

ELAPSED SIMULATION TIME 5.4750E+04 DAYS (4.7304E+09 SECS , 150.0 YEARS)
****

TIME STEP NUMBER 913 NUMBER OF OUTER ITERATIONS 0 CURRENT TIME STEP 70.00 DAYS

COMP. 1 NO. OF L2SOR ITERATIONS 1 CONVERGENCE-1.7846E-12

PARENT MAXIMUM CHANGE AT (31,61, 2)
OVER LAST TIME STEP 1.4386E-09

MATERIAL BALANCE SUMMARY OF DISSOLVED AND SORBED RADIOACTIVE COMPONENTS -- (LB)

NO	COMPONENT	IN-PLACE	SOURCES	SINKS	GENERATION	DECAY	E-FLUX	BALANCE
1	URANIUM	1.9698E+04	0.0000E+00	33.86	0.0000E+00	0.0000E+00	263.5	1.0000

SUMMARY OF RADIONUCLIDE MASS BY LAYER

COMPONENT 1 URANIUM

LAYER	DISSOLVED MASS(LB)	SORBED MASS(LB)
1	32.24685	1564.531
2	59.26946	3811.787
3	75.70985	4905.348
4	61.98614	4776.360
5	65.95327	4094.947
6	3.952474	245.4036

ELAPSED SIMULATION TIME 7.3000E+04 DAYS (6.3072E+09 SECS , 200.0 YEARS)
****

TIME STEP NUMBER 1217 NUMBER OF OUTER ITERATIONS 0 CURRENT TIME STEP 70.00 DAYS

COMP. 1 NO. OF L2SOR ITERATIONS 1 CONVERGENCE 1.3498E-12

PARENT MAXIMUM CHANGE AT (31,61, 2)
OVER LAST TIME STEP 1.0641E-09

MATERIAL BALANCE SUMMARY OF DISSOLVED AND SORBED RADIOACTIVE COMPONENTS -- (LB)

NO	COMPONENT	IN-PLACE	SOURCES	SINKS	GENERATION	DECAY	E-FLUX	BALANCE
1	URANIUM	1.9507E+04	0.0000E+00	46.59	0.0000E+00	0.0000E+00	441.0	1.0000

SUMMARY OF RADIONUCLIDE MASS BY LAYER

COMPONENT 1 URANIUM

LAYER	DISSOLVED MASS(LB)	SORBED MASS(LB)
1	28.40158	1377.969
2	53.42373	3435.266
3	68.88575	4460.020
4	61.73945	4757.323
5	78.52522	4875.522
6	4.915651	305.2060

ELAPSED SIMULATION TIME 9.1250E+04 DAYS (7.8840E+09 SECS , 250.0 YEARS)

TIME STEP NUMBER 1521 NUMBER OF OUTER ITERATIONS 0 CURRENT TIME STEP 70.00 DAYS

COMP. 1 NO. OF L2SOR ITERATIONS 1 CONVERGENCE 9.7313E-13

PARENT MAXIMUM CHANGE AT (31,61, 2)
OVER LAST TIME STEP 7.8165E-10

MATERIAL BALANCE SUMMARY OF DISSOLVED AND SORBED RADIOACTIVE COMPONENTS -- (LB)

5489

000126

NO	COMPONENT	IN-PLACE	SOURCES	SINKS	GENERATION	DECAY	E-FLUX	BALANCE
1	URANIUM	1.9293E+04	0.0000E+00	59.37	0.0000E+00	0.0000E+00	642.3	1.0000

SUMMARY OF RADIONUCLIDE MASS BY LAYER

COMPONENT 1 URANIUM

LAYER	DISSOLVED MASS(LB)	SORBED MASS(LB)
1	25.47891	1236.169
2	48.96617	3147.355
3	63.59230	4114.106
4	60.61141	4670.371
5	88.24718	5479.145
6	5.692594	353.4453

ELAPSED SIMULATION TIME 1.0950E+05 DAYS (9.4608E+09 SECS , 300.0 YEARS)

TIME STEP NUMBER 1827 NUMBER OF OUTER ITERATIONS 0 CURRENT TIME STEP 40.00 DAYS

COMP. 1 NO. OF L2SOR ITERATIONS 1 CONVERGENCE-8.1872E-10

PARENT MAXIMUM CHANGE AT (31,61, 2)
OVER LAST TIME STEP 3.2200E-10

MATERIAL BALANCE SUMMARY OF DISSOLVED AND SORBED RADIOACTIVE COMPONENTS -- (LB)

NO	COMPONENT	IN-PLACE	SOURCES	SINKS	GENERATION	DECAY	E-FLUX	BALANCE
1	URANIUM	1.9063E+04	0.0000E+00	72.20	0.0000E+00	0.0000E+00	859.9	1.0000

SUMMARY OF RADIONUCLIDE MASS BY LAYER

COMPONENT 1 URANIUM

000127

5489

LAYER	DISSOLVED MASS(LB)	SORBED MASS(LB)
1	23.20226	1125.712
2	45.42763	2918.528
3	59.32211	3835.104
4	59.06347	4551.062
5	95.83795	5950.446
6	6.325104	392.7170

ELAPSED SIMULATION TIME 1.2775E+05 DAYS (1.1038E+10 SECS , 350.0 YEARS)

****

TIME STEP NUMBER 2130 NUMBER OF OUTER ITERATIONS 0 CURRENT TIME STEP 20.00 DAYS

COMP. 1 NO. OF L2SOR ITERATIONS 1 CONVERGENCE-3.3037E-10

PARENT MAXIMUM CHANGE AT (31,61, 3)
OVER LAST TIME STEP 1.2416E-10

MATERIAL BALANCE SUMMARY OF DISSOLVED AND SORBED RADIOACTIVE COMPONENTS -- (LB)

NO	COMPONENT	IN-PLACE	SOURCES	SINKS	GENERATION	DECAY	E-FLUX	BALANCE
1	URANIUM	1.8821E+04	0.0000E+00	85.12	0.0000E+00	0.0000E+00	1089.	1.0000

SUMMARY OF RADIONUCLIDE MASS BY LAYER

COMPONENT 1 URANIUM

LAYER	DISSOLVED MASS(LB)	SORBED MASS(LB)
1	21.38850	1037.713
2	42.52149	2730.600
3	55.76660	3603.111
4	57.34321	4418.469
5	101.7973	6320.452
6	6.842588	424.8468

- 5489

000128

ELAPSED SIMULATION TIME 1.4600E+05 DAYS (1.2614E+10 SECS , 400.0 YEARS)
****

TIME STEP NUMBER 2436 NUMBER OF OUTER ITERATIONS 0 CURRENT TIME STEP 20.00 DAYS

COMP. 1 NO. OF L2SOR ITERATIONS 1 CONVERGENCE-2.7639E-10

PARENT MAXIMUM CHANGE AT (31,61, 3)
OVER LAST TIME STEP 1.0096E-10

MATERIAL BALANCE SUMMARY OF DISSOLVED AND SORBED RADIOACTIVE COMPONENTS -- (LB)

NO	COMPONENT	IN-PLACE	SOURCES	SINKS	GENERATION	DECAY	E-FLUX	BALANCE
1	URANIUM	1.8571E+04	0.0000E+00	98.11	0.0000E+00	0.0000E+00	1326.	1.0000

SUMMARY OF RADIONUCLIDE MASS BY LAYER

COMPONENT 1 URANIUM

LAYER	DISSOLVED MASS(LB)	SORBED MASS(LB)
1	19.91347	966.1483
2	40.06717	2572.034
3	52.72948	3405.368
4	55.58047	4282.599
5	106.4847	6611.490
6	7.266832	451.1875

ELAPSED SIMULATION TIME 1.6425E+05 DAYS (1.4191E+10 SECS , 450.0 YEARS)
****

TIME STEP NUMBER 2739 NUMBER OF OUTER ITERATIONS 0 CURRENT TIME STEP 20.00 DAYS

COMP. 1 NO. OF L2SOR ITERATIONS 1 CONVERGENCE-2.3558E-10

000129

5489

PARENT MAXIMUM CHANGE AT (31,61, 3)
OVER LAST TIME STEP 9.1569E-11

MATERIAL BALANCE SUMMARY OF DISSOLVED AND SORBED RADIOACTIVE COMPONENTS -- (LB)

NO	COMPONENT	IN-PLACE	SOURCES	SINKS	GENERATION	DECAY	E-FLUX
1	URANIUM	1.8316E+04	0.0000E+00	111.2	0.0000E+00	0.0000E+00	1568.

SUMMARY OF RADIONUCLIDE MASS BY LAYER

COMPONENT 1 URANIUM

LAYER	DISSOLVED MASS(LB)	SORBED MASS(LB)
1	18.69244	906.9072
2	37.94959	2435.432
3	50.08440	3233.597
4	53.84370	4148.724
5	110.1597	6839.663
6	7.614008	472.7432

ELAPSED SIMULATION TIME 1.8250E+05 DAYS (1.5768E+10 SECS , 500.0 YEARS)

TIME STEP NUMBER 3045 NUMBER OF OUTER ITERATIONS 0 CURRENT TIME STEP 20.00 DAYS

COMP. 1 NO. OF L2SOR ITERATIONS 1 CONVERGENCE-2.0374E-10

PARENT MAXIMUM CHANGE AT (31,61, 3)
OVER LAST TIME STEP 8.1512E-11

MATERIAL BALANCE SUMMARY OF DISSOLVED AND SORBED RADIOACTIVE COMPONENTS -- (LB)

NO	COMPONENT	IN-PLACE	SOURCES	SINKS	GENERATION	DECAY	E-FLUX	BALANCE
1	URANIUM	1.8057E+04	0.0000E+00	124.3	0.0000E+00	0.0000E+00	1814.	1.0000

5489

SUMMARY OF RADIONUCLIDE MASS BY LAYER

COMPONENT 1 URANIUM

LAYER	DISSOLVED MASS(LB)	SORBED MASS(LB)
1	17.66456	857.0375
2	36.09055	2315.734
3	47.74428	3082.047
4	52.16615	4019.409
5	113.0194	7017.218
6	7.896983	490.3127

ELAPSED SIMULATION TIME 2.0075E+05 DAYS (1.7345E+10 SECS , 550.0 YEARS)

TIME STEP NUMBER 3348 NUMBER OF OUTER ITERATIONS 0 CURRENT TIME STEP 20.00 DAYS

COMP. 1 NO. OF L2SOR ITERATIONS 1 CONVERGENCE-1.7819E-10

PARENT MAXIMUM CHANGE AT (31,61, 3)
OVER LAST TIME STEP 7.1453E-11

MATERIAL BALANCE SUMMARY OF DISSOLVED AND SORBED RADIOACTIVE COMPONENTS -- (LB)

NO	COMPONENT	IN-PLACE	SOURCES	SINKS	GENERATION	DECAY	E-FLUX	BALANCE
1	URANIUM	1.7796E+04	0.0000E+00	137.5	0.0000E+00	0.0000E+00	2062.	1.0000

SUMMARY OF RADIONUCLIDE MASS BY LAYER

COMPONENT 1 URANIUM

LAYER	DISSOLVED MASS(LB)	SORBED MASS(LB)
1	16.78578	814.4014
2	34.43580	2209.406
3	45.64795	2946.650

000131

3489

4	50.56244	3895.778
5	115.2149	7153.531
6	8.126016	504.5331

ELAPSED SIMULATION TIME 2.1900E+05 DAYS (1.8922E+10 SECS , 600.0 YEARS)
****

TIME STEP NUMBER 3654 NUMBER OF OUTER ITERATIONS 0 CURRENT TIME STEP 20.00 DAYS

COMP. 1 NO. OF L2SOR ITERATIONS 1 CONVERGENCE-1.5717E-10

PARENT MAXIMUM CHANGE AT (31,61, 3)
OVER LAST TIME STEP 6.1789E-11

MATERIAL BALANCE SUMMARY OF DISSOLVED AND SORBED RADIOACTIVE COMPONENTS -- (LB)

NO	COMPONENT	IN-PLACE	SOURCES	SINKS	GENERATION	DECAY	E-FLUX	BALANCE
1	URANIUM	1.7533E+04	0.0000E+00	150.7	0.0000E+00	0.0000E+00	2311.	1.0000

SUMMARY OF RADIONUCLIDE MASS BY LAYER

COMPONENT 1 URANIUM

LAYER	DISSOLVED MASS(LB)	SORBED MASS(LB)
1	16.02362	777.4232
2	32.94641	2113.899
3	43.75102	2824.439
4	49.03701	3778.175
5	116.8637	7255.906
6	8.309425	515.9207

ELAPSED SIMULATION TIME 2.3725E+05 DAYS (2.0498E+10 SECS , 650.0 YEARS)
****

5489

000132

TIME STEP NUMBER 3957 NUMBER OF OUTER ITERATIONS 0 CURRENT TIME STEP 20.00 DAYS

COMP. 1 NO. OF L2SOR ITERATIONS 1 CONVERGENCE-1.3939E-10

PARENT MAXIMUM CHANGE AT (31,61, 3)
OVER LAST TIME STEP 5.2699E-11

MATERIAL BALANCE SUMMARY OF DISSOLVED AND SORBED RADIOACTIVE COMPONENTS -- (LB)

NO	COMPONENT	IN-PLACE	SOURCES	SINKS	GENERATION	DECAY	E-FLUX	BALANCE
1	URANIUM	1.7271E+04	0.0000E+00	164.0	0.0000E+00	0.0000E+00	2560.	1.0000

SUMMARY OF RADIONUCLIDE MASS BY LAYER

COMPONENT 1 URANIUM

LAYER	DISSOLVED MASS(LB)	SORBED MASS(LB)
1	15.35382	744.9262
2	31.59371	2027.323
3	42.02041	2713.192
4	47.58900	3666.533
5	118.0589	7330.116
6	8.454031	524.8991

ELAPSED SIMULATION TIME 2.5550E+05 DAYS (2.2075E+10 SECS , 700.0 YEARS)

TIME STEP NUMBER 4263 NUMBER OF OUTER ITERATIONS 0 CURRENT TIME STEP 20.00 DAYS

COMP. 1 NO. OF L2SOR ITERATIONS 1 CONVERGENCE-1.2610E-10

PARENT MAXIMUM CHANGE AT (31,61, 4)
OVER LAST TIME STEP 4.4430E-11

MATERIAL BALANCE SUMMARY OF DISSOLVED AND SORBED RADIOACTIVE COMPONENTS -- (LB)

000133

5489

NO	COMPONENT	IN-PLACE	SOURCES	SINKS	GENERATION	DECAY	E-FLUX	BALANCE
1	URANIUM	1.7008E+04	0.0000E+00	177.2	0.0000E+00	0.0000E+00	2809.	1.0000

SUMMARY OF RADIONUCLIDE MASS BY LAYER

COMPONENT 1 URANIUM

LAYER	DISSOLVED MASS(LB)	SORBED MASS(LB)
1	14.75803	716.0203
2	30.35593	1948.241
3	40.43073	2611.203
4	46.21479	3560.574
5	118.8750	7380.785
6	8.565488	531.8193

ELAPSED SIMULATION TIME 2.7375E+05 DAYS (2.3652E+10 SECS , 750.0 YEARS)

TIME STEP NUMBER 4566 NUMBER OF OUTER ITERATIONS 0 CURRENT TIME STEP 20.00 DAYS

COMP. 1 NO. OF L2SOR ITERATIONS 1 CONVERGENCE-1.1503E-10

PARENT MAXIMUM CHANGE AT (31,61, 4)
OVER LAST TIME STEP 3.6876E-11

MATERIAL BALANCE SUMMARY OF DISSOLVED AND SORBED RADIOACTIVE COMPONENTS -- (LB)

NO	COMPONENT	IN-PLACE	SOURCES	SINKS	GENERATION	DECAY	E-FLUX	BALANCE
1	URANIUM	1.6747E+04	0.0000E+00	190.4	0.0000E+00	0.0000E+00	3057.	1.0000

SUMMARY OF RADIONUCLIDE MASS BY LAYER

COMPONENT 1 URANIUM

000134

5489

LAYER	DISSOLVED MASS(LB)	SORBED MASS(LB)
1	14.22226	690.0262
2	29.21623	1875.539
3	38.96218	2517.139
4	44.90965	3459.935
5	119.3721	7411.650
6	8.648512	536.9741

ELAPSED SIMULATION TIME 2.9200E+05 DAYS (2.5229E+10 SECS , 800.0 YEARS)
****

TIME STEP NUMBER 4872 NUMBER OF OUTER ITERATIONS 0 CURRENT TIME STEP 20.00 DAYS

COMP. 1 NO. OF L2SOR ITERATIONS 1 CONVERGENCE-1.0468E-10

PARENT MAXIMUM CHANGE AT (31,61, 4)
OVER LAST TIME STEP 3.0046E-11

MATERIAL BALANCE SUMMARY OF DISSOLVED AND SORBED RADIOACTIVE COMPONENTS -- (LB)

NO	COMPONENT	IN-PLACE	SOURCES	SINKS	GENERATION	DECAY	E-FLUX	BALANCE
1	URANIUM	1.6488E+04	0.0000E+00	203.6	0.0000E+00	0.0000E+00	3303.	1.0000

SUMMARY OF RADIONUCLIDE MASS BY LAYER

COMPONENT 1 URANIUM

LAYER	DISSOLVED MASS(LB)	SORBED MASS(LB)
1	13.73568	666.4184
2	28.16121	1808.328
3	37.59882	2429.928
4	43.66840	3364.216
5	119.5995	7425.765
6	8.707069	540.6098

ELAPSED SIMULATION TIME 3.1025E+05 DAYS (2.6806E+10 SECS , 850.0 YEARS)
****

TIME STEP NUMBER 5175 NUMBER OF OUTER ITERATIONS 0 CURRENT TIME STEP 20.00 DAYS

COMP. 1 NO. OF L2SOR ITERATIONS 1 CONVERGENCE-9.5383E-11

PARENT MAXIMUM CHANGE AT (31,61, 4)
OVER LAST TIME STEP 2.3985E-11

MATERIAL BALANCE SUMMARY OF DISSOLVED AND SORBED RADIOACTIVE COMPONENTS -- (LB)

NO	COMPONENT	IN-PLACE	SOURCES	SINKS	GENERATION	DECAY	E-FLUX	BALANCE
1	URANIUM	1.6229E+04	0.0000E+00	216.8	0.0000E+00	0.0000E+00	3548.	1.0000

SUMMARY OF RADIONUCLIDE MASS BY LAYER

COMPONENT 1 URANIUM

LAYER	DISSOLVED MASS(LB)	SORBED MASS(LB)
1	13.28989	644.7902
2	27.18018	1745.898
3	36.32783	2348.711
4	42.48608	3273.036
5	119.5975	7425.642
6	8.744500	542.9339

ELAPSED SIMULATION TIME 3.2850E+05 DAYS (2.8382E+10 SECS , 900.0 YEARS)
****

TIME STEP NUMBER 5481 NUMBER OF OUTER ITERATIONS 0 CURRENT TIME STEP 20.00 DAYS

COMP. 1 NO. OF L2SOR ITERATIONS 1 CONVERGENCE-8.6847E-11

5480

000136

PARENT MAXIMUM CHANGE AT (31,61, 4)
OVER LAST TIME STEP 1.9416E-11

MATERIAL BALANCE SUMMARY OF DISSOLVED AND SORBED RADIOACTIVE COMPONENTS -- (LB)

NO	COMPONENT	IN-PLACE	SOURCES	SINKS	GENERATION	DECAY	E-FLUX	BALANCE
1	URANIUM	1.5973E+04	0.0000E+00	229.8	0.0000E+00	0.0000E+00	3791.	1.0000

SUMMARY OF RADIONUCLIDE MASS BY LAYER

COMPONENT 1 URANIUM

LAYER	DISSOLVED MASS(LB)	SORBED MASS(LB)
1	12.87829	624.8203
2	26.26428	1687.665
3	35.13853	2272.773
4	41.35794	3186.029
5	119.3998	7413.366
6	8.763645	544.1226

ELAPSED SIMULATION TIME 3.4675E+05 DAYS (2.9959E+10 SECS , 950.0 YEARS)

TIME STEP NUMBER 5784 NUMBER OF OUTER ITERATIONS 0 CURRENT TIME STEP 20.00 DAYS

COMP. 1 NO. OF L2SOR ITERATIONS 1 CONVERGENCE-7.9128E-11

PARENT MAXIMUM CHANGE AT (31,61, 4)
OVER LAST TIME STEP 1.7230E-11

MATERIAL BALANCE SUMMARY OF DISSOLVED AND SORBED RADIOACTIVE COMPONENTS -- (LB)

NO	COMPONENT	IN-PLACE	SOURCES	SINKS	GENERATION	DECAY	E-FLUX	BAL
1	URANIUM	1.5720E+04	0.0000E+00	242.8	0.0000E+00	0.0000E+00	4032.	1.0

000137

5489

SUMMARY OF RADIONUCLIDE MASS BY LAYER

COMPONENT 1 URANIUM

LAYER	DISSOLVED MASS(LB)	SORBED MASS(LB)
1	12.49565	606.2556
2	25.40623	1633.146
3	34.02206	2201.523
4	40.27969	3102.866
5	119.0343	7390.678
6	8.766921	544.3260

ELAPSED SIMULATION TIME 3.6500E+05 DAYS (3.1536E+10 SECS , 1000. YEARS)

TIME STEP NUMBER 6090 NUMBER OF OUTER ITERATIONS 0 CURRENT TIME STEP 20.00 DAYS

COMP. 1 NO. OF L2SOR ITERATIONS 1 CONVERGENCE-7.2169E-11

PARENT MAXIMUM CHANGE AT (31,61, 4)
OVER LAST TIME STEP 1.5175E-11

MATERIAL BALANCE SUMMARY OF DISSOLVED AND SORBED RADIOACTIVE COMPONENTS -- (LB)

NO	COMPONENT	IN-PLACE	SOURCES	SINKS	GENERATION	DECAY	E-FLUX	BALANCE
1	URANIUM	1.5469E+04	0.0000E+00	255.7	0.0000E+00	0.0000E+00	4270.	1.0000

SUMMARY OF RADIONUCLIDE MASS BY LAYER

COMPONENT 1 URANIUM

LAYER	DISSOLVED MASS(LB)	SORBED MASS(LB)
1	12.13780	588.8937
2	24.59988	1581.937
3	32.97091	2134.464

5489

000138

4	39.24748	3023.250
5	118.5248	7359.041
6	8.756395	543.6724